THEORETICAL AND EXPERIMENTAL STUDY OF THE MECHANISM OF EXCLUSION CHROMATOGRAPHY

by

FORBES McLENNAN, B.Sc.

Thesis submitted for the Degree of
Doctor of Philosophy

University of Edinburgh 1978

To Mum, Dad and Fiona

I declare that the work described in this thesis has not been submitted for any other degree and is the original work of the author except where acknowledgment is made by reference. The work has been carried out in the Chemistry Department of the University of Edinburgh between October 1975 and September 1978 under the supervision of Professor J.H. Knox.

Post-graduate courses attended include: Chemistry of the Atmosphere (Dr. R.J. Donovan, 1975); From Crawford to Kemball-260 Years a-growing (Dr. W.P. Doyle, 1977); Computer facilities in the Chemistry Department (Dr. P.J. Robertson and Dr. M.A.D. Fluendy, 1977); Exploitation of Inventiveness in the Oil Industry (B.P. Research, 1977); Chemical Society Intensive Liquid Chromatography Courses (Professor J.H. Knox, 1977 and 1978); Chromatography Discussion Group (1977/78); S.R.C. CRAC Course (Liverpool, 1977); Chemistry Department Seminars (1975 - 78).

A C K N O W L E D G M E N T S

The author would like to thank

Professor John H. Knox for his enthusiastic and invaluable encouragement, guidance and discussion,

The University of Edinburgh Chemistry Department for the research facilities provided,

Mrs. M. Duncan for typing this thesis,

the Chemistry Department staff and research students for their advice, criticism and friendship during the course of this work.

ABSTRACT

This thesis describes the mechanism of exclusion chromatography in terms of conventional liquid chromatography terminology.

The various theories for sample retention are discussed and it is concluded that elution under ordinary conditions with a rigid pore structure is governed by the equilibrium theory of steric exclusion. Using the steric exclusion mechanism, calibration curves were computed for various pore geometries and spherical macromolecules which gave an exceptionally good fit to experimental data.

In exclusion chromatography, band broadening or dispersion of a polymer sample arises from both the polydispersity, P, of the sample and from the kinetic processes occurring within the column. It is shown that the plate height due to kinetic processes within the column, H, is given by

$$H = H_{app} - \frac{L\,(P-1)\,(1+\alpha)}{x^2}$$

where H_{app} is the apparent plate height calculated from the experimental peak, L is the column length, α is a function of (P-1) and x is a measure of the relative molecular mass range covered by the packing material.

By varying the column length and extrapolating to zero length, the true plate height (due to kinetic effects) was obtained as a function of velocity. This dependence of plate height upon velocity followed the well known trend in liquid chromatography giving a minimum plate height of around 2 particle diameters. This

was verified by measuring the plate height for monodisperse polymer fractions obtained by adsorption chromatography.

By manipulation of this plate height versus velocity data to account for longitudinal diffusion and flow effects, the stationary phase mass transfer coefficients were obtained. Interpretation of these coefficients in terms of the non-equilibrium theory of chromatography leads to the conclusion that within the pores of the material, diffusion of molecules is restricted with the degree of restriction increasing as molecular size approaches the pore size. However, this restriction is small enough and mass transfer fast enough so as not to negate the near-equilibrium assumption of chromatography which is shown by the narrow and symmetrical peaks obtained for monodisperse polymers.

These results finally confirm that the theory of retentive chromatography applies with only minor adjustments to exclusion chromatography, thereby solving a long standing argument as to the nature of the processes occurring in exclusion chromatography.

Sample loading is discussed and it is shown that sample loads must be kept below about 10 μg for analytical columns: larger loads lead to loss of efficiency and change in retention volume.

C O N T E N T S

C H A P T E R 1

INTRODUCTION TO LIQUID CHROMATOGRAPHY

Chapter 1.1. Historical Introduction

Chapter 1.2. Resolution, Retention and Dispersion

1.2.1. Solute Retention

1.2.2. Band Broadening

Chapter 1.3. Different Modes of Liquid Chromatography

CHAPTER 1.1.

HISTORICAL INTRODUCTION

The earliest reported account of a separation which can be considered as an example of liquid chromatography has been attributed to Tswett (1) who, in 1903, described the separation of plant pigments in a column filled with powdered chalk. This discovery, however, received little notice until 1931 when Kuhn, Lederer and Winterstein (2) virtually repeated Tswett's work and separated pigments on a column filled with alumina and calcium carbonate. There was, however, little advance in either the theory or practice of chromatography until 1941 when Martin and Synge (3) published their classic paper describing liquid-liquid partition chromatography in which the different rates of migration of solutes arose from their different partition ratios between the flowing mobile phase and a stationary phase held on the surface of a porous support. They introduced to chromatography the concept of the number of theoretical plates and the height equivalent to a theoretical plate (H.E.T.P.) which was defined as "the thickness of a layer such that the solution issuing from it is in equilibrium with the mean concentration of solute in the non-mobile phase throughout the layer ". They realised that there was an optimum rate of flow since at very low flow velocities, molecular diffusion becomes important, and that since the H.E.T.P. was proportion to the flow rate and the particle diameter squared, the smallest H.E.T.P. should be obtained by using very small particles and a high pressure difference across the length of the column. It was noted that separation efficiency may be affected by non-equilibrium considerations and also that the other great source of loss of efficiency is the lack of uniformity of

flow through the column.

Martin and Synge outlined the advantages of using a gas as mobile phase and so foreshadowed gas chromatography which was not experimentally demonstrated until 1952 (4). Gas chromatography made rapid advances during the next two decades but liquid chromatography lagged well behind and it was only around 1968 that the first papers appeared showing analyses of liquid chromatography comparable in speed to gas chromatography (5,6,7).

CHAPTER 1.2.

RESOLUTION, RETENTION AND DISPERSION

The separation of compounds on a chromatographic column arises from the different migration rates along the column. The degree of separation of adjacent zones is quantitatively described by the resolution, R_s, defined as

$$R_s = \frac{\Delta Z}{\bar{w}} \qquad (1.1.)$$

where ΔZ is the distance between adjacent peak maxima and $\bar{w}$ is the mean width of the peaks at the base.

For a peak whose concentration profile is Gaussian, the base width is equal to four standard deviations. In the case of adjacent peaks the standard deviations, and hence the peak widths, will differ slightly and an average value is taken. Resolution is therefore given by

$$R_s = \frac{V_{r(1)} - V_{r(2)}}{\frac{1}{2}(w_1 + w_2)} \qquad (1.2.)$$

where $V_{r(1)}$, $V_{r(2)}$ are the elution volumes of peaks of base width w_1 and w_2 respectively, as is shown in Figure 1.

Thus resolution is composed of two factors, separating power reflected in ΔZ and band spreading, reflected in $\bar{w}$. These two factors can be considered to be governed by thermodynamic and kinetic properties respectively, which are essentially independent, and may therefore be treated separately.

1.2.1. Solute Retention

A chromatographic column may be considered to consist of two zones, a flowing mobile zone (the fluid outside the particles) and a stationary zone (the material, usually partly fluid, within the particles). The separation of solutes arises from the different solute migration rates along the column which are controlled by the distribution of solutes between the mobile and stationary zones. It is assumed that the solute molecules equilibrate rapidly between the mobile and stationary zones and that during elution, molecules only move while in the mobile zone, at the mean linear velocity of the eluent, u_o.

It therefore follows that the speed of a band of solute molecules relative to the mobile zone is given by

$$\frac{u_{band}}{u_o} = \text{fraction of solute in the mobile zone} = \frac{q_{mz}}{q_{mz} + q_{sz}} = \frac{1}{1+q_{sz}/q_{mz}} = \frac{1}{1+k''} \qquad (1.3.)$$

where q_{mz} and q_{sz} are the quantities of solute in the mobile and stationary zones and k", called the zone capacity factor is given by

$$k'' = \frac{q_{sz}}{q_{mz}} \qquad (1.4.)$$

Because of the near equilibrium assumption q_{sz} and q_{mz} may be regarded as equilibrium values and so

$$k'' = \frac{C_{sz}\,V_{sz}}{C_{mz}\,V_{mz}} = K\,\frac{V_{sz}}{V_{mz}} \qquad (1.5.)$$

where C_{sz} and C_{mz} are the equilibrium concentrations of the solute

in the stationary and mobile zones while V_{sz} and V_{mz} are the volumes of the stationary and mobile zones respectively. K is the distribution coefficient of the solute between the stationary and mobile zones.

Since the volume of the stationary zone is equal to the pore volume in the column, V_p, and the volume of the mobile zone is the void volume of the column, V_o, equation (1.5) may be written as

$$k'' = K \frac{V_p}{V_o} \qquad (1.6.)$$

Since the linear velocity of a solute band is inversely proportional to its elution volume

$$\frac{u_{band}}{u_o} = \frac{V_o}{V_r} = \frac{1}{1+k''} \qquad (1.7.)$$

where V_r is the elution volume of a solute band.

By combining equations (1.6.) and (1.7.) we see that

$$V_r = V_o(1+k'') \qquad (1.8.)$$

and

$$V_r = V_o + K V_p \qquad (1.9.)$$

Only in exclusion chromatography is the rate of movement of the solute band normally referred to the rate of movement of the mobile zone. In retentive chromatography (adsorption, partition, ion exchange), the mobile zone is not identical to the mobile phase since part of the eluent will be held within the pores of the

support and similarly the stationary zone does not correspond to the stationary phase.

The rate of movement of a solute band in retentive chromatography is usually referred to the rate of movement of the mobile phase, u.

Thus it follows that the speed of a band of solute molecules relative to the mobile phase is given by

$$\frac{u_{band}}{u} = \text{fraction of solute in the mobile phase} = \frac{q_m}{q_m + q_s} = \frac{1}{1 + q_s/q_m} = \frac{1}{1 + k'} \qquad (1.10.)$$

where q_m and q_s are the quantities of solute in the mobile and stationary phase and k', called the phase capacity factor, is given by

$$k' = \frac{q_s}{q_m} \qquad (1.11.)$$

Because of the near equilibrium assumption q_s and q_m may be regarded as equilibrium values and so

$$k' = \frac{C_s V_s}{C_m V_m} = D\frac{V_s}{V_m} \qquad (1.12)$$

where C_s and C_m are the equilibrium concentrations of the solute in the stationary and mobile phases while V_s and V_m are the volumes of the stationary and mobile phases respectively. D is the distribution coefficient of the solute between the stationary and mobile phases.

Since the linear velocity of a solute band is inversly proportion to its elution volume

$$\frac{u_{band}}{u} = \frac{V_m}{V_r} = \frac{1}{1 + k'} \qquad (1.13.)$$

where V_r is the elution volume of a solute band.

by combining equations (1.12.) and (1.13.) we see that

$$V_r = V_m (1 + k') \qquad (1.14.)$$

and $$V_r = V_m + DV_s \qquad (1.15.)$$

Thermodynamically, the standard free energy change, ΔG^o, for the transfer of solute molecules from the mobile phase or zone to the stationary phase or zone is given by equation (1.16.)

$$\begin{aligned} \Delta G^o &= -k\ T\ \ln D \\ \Delta G^o &= -k\ T\ \ln K \end{aligned} \qquad (1.16.)$$

where D or K is the distribution coefficient and k is Boltzmann's constant.

Combining equations (1.6.) and (1.12.) with equations (1.16.) and (1.17.)

$$\Delta G = \Delta H - T\Delta S \qquad (1.17.)$$

we have that

$$\begin{aligned} k' &= \exp(-\frac{\Delta H}{kT}) \exp(\frac{\Delta S}{k})(\frac{V_s}{V_m}) \\ k'' &= \exp(-\frac{\Delta H}{kT}) \exp(\frac{\Delta S}{k})(\frac{V_p}{V_o}) \end{aligned} \qquad (1.18.)$$

In retentive chromatography (adsorption, partition, ion exchange) it is generally found that ΔH is the factor which is varied in order to change k', the entropy changes are usually similar. In exclusion chromatography, enthalpy changes are as far as possible eliminated and k'' is determined only by an entropy change.

1.2.2. Band Broadening

Band broadening is universally characterized by the number of theoretical plates N and the height equivalent to a theroetical plate H (3).

$$H = L\left(\frac{\sigma_v}{V_r}\right)^2 \qquad (1.19.)$$

$$N = \frac{L}{H} = \left(\frac{V_r}{\sigma_v}\right)^2 \qquad (1.20.)$$

where L is the length of the column, σ_v is the standard deviation of the peak in volume units and V_r is the elution volume.

The plate height theory is a convenient tool for assessing the efficiency or performance of a column, but in itself affords no explanation of real behaviour in the column.

Martin and Synge (3) recognised the role which is played by molecular diffusion, mass transfer, non-equilibrium and non-uniform flow through the column and realized that since the influence of flow rate on mass transfer and molecular diffusion were opposed there would be an optimum flow rate.

All the main near-equilibrium theories of band broadening in liquid chromatography (which are discussed in detail in Chapter 2.5.) give rise to a dependence of H on the linear velocity which may be approximated by the empirical equation (8)

$$H = \frac{B}{u} + Au^{0.33} + Cu \qquad (1.21.)$$

In this equation, B described the molecular diffusion, C the mass transfer characteristics and A reflects the dispersive power of the interparticle space (flow effects).

In order to discuss a multi-component separation, Giddings (9) introduced the concept of peak capacity. The peak capacity is defined as the number of peaks, n, that can be placed within a certain time (volume) period in which all the bands have a resolution of unity. If the same number of theoretical plates is assumed for all solutes then n is given by equation (1.22.).

$$n = 1 + 0.25\, N^{\frac{1}{2}} \ln \left(\frac{V_{max}}{V_{min}}\right) \qquad (1.22.)$$

In retentive chromatography, k' of the nth peak is given by

$$k' = \frac{V_{max} - V_{min}}{V_{min}} \qquad (1.23.)$$

and hence

$$n = 1 + 0.25\, N^{\frac{1}{2}} \ln (1 + k') \qquad (1.24.)$$

In exclusion chromatography $V_{max} = V_o + V_p$ where $V_{min} = V_o$, hence

$$n = 1 + 0.25\, N^{\frac{1}{2}} \ln \left(1 + \frac{V_p}{V_o}\right) \qquad (1.25.)$$

CHAPTER 1.3.

DIFFERENT MODES OF LIQUID CHROMATOGRAPHY

The different modes of liquid chromatography all have a common theoretical basis and can generally be carried out with the same basic equipment. The only difference between the different modes is in the nature, composition and structure of the stationary phase, and in the nature of the molecular forces that hold the solute molecules within the mobile and stationary phases.

Adsorption Chromatography (Liquid-Solid Chromatography)

Adsorption chromatography was the original chromatographic technique used by Tswett (1). It is based on differences in the relative affinity of compounds for the solid adsorbent used as stationary phase. Silica is the most widely used adsorbent and the active sites on the surface of the silica are normally hydroxyl groups. Affinity is determined almost entirely by polar interactions. This means that polar groupings in the molecule to be separated exerts a much stronger effect than non-polar hydrocarbon chains and adsorption chromatography therefore tends to separate mixtures into classes characterized by the number and type of polar groups.

Partition Chromatography (Liquid-Liquid Chromatography)

Partition chromatography is based on the relative distribution characteristics of solutes between the mobile phase and a liquid phase held stationary on a porous inert support. If the stationary phase is more polar than the mobile phase, the technique is called Straight-Phase Partition Chromatography and if the roles

are reversed it is called Reverse-Phase Partition Chromatography. Separations essentially depend on the balance between polar and apolar groups in the solutes and the two liquid phases. Reverse-phase systems are much more difficult to handle since the physical forces between the stationary phase and the support are relatively weak and this is one of the reasons for the development of chemically bonded stationary phases which are discussed below.

Ion-Exchange Chromatography

Ion-exchange chromatography is based on the differing affinity of ions in solution for sites of opposite charge in the stationary phase. Ion exchange materials contain either acidic sites (such as sulphonic acid) for the separation of cations or basic sites (such as quaternary amine) for the separation of anions. The best efficiencies have been obtained by chemically bonding these ion groups onto 5 - 10um porous silica particles.

Exclusion Chromatography

Exclusion chromatography is based on the distribution of solutes between bulk solvent and the solvent contained within the interstices of porous particles. The bulk solvent may be considered analogous to a mobile phase and the solvent within the pores to a stationary phase. Separation is based upon the fact that the pores are of molecular dimensions and the degree of penetration of a solute molecule into the pores is determined by the size of the solute. Very large molecules are unable to enter the pores and are eluted in a volume of solvent equal to the void volume of the column, V_o. If the solute molecules are of such

a size that they can penetrate the entire volume of the pores, they are eluted in a volume equal to the void volume plus the volume of the pores, V_p. Molecules of intermediate size are eluted in a volume (between V_o and $V_o + V_p$) described by the relationship

$$V_r = V_o + K V_p \qquad (1.26.)$$

where K is the distribution coefficient of the solute between the two phases.

Bonded-Phase Chromatography

Adsorption chromatography is not usually applicable to the separation of very polar or ionic molecules and liquid-liquid partition chromatography can be experimentally troublesome due to the need for a thermostatted pre-column loaded with stationary phase to prevent stripping of the stationary phase from the analytical column. For these reasons, chromatography on chemically bonded stationary phases (prepared by bonding organic groups to the surface of an adsorbent) has developed. The main types of organic groups utilized commercially are (a) hydrophobic groups such as octadecyl groups and shorter alkyl chains, (b) polar groups such as cyanopropyl, (c) ion exchange groups such as sulphonic acids and quaternary ammonium salts.

The preparation and applications of chemically bonded stationary phases for retentive liquid chromatography has been well reviewed (10). For exclusion chromatography it may also be useful to bond organic groups to a packing material in order to eliminate adsorption. This is particularly necessary when working with very polar molecules such as proteins or nucleic acids.

CHAPTER 2

INTRODUCTION TO EXCLUSION CHROMATOGRAPHY

2.1. Historical Introduction and Nomenclature

2.2. Principle of Exclusion Chromatography

2.3. Support Materials for Exclusion Chromatography

2.4. Sample Retention in Exclusion Chromatography

- 2.4.1. Equilibrium Models
- 2.4.2. Diffusion Models
- 2.4.3. Flow Models
- 2.4.4. Summary

2.5. Peak Broadening in Exclusion Chromatography

- 2.5.1. Near-Equilibrium Theory
- 2.5.2. Non-Equilibrium Theory
- 2.5.3. Extra-Column Band Broadening
- 2.5.4. Peak Capacity Factor

CHAPTER 2.1.

HISTORICAL INTRODUCTION AND NOMENCLATURE

Exclusion chromatography is the newest of the four modes of liquid chromatography (liquid-liquid, liquid-solid, ion exchange and exclusion chromatography) and it is also unique in that the method of separation relies entirely on the physical restriction of molecules moving through a packed bed rather than any interactive effect e.g. adsorption or partition into a stationary phase. Although other more complex physical effects may be involved to an extent dictated by the nature of the gel system and the sample under investigation, such effects are usually undesirable and can often be minimised by careful design of the chromatographic conditions.

Although porous zeolites (11) and agar gels (12) were used for separations before 1930, the technique was not widely used until 1959 when Porath and Flodin (13) developed organic gels (cross-linked dextran gels) which were suitable for the separation of biopolymers in aqueous media and called their technique Gel Filtration.

The term Gel Permeation chromatography was first employed by Moore (14) for the separation of polymers in organic media using cross-linked polystyrene gels.

During the 1960's, a dual literature grew up. The term Gel Filtration being used in relation to chromatography using hydrophilic packings and aqueous solvents to separate mainly natural products and Gel Permeation Chromatography being used in relation to chromatography using hydrophobic packings and organic solvents for the separation of synthetic macromolecules.

Also during this period a vast number of other names were coined to describe this type of separation: Molecular Sieve Filtration (15), Exclusion Chromatography (16), Restricted Diffusion Chromatography (17), Molecular Sieve Chromatography (18), Gel Chromatography (19), Gel Diffusion Filtration (20), Molecular Exclusion Chromatography (21), Steric Chromatography (22), Gel Exclusion Chromatography (23), Permeation Chromatography (24), Size Exclusion Chromatography (25), Liquid Exclusion Chromatography (26). Throughout this work I shall use the name Exclusion Chromatography which along with Size Exclusion Chromatography and Liquid Exclusion Chromatography give the clearest indication of the mechanism of separation.

Organic gels (13, 14) are highly sensitive to pressure and although efficient separations may be accomplished with these materials, the separations are slow and the equipment cumbersome. A typical arrangement (14) would consist of four columns, each 6 feet long, 3/8" outside diameter, coupled in series and the separation time would then be a few hours. As in other forms of liquid chromatography, great increases in speed and resolution may be achieved by using rigid, porous, inorganic microparticles (27, 28) and it was the advent of these materials which brought about the renaissance of interest in the mechanism of exclusion chromatography. Using these materials typical columns are 100 - 250mm long and 5 - 8mm internal diameter. Although it may still be necessary to couple columns together to achieve the required separation, typical separation times may be less than 15 mins, and this has led to the use of the terms High Speed, High Pressure and High Performance to prefix many of the names given above for this type of separation.

CHAPTER 2.2.

PRINCIPLE OF EXCLUSION CHROMATOGRAPHY

Exclusion chromatography is a form of liquid chromatography which sorts molecules by elution through a packed column according to their size in solution. The mechanism of this size sorting will be discussed in Chapter 2.4.

The packing material is a rigidly structured porous network and may consist of materials such as cross-linked dextrans (13), (soft gels), polystyrene cross-linked with divinylbenzene (14) (semi-rigid gels) or porous glass (27) or silica(28) (rigid gels). Solvent is pumped continuously through the column by means of an external pumping system. A solution of the sample is injected onto the top of the column, and the sample is transported through the column by means of the flowing solvent stream.

The size sorting of the polymer molecules takes place in the pores of the gel. Very large molecules are unable to enter the pores and are eluted in a volume of solvent equal to the void volume of the column, V_o. If the solute molecules are sufficiently small so that they can penetrate the entire volume of the gel pores, they are eluted in a volume of solvent equal to the void volume of the column, V_o, plus the volume of solvent contained within the pores, V_p. Molecules intermediate in size are eluted in a volume between these two extremes. Thus, providing adsorption effects are absent, exclusion chromatography separates according to size, large molecules being eluted before small molecules. All solutes are eluted in the comparatively narrow range of elution volumes between the void volume of the column and the total volume of the solvent in

the column. Between the two extremes the elution volume can be described by a relation similar to that found for partition chromatography (see Chapter 1.2.1.)

$$V_r = V_o + K V_p \qquad (2.1.)$$

where V_r is the elution volume of the solute and K is the distribution coefficient of the solute between the solvent in the column void volume and the solvent contained within the pores i.e. K may be interpreted as the fraction of the pore volume available to the solute in question. Evidently completely excluded solutes have K = 0 while totally permeating solutes have K = 1.

The total volume of eluent within the column is given by

$$V_m = V_o + V_p \qquad (2.2.)$$

From Chapter 1.2.1. we have

$$k' = \frac{V_r - V_m}{V_m} \qquad (2.3.)$$

and

$$k'' = \frac{V_r - V_o}{V_o} \qquad (2.4.)$$

where k' and k'' are the phase capacity ratio and the zone capacity ratio respectively.

Combining equations (2.3.) and (2.4.) with equation (2.1.) we see that

$$k' = (K - 1)\, V_p/V_m \qquad (2.5.)$$

$$k'' = K\, V_p/V_m \qquad (2.6.)$$

k' is negative for partially excluded solutes while k'' falls in the range zero to V_p/V_m and is always positive.

As the molecules exit from the column they may be detected by differential refractometry (29), ultraviolet photometry (30), flame ionization (31), infrared adsorption (32) or thermal adsorption (33). Discontinuous detection may also be used. For example, fractions may be collected and the viscosities measured (34) or the solvent may be evaporated and the residue weighed.

The normal way of expressing exclusion data is in the form of a semi-logarithmic calibration curve relating molecular weight to either V_r or K. A typical calibration curve for a single matrix material is shown in Figure 2. The figure also indicates the equivalent values of k" and k' and the volume of the solid of the matrix, V_s. Such calibration curves normally have a fairly sharp cut off corresponding to the exclusion limit at the high molecular weight end, an approximately linear intermediate portion, and a more gradual curve away from the linear portion towards the region of total permeation. The extent of the linear region generally covers about 1.5 - 2 orders of magnitude of molecular weight depending on the pore size distribution of the packing material. If the pore size distribution is narrow, the exclusion curve is relatively flat giving rise to selective permeation over a small range of molecular weight and good resolution per unit of molecular weight. A wide pore size distribution gives rise to a steeper exclusion curve, selective permeation over a wider range of molecular weight but poorer resolution per unit of molecular weight. Hypothetical calibration curves for a narrow and a wide pore size distribution is shown in Figure 3.

To cover wide ranges of molecular weight it is usual to employ several columns connected in series, each column covering a

different molecular weight range (14).

These semi-logarithmic calibration curves are usually arrived at by using narrow-distribution polymers of known molecular weight.

In the absence of well characterised samples of the polymer under test, the calibration curve can only be obtained by assuming that the size of the polymer in solution controls exclusion chromatography separation (i.e. it assumes a steric exclusion mechanism) and then using a known or assumed size-molecular weight relationship. Theoretical analysis (35) of the behaviour of dilute polymer solutions shows that, for monodisperse polymers, the product of intrinsic viscosity and molecular weight is proportional to the hydrodynamic volume of the polymer molecule. Therefore if hydrodynamic volume controls exclusion chromatography separation a plot of log ($[\eta]$ M) against V_r should provide a universal calibration curve valid for all polymers. This hypothesis has been established experimentally by a number of workers (36, 37). If a universal calibration curve holds, then it follows that for any two polymers having the same retention volume

$$\log M_p - \log M_s = \log [\eta_s] - \log [\eta_p] \qquad (2.7.)$$

where subscripts p and s refer to the polymer under test and the standard polymer respectively.

The right-hand side of equation (2.7.) can be determined experimentally by collecting the eluted samples from the exclusion chromatography instrument in an automatic viscometer and measuring the intrinsic viscosity of each fraction in this way.

Alternatively equation (2.7.) can be converted into a different form by using the Mark-Houwink equation

$$[\eta] = K_M M^a \qquad (2.8.)$$

where K_M and a are approximate constants for a given polymer-solvent combination.

Combining equations (2.7.) and (2.8.) gives

$$\log M_p - \frac{1 + a_s}{1 + a_p} \log M_s = \frac{1}{1 + a_p} \log \frac{K_{Ms}}{K_{Mp}} \qquad (2.9.)$$

which allows the calibration curve for an unknown polymer to be obtained from the corresponding curve for a standard, provided that K_M and a are known for both polymers in the solvent being used.

The need for a calibration curve, which is the relationship between molar mass and elution volume, could be eliminated if a detector which responded to the molar mass of the eluting polymer at any instant was used. Detectors of this type are in their early stages of development. Ouano (38) has for example described a continuous in-line viscometer which may be coupled to the exclusion chromatography instrument in series with a conventional detector, but this method is not absolute since it depends upon the calibration of the viscosity-molar mass relationship.

More recently the same author has produced a series of publications (39, 40) describing a continuous light-scattering detector using laser excitation. This technique can be made absolute but there are still very difficult experimental problems to solve.

CHAPTER 2.3.

SUPPORT MATERIALS FOR EXCLUSION CHROMATOGRAPHY

These materials, historically known as gels, may be conveniently divided up into three categories: soft, semi-rigid and rigid.

Soft-gels in the form of cross-linked dextran gels, were first described (13) in 1959 and were the first gels commercially available for exclusion chromatography (gel filtration). Other gels of this type include polyacrylamide gels, agar gels and agarose gels. The preparation of these materials have been well reviewed (41) elsewhere and I will not go into details here.

Soft-gels are lightly cross-linked structures capable of inbibing large quantities of solvent into their pores. These materials swell to many times their dry volume and their porosity is proportional to the amount of solvent inbibed. Since the degree of cross-linking of these gels is inversely related to the pore size of the resulting gel, the cross-linking density must be kept low for polymer separations. Consequently these soft gels have poor mechanical stability, which deteriorates as pore size increases, and they can only be used at low pressures (gravity feed) with slow eluent flow rates. For this reason they tend to be more usable with small molecules and are only suitable for use with aqueous solvents.

Commercially these materials are available under the trade names of Sephadex, Bio Gel and Sepharose. The preparation and properties of these commercially available materials have been well reviewed (42).

The credit for the development of semi-rigid gels is usually given to Moore (14) for the development of polystyrene gels, suitable for non-aqueous exclusion chromatography, in 1964. These materials are generally prepared by suspension polymerisation of styrene and divinylbenzene as cross-linking agent in the presence of organic dilutents which determine the pore size. Because of extensive cross-linking these gels have a smaller total pore volume and consequently are mechanically more stable than dextran gels and may be used at up to 1500 p.s.i.

These are available under the trade names of AR Gel, Bio Beads S, HSG, Shodex, Styragel, TSK Gel, Poragel, and are compatible with a wide range of organic solvents. Preparation, properties and experimental data for most of these materials have been given by Dark et al (42).

Rigid gels may be classified either as silica gels or porous glasses. In exclusion chromatography these materials offer several significant experimental advantages over organic gels. There is no swelling therefore very little conditioning time is necessary. Their rigid structure and narrow pore size distribution gives a high permeability, a constant bed volume and constant pore size regardless of the temperature or composition of the eluent, its flow-rate, ionic strength, or applied pressure. Packed columns may be regenerated or cleaned and approximate molecular weight calibration curves can be predicted from pore size distribution data.

The preparation and application of porous glass in exclusion chromatography is popularly credited to Haller (43) but credit must also be given to earlier workers (44-48). Glasses made by the Haller process are marketed under the trade name of Corning

Porous Glasses (C.P.G.). Because of the way these glasses are prepared, they have a very narrow pore size distribution with a standard deviation of approximately 5%. This leads to a relatively flat calibration curve.

A porous glass which contains a continuum of pore sizes is available as Bio-Glass.

Because the surface of porous glass contains many hydroxyl groups, it may be necessary, particularly in aqueous solution, to block these adsorption sites. This may be achieved by chemically bonding a hydrophobic non-ionic monolayer onto the surface. The only such material currently on the market is C.P.G. - Glycophase which is C.P.G. with a "glycerol" group covering the active sites on the glass.

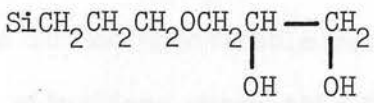

In other forms of liquid chromatography great increases in speed and resolution have been obtained by the development of column packings consisting of porous silica microspheres (49 - 56). Very high column efficiency is the result of rapid equilibrium of solute molecules in a packed bed of such small molecules. Studies have suggested that particles in the size range 5 - 10μm offer a good compromise between column efficiency and practical difficulties (50 - 55). For these particles to be of use in exclusion chromatography they must be available in a number of different pore sizes. Most of the porous silica microspheres are prepared by a process in which the particles are produced by the aggregation of colloidal silica particles to form spherical microparticles of uniform diameters (57 - 60). The particles generally consist of

an array of uniform-sized colloidal silica particles arranged in an interconnected three dimensional lattice defining a system of internal pores having controlled dimensions. The size of the pores is determined by the size of the colloidal particles used to form the microspheres and 10um microspheres have been produced in a variety of pore sizes from 40Å to 3500Å (61).

Typically the colloidal silica particles occupy about 50% of the microsphere while the remaining volume is occupied by the interconnecting pores. Ideally for exclusion chromatography we would like the particles to be 100% porous but results in this laboratory have shown that if the microspheres are more than 80% porous by volume, the solid matrix becomes mechanically unstable at pressure of around 2000 p.s.i.

As with porous glasses, the main disadvantage of these silica particles is the undesirable retention of solutes by adsorption. In situations where this is a problem, the silica particles can be exhaustively modified with organic functional groups to eliminate absorptive interactions that interfere with the desired size exclusion process.

Several workers (25, 62)found adsorption problems eliminated by exhaustively bonding various chlorosilanes onto the surface hydroxyl groups according to the general reaction.

$$\text{Si} - \text{OH} + \text{Cl} - \text{Si} - \text{R}_3 \rightarrow \text{Si} - \text{O} - \text{Si} - \text{R}_3 + \text{HCl}$$

Typical chlorosilanes used have been chlorotrimethylsilane (61, 63) and phenylchlorosilanes (64).

It has been shown that silanization effects no significant change in the molecular weight calibration plots compared to untreated particles (25, 61) and that for a totally permeating solute, no difference in plate height was found for columns of untreated or silanized particles (25). However, when these hydrophobic bonded phases are used with biological molecules such as proteins or dextrans, there is still adsorption and/or denaturation of these polymers. Various bonded groups (65, 66) which show slightly more hydrophilic properties have been used and the best results to date have been obtained by chemically bonding an "amide" or a "glycinamide" functional group (67) onto the surface.

Kirkland (68) has recently suggested the use of column packings with bimodal pores for exclusion chromatography; using 10um material containing only two discrete pore sizes, having about one decade difference in pore size. The pore sizes of these materials may be closely controlled to give minimum overlap of the individual column molecular weight calibration curves and to ensure that the linear portions of the calibration curves are essentially parallel.

CHAPTER 2.4.

SAMPLE RETENTION IN EXCLUSION CHROMATOGRAPHY

Despite the large volume of quantitative information that has been amassed, no universal consensus has been achieved concerning the dominant mechanism in exclusion chromatography separation, except for the evident fact that it is somehow effected on the basis of molecular size.

In this chapter I shall only deal with processes which determine the position of the elution peak in the chromatogram of a homogeneous substance , the question of peak broadening will be dealt with in Chapter 2.5.

It was shown in Chapter 2.2. that the elution volume, V_r, of a sample can be expressed by

$$V_r = V_o + K V_p \qquad (2.10)$$

where V_o is the void volume of the column, V_p is the pore volume in the column, K is the distribution coefficient of the solute and that if adsorption effects are absent $0 \leqslant K \leqslant 1$.

Equation (2.10) implies virtually nothing about a mechanism for sample retention, but a theory for retention must be able to be cast in this form. The meaningful content of a theory lies in what it predicts about K: how K depends upon the structure of the packing material, on solute and solvent, and on general operating parameters such as flow rate. For a model to be satisfactory it must fulfil two conditions: the physical processes which the model describes must be realistic and secondly, the predicted values for K must be in close agreement with experimental results. The main theories that have been put forward can be

conveniently considered under three headings: equilibrium models, diffusion models and flow models.

2.4.1. Equilibrium Models

The equilibrium theory is both practically and conceptionally the easiest to consider. We assume that the elution volume of a molecule in solution is determined by the equilibrium partitioning between the interstitial volume and the pore volume. Thus K is just an equilibrium constant, the ratio of solute concentration inside to outside the pores. This theory is attractive for two reasons: firstly, equilibrium calculations are inherently easier than non-equilibrium ones and secondly, equilibrium must be a limiting condition for actual behaviour.

In this model it is assumed that the standard free energy change for transporting a macromolecule from the interstitial space to the interior of a micropore is entirely due to the entropy change connected with a constraint imposed upon the macromolecule by the presence of the rigid, impenetrable barrier defining the pores and that if there are any other entropy contributions or enthalpy changes, (interaction between solute and gel), these are negligible in comparison with the entropy change associated with steric hinderence.

The equilibrium constant (or exclusion coefficient), K, may therefore be obtained from the ratio of the partition functions for the two states in question (69): the liquid in the micropores and the bulk liquid

$$K = \frac{q \text{ pores}}{q \text{ bulk}} \qquad (2.11.)$$

where q_{pores} and q_{bulk} are the respective partition functions. Equation (2.11.) is an absolute definition of K. The difficulty in evaluating K by this equation arises from the difficulty of reasonably characterising the experimental system and at the same time keeping the mathematics (involved in evaluating the partition functions) within reasonable limits of complexity.

Many model systems and experical rules have been used to obtain equations for the dependence of the partition coefficient on molecular and pore size dimensions (70). The theoretical models have generally been limited to spherical molecules and simple pore geometries. (Some of these are considered in more detail in Chapter 4).

In the first rigorous treatment of such a model, Porath treated an equivalent spherical molecule in conical pores (13). He recognised that the volume available to a penetrating molecule was less than that of the pore because of the finite molecular radius. A different pore network was treated by Laurent and Killander (71) to determine the partitioning of a sphere in a network of random rods.

Cassassa (72) calculated the equilibrium distribution of flexible polymer chains between the interstitial volume and the pore volume for simple voids (spheres, slabs and cylinders) and compared these with experimental results (73). The fit was not very good and predicted a large dependence on pore shape. A shape factor (74) was introduced into this theory to force these curves together and to give a closer fit with the experimental data but it was admitted that the good agreement between theory and experiment may well be coincidental because of possible large uncertainties in the experimental data used and the inclusion of

the empirical shape factor. However, it was concluded (72, 74) that for linear and branched flexible chain molecules the permeation depends upon the hydrodynamic volume of the polymer molecule as suggested by Benoit et al (36, 37). Giddings (69) carried these arguments one step forward by considering not only spherical molecules (or their spherical equivalent), but also exclusion of rigid particles of various shapes from simple voids. They considered not merely exclusion from cartesian space (which is only possible for an isotropically spherical particle whose configuration is completely specified by the locus of a single point) but rather exclusion from a part of the configuration space of all coordinates of the particle. This is probably the most fundamental publication on this subject to date but unfortunately there is no attempt to compare the theoretical results with that of experimental data. However, despite the large amount of work carried out with complex macromolecular shapes and simple pore structures, the best results have been obtained using models based on using spherical molecules and more complex and realistic pore models (see Chapter 4).

Van Kreveld and Van den Hoed (75) used the random spheres model (27) to build up a model for the matrix which was composed of ramdomly arranged overlapping spheres of equal radius. The polymer molecules were considered to be spheres of radius 0.89 times their mean hydraulic radius which was then related to the molecular weight of the polymer for the polymer-solvent system under study. By measuring the pore size and pore volume of the experimental material they were able to predict the experimental calibration curve, for polystyrene samples eluted from Porasil, within the limits of accuracy of the experimental data using no further adjustable parameters.

2.4.2. Diffusion Models

The credit for a diffusion controlled separation mechanism for exclusion chromatography is given to Ackers (76). In this treatment, the gel phase is considered to consist of cylindrical pores in which free diffusion of the molecules is hindered sterically and by friction. The steric hinderence is the same as that discussed in Chapter 2.4.1. However, Ackers argues that if a molecule does enter a pore, it encounters increased hydrodynamic frictional resistance to motion and therefore has a lower diffusion coefficient.

Using a previously derived equation (77) linking the equivalent Stoke's radius of macromolecules, r, to the effective radius of the pore, R, he arrives at

$$K = (1 - \frac{r}{R})^2 \left[1 - 2.104(\frac{r}{R}) + 2.09(\frac{r}{R})^3 - 0.95(\frac{r}{R})^5\right] \quad (2.12.)$$

In this equation, the first term represents the equilibrium constant for partitioning of rigid spheres of radius, r, between cylindrical pores of radius, R, and a macroscopic solution phase (see Chapter 4). It is claimed that the second term arises from a restricted diffusion rate, but if so it would necessarily contain a flow rate dependence so that it would equal unity at the limit of slow flow. Equation (2.12.) in fact is a purely geometrical equation and therefore must apply to a specific geometric model. In the sense that it accommodates restricted diffusion the restriction relates the regions into which diffusion is restricted or barred not the rate at which diffusion occurs into such regions. Thus I do not consider this to be a diffusion model and suggest that equation (2.12.) represents the result for

steric exclusion of molecules from cylindrical pores with a geometrical correction factor.

In a derivation by Yau and Malone (78) exclusion chromatography separation is attributed to lateral diffusion in the column and they produce an expression for the distribution coefficient which is a complicated function of the diffusion coefficient within the pores and the flow rate. Through arbitrary adjustment of parameters they can enable this theory to conform fairly well to typical exclusion chromatography data. This theory breaks down at very low flow rates when it predicts that the distribution coefficient, K, approaches unity, thus, in succeeding papers, Yau et al (79, 80) combine this diffusion theory with the equilibrium theory by writing K as a product of the equilibrium K and the distribution coefficient given by the diffusion model.

2.4.3. Flow Models

Detailed theories on separation by mass flow effects have been put forward (81, 82, 83) and have been well reviewed by Cassassa (84). The results obtained are analagous to those of Ackers (76) which again show no flow rate dependence and I believe that these are essentially the same as the steric exclusion models.

2.4.4. Summary

Considering all the data and models discussed above to account for the mechanism of separation in exclusion chromatography I consider that the equilibrium theory of steric exclusion is the dominant mechanism. The evidence in favour of this mechanism is very strong:

(1) Using the principle of steric exclusion and a realistic pore model, the theoretically derived pore size, pore volume and calibration curves give good agreement with experimental data without the need to arbitrarily adjust parameters (75).

(2) On fundamental theoretical grounds, a large departure from equilibrium is totally incompatible with the narrow symmetrical peaks obtainable from a good exclusion chromatography system (see Chapter 5). If there are severe departures from equilibrium, peaks according to theory will be both wide and unsymmetrical as discussed in Chapter 2.5.2.

(3) Peak maximum in exclusion chromatography columns show no dependence upon flow rate (79).

(4) Using narrow-distribution polystyrenes and porous glass beads excellent agreement was found between the results of static and elution experiments (79). However, Ackers (76) studied the behaviour of proteins on organic gels and found that for tightly cross-linked materials the results for static and elution studies were in good agreement but large differences appeared with very highly swollen loosely cross-linked gels.

All this evidence suggests that elution under ordinary conditions with a comparatively rigid pore structure is governed by the equilibrium theory of steric exclusion.

Since most of the evidence is in favour of universal calibration on the basis of the hydrodynamic volume, there should be little or no change in the theoretically predicted calibration curves by introducing complex functions to describe

the molecular shape. This, coupled with the excellent work of Van Kreveld (75) suggests, that in order to predict molecular weight dependence upon elution volume for a column, we should be concentrating on producing more realistic representations of the pore model and treating the macromolecule as an equivalent sphere.

CHAPTER 2.5.

PEAK BROADENING IN EXCLUSION CHROMATOGRAPHY

When a packet of molecules of a monodisperse substance is passed through a chromatographic column the individual molecules are eluted with a distribution of elution volumes, so the initially compact packet emerges as a band more or less spread out. Such broadening phenomena is well known but the detailed mechanisms which cause such broadening are so complex that they are still not totally understood.

Knowledge of the variables which cause this broadening is essential for the optimisation of chromatographic conditions, and for the design of improved separation systems.

What is required is a mathematical model of idealized physical processes, closely related to the dispersion processes occurring on a molecular scale, that allows us to predict broadening behaviour.

Peak broadening can result from (a) non-linear distribution isotherms which are not relevent here and will not be considered, (b) polydispersity of a polymer which is a thermodynamic effect and is discussed in Chapter 5, (c) extra-column effects discussed in Chapter 2.5.3. and (d) kinetic effects.

The kinetic broadening in a chromatographic column may be described either on the basis (1) that the near equilibrium assumption holds i.e. there is a large number of transitions during passage through the column or (2) that the near equilibrium assumption does not hold i.e. there is only a relatively small number of transitions during passage through the column. Only case (1) is capable of rigorous theoretical treatment and case (2)

which results in broad elution peaks will be considered qualitatively as a breakdown of the near-equilibrium theory.

2.5.1. Near-Equilibrium Theory

As discussed in Section 1.2.2., this theory was first described by Martin and Synge (3). In this so called "plate model" band broadening is characterised by the plate height, H, and the number of theoretical plates, N.

$$H = L\left(\frac{\sigma_v}{V_r}\right)^2 \qquad (2.13.)$$

$$N = \frac{L}{H} = \left(\frac{V_r}{\sigma_v}\right)^2 \qquad (2.14)$$

where L is the length of the column, σ_v is the standard deviation of the peak in volume units and V_r the elution volume.

In general, the plate height, H, may be expressed in the form

$$H = 2\frac{Dn}{u} + (\text{a mass transfer contrib.}) \qquad (2.15.)$$

where D_m is an overall dispersion number and u is the mobile phase velocity.

Using this equation Van Deemter (85) assumed that the dispersion number was composed of a longitudinal molecular-diffusion term and an eddy diffusion term and that the mass-transfer term was a linear function of velocity. This resulted in an overall plate height of the general form

$$H = A + \frac{B}{u} + Cu \qquad (2.16)$$

where the first term accounts for eddy diffusion, the second for

molecular diffusion and the third for mass transfer resistances in the stationary and mobile phases. Using the random walk model, Giddings (86) analysed the behaviour of individual solute molecules as they progress through the chromatographic bed. These molecules are moving in a series of random steps. Each chromatographic process has a mean characteristic step length, l, and during the elution of the solute there are n such steps. When a molecule starts moving in random fashion with a series of n steps, each of length, l, there is a high probability that, after a certain time, the molecule will no longer be at its starting point, but rather some distance away from it. If a large number of such molecules start moving randomly, then, after a certain time they will be distributed around the starting point. This distribution may be represented by its variance

$$\sigma^2 = l^2 n \qquad (2.17.)$$

or by its standard deviation

$$\sigma = \sqrt{l^2 n} \qquad (2.18.)$$

In this model, each process occurring in the column has its own value of n and l. Giddings identified these processes to be molecular diffusion, resistance to mass transfer in the stationary phase, resistance to mass transfer in the mobile phase and eddy diffusion, and calculated n and l for each of them.

To combine the effects of these various contributions to peak broadening, Giddings used a fundamental law of statistics, that if several processes contributed to the peak spreading and if these processes are random and independent of each other, then the variance of the peak will be the sum of the variances associated

with the individual processes.

$$\sigma^2_{v(total)} = \sigma_1^2 + \sigma_2^2 + \sigma_3^2 + \ldots \quad (2.19)$$

A rigorous mathematical treatment of this model is given (86) which leads, assuming independence of the four processes, to a plate height expression which may be written in the following general form

$$H = A + \frac{B}{u} + (C_m + C_s)u \quad (2.20.)$$

This equation is identical to the Van Deemter equation where C_m and C_s, given by equations (2.21) and (2.22.) are resistances to mass transfer in the mobile and stationary phases.

$$C_m = q_m\left(1 + \frac{\alpha k'}{1+k'}\right)^2 \frac{d_p^2}{D_m} \quad (2.21)$$

$$C_s = q_s \frac{k''}{(1+k'')^2} \frac{d_p^2}{D_s} \quad (2.22)$$

where q_m, q_s and α are geometrical factors and D_m and D_s are diffusion coefficients in the mobile and stationary phases. Appendix 1 gives a derivation of equation (2.22.) and calculation of q_s for a porous spherical material.

Giddings later pointed out, however, that the eddy diffusion processes and resistances to mass transfer in the mobile phase cannot be considered as independent but cooperate in reducing dispersion. Giddings called processes of this kind "coupled" and showed that equation (2.20) should accordingly be written in

the form

$$H = \frac{B}{u} + C_s u + \sum_i \frac{1}{\frac{1}{A_i} + \frac{1}{C_{mi} u}} \qquad (2.23.)$$

Giddings and Mallik (87) applied equation (2.23.) specifically to the theory of zone broadening in exclusion chromatography defining the parameters A_i, B, C_s and C_{mi} in the context of the exclusion chromatography process.

The final form of the equation proposed is -

$$H = \frac{4D_m(1+k'')}{3u} + \frac{1}{20}\frac{k''}{(1+k'')^2}\frac{d_p^2}{D_m}u + \sum_i \frac{1}{\frac{1}{2\lambda_i d_p} + \frac{D_m}{w_i d_p^2 u}} \qquad (2.24.)$$

where λ_i and w_i are geometrical factors of order unity.

In order to relate plate heights under different operating conditions, Giddings (88) introduced two dimensionless parameters, the reduced plate height

$$h = \frac{H}{d_p} \qquad (2.25.)$$

and the reduced velocity

$$\nu = \frac{d_p u}{D_m} \qquad (2.26.)$$

Using these parameters equation (2.24.) reduced to

$$h = \frac{4(1+k'')}{3} + \frac{1}{20}\frac{k''}{(1+k'')^2} + \sum_i \frac{1}{\frac{1}{2\lambda_i} + \frac{1}{w_i \nu}} \qquad (2.27.)$$

Written in this form (h, ν) curves are expected to be independent of d_p and D_m and experimental evidence for the use of these reduced parameters has been extensively published (89, 90, 91).

Unfortunately equation (2.23.) does not correctly reproduce experimental data which is probably due to the uncertainty in the final term of this equation. So far the "best fit" achieved has been by the use of an empirical equation (8) which has been shown to be a good fit to experimental data over a wide range of velocities in both liquid chromatography and gas chromatography.

This equation may be written as

$$h = \frac{B'}{\nu} + A'\nu^{n} + C'\nu \qquad (2.28.)$$

which is identical to the reduced form of equation (2.23.) with the empirical term $A'\nu^{n}$ replacing the coupled term in the Giddings equation to describe the contribution from the complex flow in a packed column. Typically the exponent n is around 0.33. At high velocities and over a limited range of reduced velocity equation (2.28.) can be approximated by

$$h = D'\nu^{n'} \qquad (2.29.)$$

which is the reduced form of Snyder's (92) equation.

$$H = D\,u^{n} \qquad (2.30.)$$

where D' and D are constants and n lies between 0 and 1.0. Equation (2.29.) generally fits the experimental data over a ten-fold range of reduced velocity, but over a wider range, n increases with velocity. The main advantage of Snyder's equation is that it leads to explicit expressions for optimising performance but it fails to produce the minimum in the plate height curve which is well established in liquid chromatography and this is the velocity at which one ought to operate (49).

In exclusion chromatography of polymers, under typical operating conditions, we are working in the reduced velocity range of about 100 - 1000 and equations (2.23.) and (2.28.) may be very well approximated by

$$h = C_s' \nu$$

$$\text{where} \qquad C_s' = q_s \frac{k''}{(1+k'')^2} \qquad (2.31.)$$

Another approach (94,95) has been put forward in which the Van Deemter theory is extended by incorporating an additional term to account for velocity-profile effects caused by a nonuniform velocity across the column cross section. A nonuniform velocity profile causes peak broadening, the magnitude of which is primarily determined by radial diffusion.

This term is given by (96)

$$\text{Velocity - profile effect} = h_v R_c^2 u^2 / \bar{D}_r \qquad (2.32.)$$

where h_v is a velocity-profile constant, R_c is the column radius and $\bar{D}_r$ is an average radial diffusivity. This radial diffusivity is determined by radial gradients existing within the column which come about from both molecular-diffusion and eddy-diffusion processes. This leads to an overall equation for the plate height of the general form (95)

$$H = A + \frac{B}{u} + \frac{4h_v R_c^2}{A + \frac{B}{u}} + Cu \qquad (2.33.)$$

where all the terms are as previously defined. This again leads to a coupling term similar to that proposed by Giddings but the

biggest drawback for utilizing this model has been the difficulty in evaluating the velocity profile constant h_v.

Again note that at very high reduced velocities equation (2.33.) may be approximated by equation (2.30).

An independent but equivalent theory to describe broadening in liquid chromatography has recently been developed by Huber (6). The overall expression for the plate height is again expressed as a sum of individual contributions which include mixing arising from diffusion in the mobile phase, mining due to convection in the mobile phase and contributions from mass transfer effects in the mobile and stationary phases. In formulating his theory Huber takes into account the specific volume fractions in which each broadening process occurs and the overall expression may be written in the form

$$H = \frac{a_1 D_m}{u} + \frac{a_2 d_p}{1 + a_3\left(\frac{D_m}{u d_p}\right)^{\frac{1}{2}}} + a_4\left(\frac{k''}{1+k''}\right)^2 \frac{d_p^{3/2}}{D_m^{\frac{2}{3}}} u^{\frac{1}{2}} + a_5 \frac{k''}{(1+k'')^2} \frac{d_p^2}{D_s} u \qquad (2.34.)$$

The first and the fourth terms of equation (2.34.) are identically equal to the B- and C-terms given earlier, while the second and third terms are the equivalent of the coupled term of Giddings and the empirical term of Knox.

The general shape of the reduced plate height versus reduced velocity curve for all these theories is outlined in Figure 4 and it is found experimentally that for an efficient column, the curve should show a minimum of $h \sim 2\text{-}3$ at a reduced velocity of $\nu \sim 5$.

2.5.2. Non-Equilibrium Theory

The outstanding piece of evidence in favour of the near equilibrium theory of chromatography is the narrow peaks obtainable when using a good system, but it is useful to consider, at least qualitatively, the consequences of the breakdown of the near-equilibrium theory. It is not difficult to show that non-equilibrium in a chromatographic column leads to peak broadening.

If we examine the concentration distribution within a chromatographic band it is clear that there cannot be equilibration at all points in a band and that there must be departures from equilibrium on the two sides of the peak maximum. Figure 5 illustrates this point where, as a result of the flow of mobile phase, the concentration profile of solute in the flowing zone runs slightly ahead of the corresponding zone in the stationary phase. This tendency for the two profiles to be pulled apart by the flow of mobile phase against stationary phase is countered by the equilibration process which continually tries to bring the concentrations in the mobile and stationary phases towards their equilibrium values.

The displacement of the two bands δZ is therefore given by

$$\delta Z = u_o t \qquad (2.35.)$$

where u_o is the linear velocity of the mobile zone and t is the relaxation time for equilibration.

At the centre of the band the ratio $\frac{q_s}{q_m}$ is equal to the equilibrium distribution ratio $\frac{q_{s(eq)}}{q_{m(eq)}}$ which is equal to k''_{eq}.

Upstream of the centre $\frac{q_s}{q_m}$ is greater than $\frac{q_{s(eq)}}{q_{m(eq)}}$, while downstream $\frac{q_s}{q_m}$ is less than $\frac{q_{s(eq)}}{q_{m(eq)}}$.

Hence

$$k''_{upstream} > k''_{eq} > k''_{downstream} \qquad (2.36.)$$

and since the velocity of a particular slice of the band is given by

$$u_{slice} = \frac{u_o}{1+k''} \qquad (2.37.)$$

we have that

$$u_{upstream} < u_{centre} < u_{downstream} \qquad (2.38.)$$

Thus clearly, as the band moves along the column, the wings of the band move outwards at a rate dependent on the relaxation time for equilibration.

The more severe the non-equilibrium the greater the rate of band spreading. Any theory which takes as a major postulate that slow diffusion, causing lack of equilibrium, is the major cause of differential migration rates must inevitably predict very wide peaks. Indeed if taken to a sufficiently extreme point that genuine differences in retention are produced only by differences in the rate of equilibration then peaks are predicted to be highly unsymmetrical. This form of such peaks has been used by Van Kreveld and Van den Hoed specifically to measure mass transfer coefficients (97). They used such high elution velocities with large particles (reduced velocity around 10^5) that time of equilibration was comparable to the time of elution from the column.

2.5.3. Extra Column Band Broadening

The treatments of band broadening discussed in Chapters 2.5.1. and 2.5.2. are only concerned with the dispersion of solutes as they pass through the column, but to adequately describe the complete band width, for a monodisperse sample, recorded by the detector it is necessary to modify these theories by adding terms which describe broadening that occurs outside the column. This broadening, usually termed the extra-column band broadening, arises from the appreciable volumes of the injected sample and of the various elements in the chromatographic apparatus: injection system, connecting lines, column end-fittings and detector cell. These dispersion contributions are independent of the kinetic broadening and we may write the total plate height as recorded by the detector (for a monodisperse sample) as

$$H_{total} = H_{col} + H_{app} \qquad (2.39.)$$

or in terms of the variance of the peak

$$\sigma^2_{total} = \sigma^2_{col} + \sigma^2_{app} \qquad (2.40.)$$

where σ^2_{col} is the peak variance produced by the column alone and σ^2_{app} the peak variance due to the apparatus. σ^2_{app} may be obtained experimentally by connecting the injector directly to the detector, replacing the column by a fitting where the packed section is missing. For the system used in this work, the peak width (measured as four standard deviations) determined in this way was between 30 and 40ul.

For a typical column used in this work 100mm x 7mm producing 7000 theoretical plates, typical peak widths are of the order of

80ul, it is easily seen that the contribution to peak spreading due to the extra column dispersion processes is only about 10%. It is essential in high performance exclusion chromatography that the components of the apparatus are well designed to keep the extra column band spreading around or below this level.

2.5.4. Peak Capacity Factor

From equation (1.25.) we see that the peak capacity factor in exclusion chromatography is given by

$$n = 1 + 0.25\, N^{\frac{1}{2}} \ln \left(\frac{V_o + V_p}{V_o} \right) \qquad (2.41.)$$

Thus to increase the number of resolvable components we can either increase the ratio $\frac{V_o + V_p}{V_o}$ or increase the column efficienty. Unfortunately, as was shown in Chapter 2.3., the ratio $\frac{V_o + V_p}{V_o}$ cannot exceed about 2.5 unless the mechanical stability of the gel is sacrificed and hence equation (2.41.) may be approximated by

$$n \sim 1 + 0.2\, N^{\frac{1}{2}} \qquad (2.42.)$$

Since a typical value of N for a good column is 10,000, the peak capacity in exclusion chromatography is in the region of 20.

CHAPTER 3

EQUIPMENT, EXPERIMENTAL PROCEDURE AND CALCULATION OF RESULTS.

3.1. Equipment

3.1.1. Pumps

3.1.2. Columns and Injectors

3.1.3. Detector

3.2. Column Packing, Materials and Experimental Procedure

3.3. Calculation of Results

Chapter 3.1.

EQUIPMENT

Figure 6 shows a schematic outline of the equipment used for all the chromatography carried out during the course of this work. The main features are described in detail below. Prior to use, the solvent was degassed either by reflux or by vacuum degas and then filtered by use of "Watman No. 1" filter paper to remove any large particles of foreign matter. Smaller particles were removed by inserting a 7um porosity stainless steel Nupro filter between the reservoir and the pump.

3.1.1. Pumps

Orlita DMP-AE 10.4 (Orlita, Giessen). This pump (Figure 7) operates on the counter-plunger system. A motor driven plunger reciprocates in and out of an oil filled cavity, thus creating a volume variation that is translated via the metal diaphram to the valve chamber containing the pumping liquid. The volume of liquid pumped during each cycle depends upon the swept volume of the plunger which is controlled by a regulating plunger positioned opposite the working plunger. The regulating plunger is spring-loaded and its position is determined by an adjustable stop. As the working plunger moves out of the oil cavity the regulating plunger follows, remaining in contact with it until it is retained by the stop. During the rest of the stroke the working plunger sucks up the quantity of pumping liquid through the inlet valve. On the return pressure stroke this volume is forced through the outlet valve until the working plunger again

meets the regulating plunger pushing it back against the spring and completing the cycle. This pump is capable of delivering solvent at continuously variable flow rates from 0 - 10mls per minute against back pressures of up to 7000 p.s.i. In general this pump performed satisfactorily, although at back pressures less than about 50 p.s.i. the long term flow rate tended to vary. A further disadvantage common to all pumps of this kind, is that the mode of pumping gives rise to pressure pulsing which may not be compatible with the detection system. This pulsing was adequately damped at all flow rates by using a Bourdon type pressure gauge (Negretti and Zambra, London) in series with an air-filled snubber. The snubber is a 500 x 6mm stainless steel tube capped at one end. The air in the tube is compressed as the pressure increases during the forward stroke and expands during the refil stroke. One problem with this type of pulse damper is that it introduces a poorly swept fluid-filled chamber between the pump and injector which makes eluent change a lengthy process.

In order to work at low flow rates (back pressures of less than 50 p.s.i.) a second pumping system was used. This consisted of eluent (in a pressurized reservoir) being forced through the column at a stabilized rate by nitrogen maintained at constant pressure by a pressure regulator (Negretti and Zambra, London). Using this system there was small pressure and hence flow rate fluctuations and to eliminate these it was found necessary to insert a Cartesian manostat (Edwards High Vacuum, Crawley, Sussex) in series with the pressure regulator. A mercury manometer was used to record the pressure and by using different

pressures of nitrogen this system was used to cover flow rates of 0.003mls/min - 0.5mls/min.

3.1.2. Columns and Injectors

The columns and injectors (Figures 8 and 9) were designed by the Wolfson Liquid Chromatography Unit, Edinburgh University. These are commercially available in slightly modified design from Shandon Southern Products Limited, Runcorn.

The columns were constructed from lengths of 7mm inside diameter Appollo Liquid Chromatography tube with mirror finish bore. End fittings were constructed from stainless steel (EN58J) and vacuum braised to withstand pressures of up to 10,000 p.s.i. The top of the column packing is protected by a stainless steel mesh which prevents disturbance of the packing during injection or maintenance, and also by the bed of glass beads which traps septum fragments. The column bottom is fitted with a zero dead volume connection which carries a stainless steel mesh to retain the packing material. This lower fitting terminates in 0.25mm (10 thou) bore tube which can be coupled by standard zero dead volume fittings to the detector cell.

The injector is again engineered from stainless steel (EN58J) and is specially designed with a needle guide which controls accurately both the position and penetration of the syringe needle. The geometry of the injector ensures curtain flow of mobile phase around and down the syringe needle so that the sample is applied as a point injection at the top of the packing material.

All injections were carried out using graduated syringes (Scientific Glass Engineering Ltd., 657 North Circular Road, London) fitted with dome-tipped needles which enhances the accuracy of the injection. Both injector and syringe are capable of withstanding injections at pressures up to 2000 p.s.i.

3.1.3. Detector

Cecil 212 Photometer (Cecil Instruments Ltd., Cambridge). This single beam instrument (Figure 10) may be operated at wavelengths between 220 and 400nm. The beam generated at the deuterium lamp source is attenuated before monochromation by a series of mirrors, collinator and grating. The beam passes through the sample cell and focuses on the photocell. Wavelength accuracy is specified at better than 2nm and reproducibility less than 0.5nm. Highest full scale sensitivity is 0.01 AU and zero stability better than $\pm$ 0.1% short term.

Flow cells (Figure 11) for use in the Cecil Photometer were again designed in the Wolfson Liquid Chromatography Unit, Edinburgh University. Cell volumes were either 5 or 8mm^3. To calculate the extra-column dispersion, the injector and detector were coupled together and the peak volume measured for an injection. Typical values for the peak-volume tend to lie in the range 30 - 50mm^3. To consistently keep the peak volume due to extra-column effects at the lower end of this range it is necessary to use zero dead volume fittings and short pieces of narrow bore tubing (50mm x 0.25mm). For a typical column (100 x 7mm) giving 7000 plates, peak volumes would be approximately 80mm^3 and therefore it is imperitive that this extra-column dispersion is kept as low as possible.

"Swagelok" stainless steel unions and 1.6mm (1/16") or 3.2mm (1/8") outside diameter stainless steel tubing were used to connect the component parts of the apparatus. Elution chromatograms were recorded by a "Servoscribe" potentiometric recorder.

CHAPTER 3.2.

COLUMN PACKING, MATERIALS AND EXPERIMENTAL PROCEDURE

All columns were packed with one of two porous spherical microparticulate silicas - Hypersil (Shandon Southern Products Ltd., Runcorn) or SG60F (experimental batch supplied by Materials Preparation Unit, AERE, Harwell). Material specifications are given in Table 3.1 and electron micrographs of Hypersil are shown in the Appendix.

Table 3.1.

Material	Mean particle size / um	Surface Area / m^2g^{-1}	Pore Volume/cm^3g^{-1}	Mean pore diameter/A^o
Hypersil	6 [a]	200[c]	0.68[b]	100[c]
SG60F	7.5[c]	100[c]	1.76[c]	600[c]

Notes a: measured from electron micrographs

b: calculated from elution data

c: quoted by supplier

All columns were slurry packed and a variety of pumping systems and slurry media were used but the most consistent results (especially with columns longer than 120mm) were obtained by using the method of Bristow (98).

The packing apparatus (Figure 12) consisted of a Haskel Pressure Intensifier (Haskel Engineering and Supply Co., Burbank, California, U.S.) driven by gas pressure from an air cylinder, and a slurry reservoir of volume, 40mls. The pump was charged

with methanol and pressurized to 3000 p.s.i. with the release valve shut. A slurry of Hypersil in 40mls of methanol was shaken, dispersed using an ultra-sonic bath and poured into the slurry reservoir with a funnel. The column was quickly attached, pointing upwards, and the flow started by opening the release valve. The column was judged packed when the flow-rate became constant, usually after about 100mls. of methanol had passed. The packing equipment is then dismantled and the column connected to the chromatographic pump, via the injection head, where it is flushed with the eluent to be used at 10mls/min for approximately thirty minutes. This allows for any settling of the chromatographic bed which may occur during use. Excess column packing is then removed from the column top by a microspatula until the top of the packed bed is flush with the mesh ledge. The top mesh, column top insert and ballotini glass beads can now be inserted and the injection head replaced. With the column outlet now connected to the detector, the system can be conditioned by passing eluent at approximately 5mls/min and a steady detector base-line is indicative of satisfactory conditioning. The column is now ready for use. When a change of eluent is required, the last conditioning step must be repeated and it may also speed up the process if the eluent contained in the pulse damper and pressure gauge is manually removed.

After prolonged use the column efficiency may decrease and this can usually be restored by cleaning out the top 2mm of the column packing with a microspatula, top-up the column with fresh packing material and completing the packing procedure from when the column is detached from the packing pump. The reason for this decrease in efficiency is usually due to fine dust

particles (which enter the system either from the mobile phase or the sample injection) accumulating at the top of the column.

The choice of eluent in other modes of liquid chromatography greatly affects selectivity, but in exclusion chromatography the affect is minimal if it fulfils the following requirements: a) it must be a good solvent for the sample at ambient temperatures, b) it must not be reactive towards the column packing material but must be capable of "wetting" it, c) it must be compatible with the ultra-violet photometric detector used.

Kirkland (25) has shown the effect of different solvents on the calibration curves of polystyrene and concludes that the slopes of these calibration curves are identical but the intercepts are different due to changes in the hydrodynamic volume of the polymers in different solvents. Since the choice of solvent is not critical except with regard to the three points given above, all the exclusion chromatography was carried out with dichloromethane rather than the commonly used T.H.F. because there was a local supply of chromatographic grade dichloromethane available.

The polystyrene standards used were obtained from Waters Associates Ltd., and the specifications provided for these materials is given in Table 3.2.

Table 3.2.

Sample	Molecular weight[a]	M_w[a]	M_n[a]	Diffusion coefficient/ 10^{-8} $cm^2 s^{-1}$[b]
Benzene	78	-	-	3441
m-dinitrobenzene	168	-	-	2761
PS 2K	-	2100	1950	486
PS 3K	2900	-	-	392
PS 4K	-	4000	3100	330
PS 10K	-	10,000	9600	190
PS 20K	-	20,800	20,200	123
PS 33K	-	33,000	36,000	93
PS 111K	-	111,000	111,000	40
PS 200K	-	200,000	193,000	32
PS 470K	470,000	-	-	19
PS 2700K	2,700,000	-	-	7

Notes: a: quoted by supplier

b: calculated from Wilke-Chang equation

Columns packed as described above are now ready for use. To give an indication of the column efficiency, the flow rate was set to give a reduced velocity for a totally permeating sample (benzene) of between 1 and 5 (approx. 0.1cm s^{-1}) and the mobile phase flow velocity given time to stabilize. A 0.1% (1mg/ml) solution of benzene was made up in the eluent and injected directly through a rubber septum, into the top of the column packing by glass microsyringe. Sample size was generally 1 - 5ul keeping the total load on the column below 5ug to avoid overloading (see Chapter 6). Reduced plate height was calculated for this totally permeating solute and if this value was less than 4 particle diameters, the column was deemed satisfactory. (Values of around 2 particle diameters are expected for a 10cm column). The mobile phase linear velocity was determined by injecting a sample that was totally excluded from the packing material in the column. (In this case a polystyrene of average molecular weight of 2,700,000). This solute therefore elutes at the mean velocity of the mobile phase.

Reduced calibration curves (log M_w v K) were plotted for each column using the complete set of standard polystyrenes and a totally permeating solute (benzene) as a further check on column reproducibility.

CHAPTER 3.3.

CALCULATION OF RESULTS

The various experimentally derived parameters are defined below

a) The plate height, H, is given by

$$H = \frac{L}{5.54} \left(\frac{w_{\frac{1}{2}}}{V_r}\right)^2 \qquad (3.1.)$$

where $w_{\frac{1}{2}}$ is the half-height width of the Gaussian peak, V_r is the elution volume of the peak maximum and L is the column length.

b) The reduced plate height, h, given by

$$h = \frac{H}{d_p} = \frac{L}{5.54\, d_p} \left(\frac{w_{\frac{1}{2}}}{V_r}\right)^2 \qquad (3.2.)$$

where d_p is the mean particle diameter. On a typical chromatogram, the chart speed was altered so that $w_{\frac{1}{2}}$ represented 3 - 10mm and was accurately measured by use of a travelling microscope. The reduced plate height is a measure of the H.E.T.P. expressed in particle diameters.

c) The mobile phase linear velocity, u, given by

$$u = \frac{L}{t_o} \qquad (3.3.)$$

where t_o is the elution time of a totally excluded solute.

d) The reduced velocity, ν , given by

$$\nu = \frac{u d_p}{D_m} \qquad (3.4.)$$

where D_m is the diffusion coefficient of the solute in the mobile phase. The reduced velocity may be thought of as the rate of flow over a particle relative to the rate of diffusion through a particle.

e) For the purpose of this work the diffusion coefficients, D_m, were found from the Wilke-Chang equation (99) quoted below.

$$D_m = \frac{7.4 \times 10^{-8} (\psi_2 M_2)^{0.5} T}{\eta V_1^{0.6}} \qquad (3.5.)$$

where η is the viscosity of the solvent in centipoise, M_2 the molecular weight of the solvent, V_1 the molar volume of the solute in $cm^3\ mol^{-1}$ and ψ_2 an association factor which was taken to be 1.3 for dichloromethane and T is the absolute temperature. This gives D_m in units of $cm^2\ s^{-1}$.

The diffusion coefficients for the solutes used are given in Table 3.2. and are in reasonable agreement with those used by other workers using different methods of deriving D_m (97, 100).

CHAPTER 4

MODELS FOR PREDICTING CALIBRATION CURVES IN EXCLUSION CHROMATOGRAPHY

4.1. Introduction

4.2. Calculation of Exclusion Curves for Various Pore Geometries

- 4.2.1. Infinite Parallel Plate
- 4.2.2. Infinite Cylinder
- 4.2.3. Spheres
- 4.2.4. Inverse Cylinder
- 4.2.5. Inverse Sphere

4.3. Results and Discussion

CHAPTER 4.1.

INTRODUCTION

In Chapter 2.4., the various theories for retention in exclusion chromatography have been discussed in detail and I concluded that, on the basis of the evidence available, elution under ordinary conditions with a comparatively rigid pore structure is governed by the equilibrium theory of steric exclusion.

Thus if the elution volume is written in the form

$$V_r = V_o + KV_p \qquad (4.1.)$$

where V_o is the volume outside the pores (the interstitial volume) and V_p is the total pore volume within the column, then K is an equilibrium constant, the ratio of solute concentration inside to outside the pores. The equilibrium constant (or exclusion coefficient), K, may be related to molecular parameters by using statistical mechanics and is given by the ratio of the partition functions for the two states in question (69), the liquid in the micropores and the bulk liquid.

$$K = \frac{q_{pores}}{q_{bulk}} \qquad (4.2.)$$

where q_{pores} and q_{bulk} are the respective partition functions. I will further assume that the macromolecules can be approximated as spheres, the radius of which may be related to the molecular weight of the macromolecule by equation 4.3.

$$r = a M^b \qquad (4.3.)$$

where a and b are constants for a particular solute-solvent system.

Using classical partition functions, equation 4.2. may be expanded in terms of the ratio of two configuration integrals.

$$K = \frac{\frac{1}{h^3}\iiint \exp\left(-\frac{Ep}{kT}\right) d\underline{r}\, d\underline{\Psi}\, d\underline{\lambda}}{\frac{1}{h^3}\iiint \exp\left(-\frac{Eb}{kT}\right) d\underline{r}\, d\underline{\Psi}\, d\underline{\lambda}} \qquad (4.4.)$$

where E is the energy of the system and the generalized coordinates $\underline{r}$, $\underline{\Psi}$ and $\underline{\lambda}$ describe molecular position, orientation and conformation respectively.

If we restrict ourselves to dealing with only spherical molecules, then E is a function only of position and equation 4.4. reduces to

$$K = \frac{\int \exp\left(-\frac{Ep(\underline{r})}{kT}\right) d\underline{r}}{\int \exp\left(-\frac{Eb(\underline{r})}{kT}\right) d\underline{r}} \qquad (4.5.)$$

In the bulk phase, the energy is independent of position if we assume that the dimensions of an interstitial pore is large compared to the molecular size and therefore the denominator reduces to $\int d\underline{r}$.

Since the size of the micropores are of the same order of magnitude as the macromolecules there will be a potential arising from interaction between the macromolecule and the pore wall. The simplest potential to assume is the "hard sphere" potential which requires that $Ep(\underline{r}) = \infty$ if the macromolecule and the pore wall overlap and $Ep(\underline{r}) = 0$ otherwise.

Thus we have that

$$K = \frac{\int \exp\left(\frac{-Ep(\underline{r})}{kT}\right) d\underline{r}}{\int d\underline{r}} \qquad (4.6.)$$

The Boltzmann factor in the numerator may be replaced by a probability function $P(\underline{r})$ which gives the probability that a molecule is found at position $\underline{r}$. Using the boundary conditions of a hard-sphere potential we see that

$P(\underline{r}) = 0$ if the molecule overlaps the pore wall, and
$P(\underline{r}) = 1$ otherwise.

and the equilibrium constant may be written as

$$K = \frac{\int P(\underline{r})\, dr}{\int d\underline{r}} \qquad (4.7.)$$

Figure 13 shows the implication of equation 4.7. If a surface is drawn, a distance from the pore wall equal to the molecular radius, then $P(\underline{r}) = 1$ if the centre of the molecule lies outside this surface and $P(\underline{r}) = 0$ if the centre of the molecule lies inside this surface. Thus K is the ratio of the volume free to the centre of mass of a molecule, to the total volume of the micropores.

CHAPTER 4.2.

CALCULATION OF EXCLUSION CURVES FOR VARIOUS PORE GEOMETRIES

In the previous section I have shown that the equilibrium constant (exclusion coefficient), K, is given by the ratio of the volume available to a molecule to the total volume of the pore and this construction can be used to calculate exclusion curves for various pore geometries which are then compared with experimental exclusion curves.

4.2.1. Infinite Parallel Plates

The construction for this pore geometry is straightforward and shown in Figure 14. The pore radius is given by R and the molecular radius by r. It is obvious that if $r > R$, the molecule will be completely excluded from the pores and $K = 0$. Smaller molecules of radius r will be excluded from the shaded region in Figure 14 and the exclusion coefficient K is given by

$$K = \frac{V_{available}}{V_{total}} = \frac{R - r}{R} \qquad (4.8.)$$

4.2.2. Infinite Cylinder

Figure 15 shows a cross-section of an infinite cylinder. Again if $r > R$, the molecule is completely excluded from the pores, smaller molecules of radius r will be excluded from the shaded region and K is given by

$$K = \frac{(R - r)^2}{R^2} \qquad (4.9.)$$

4.2.3. Spheres

In this construction, the pores are assumed to be spherical and the result is analogous to that for the infinite cylinder except that we are now dealing with a ratio of volumes and K is given by

$$K = \frac{(R - r)^3}{R^3} \qquad (4.10.)$$

4.2.4. Inverse Cylinder

In this pore model, the pore volume is the volume outside a packed arrangement of infinite cylinders as shown in Figure 16. The volume available to a molecule of radius r is the unshaded region outside the cylinders so that K is the ratio of the area of this unshaded region to the total area of the pore. The construction used to calculate these areas is shown in Figure 17 which shows one-quarter of the total pore but since the construction is symmetrical, this is sufficient. The radius of the cylinder defining the pore is represented by R' and the pore radius by R, so that if the molecular radius r is greater than R, then the molecule is completely excluded and K = 0.

From Figure 17 we see that the pore volume V_{total} is given by

$$V_{total} = \text{area (ABC)}$$
$$= R'^2 - \frac{\pi R'^2}{4}$$
$$= \frac{(4 - \pi) R'^2}{4}$$

If we now define R'' = R' + r, then it is easily seen that the distance OH is given by $(R''^2 - R'^2)^{\frac{1}{2}}$ which I will represent by R'''.

The volume available to a molecule of radius r, $V_{available}$ is given by

$$V_{available} = \text{area(EBF)}$$

$$= \text{area(OABC)} - \text{area(OAEH)} - \text{area(HEFC)}$$

$$\text{area(OABC)} = R'^2$$

$$\text{area(OAEH)} = R' R'''$$

$$\text{area(HEFC)} = \int_{R'''}^{R'} (R''^2 - x^2)^{\frac{1}{2}}\, dx$$

$$= \left[\frac{x}{2}(R''^2 - x^2)^{\frac{1}{2}} + \frac{R''^2}{2} \sin^{-1} \frac{x}{R''} \right]_{x=R'''}^{x=R'}$$

Therefore

$$V_{available} = R'^2 - R' R''' - \left[\frac{x}{2}(R''^2 - x^2)^{\frac{1}{2}} + \frac{R''^2}{2} \sin^{-1} \frac{x}{R''} \right]_{x=R'''}^{x=R'}$$

and the exclusion coefficient K is given by

$$K = \frac{V_{available}}{V_{total}}$$

$$= 4 \left\{ R'^2 - R' R''' - \left[\frac{x}{2}(R''^2 - x^2)^{\frac{1}{2}} + \frac{R''^2}{2} \sin^{-1} \frac{x}{R''} \right]_{x=R'''}^{x=R'} \right\} \Big/ (4 - \pi) R'^2 \qquad (4.11.)$$

where $R' = \dfrac{R}{\sqrt{2}-1}$

$$R'' = R' + r$$

$$R''' = (R''^2 - R'^2)^{\frac{1}{2}}$$

4.2.5. Inverse Sphere

This construction shown in Figure 18 is similar to that for the inverse cylinder except that we must now work in three dimensions.

Simple geometry shows that $R = (\sqrt{3}-1)R'$. In this pore model I shall only consider values of r from r = 0 to $r = (\sqrt{2}-1)R'$ since at higher values of r, the geometry becomes impossibly complex, i.e. we are only considering values of r for which

$$r \leq \frac{\sqrt{2}-1}{\sqrt{3}-1} R$$

$$r < 0.56\ R$$

The pore volume V_{total} is given by

$$V_{total} = (8 - \tfrac{4}{3}\pi)R'^3$$

The volume available to a molecule of radius r is given by

$$V_{available} = \text{vol.(EBF)}$$

$$= \text{vol.(OABC)} - \text{vol.(OAEFC)}$$

$$\text{vol.(OABC)} = 8R'^3$$

If we now define $R'' = R' + r$, then

$$\text{vol.(OAEFC)} = \tfrac{4}{3}\pi R''^3 - 6_x \text{ vol.(CFG) rotated about x-axis}$$

$$\text{vol. (CFG)} = \pi \int_{R'}^{R''} (R''^2 - x^2)dx$$

$$= \pi \left[R''^2 x - \tfrac{1}{3}x^3 \right]_{x=R'}^{x=R''}$$

Therefore

$$V_{available} = 8R'^3 - \frac{4}{3}\pi R''^3 + 6\pi\left[R''^2 x - \tfrac{1}{3}x^3\right]_{x=R'}^{x=R''}$$

and the exclusion coefficient K is given by

$$K = \frac{V_{available}}{V_{total}}$$

$$= \frac{8R'^3 - \frac{4}{3}\pi R''^3 + 6\pi\left[R''^2 x - \tfrac{1}{3}x^3\right]_{x=R'}^{x=R''}}{(8 - \frac{4}{3}\pi)R'^3} \qquad (4.12.)$$

where $R' = \dfrac{R}{\sqrt{3}-1}$

$$R'' = R' + r$$

and is valid for values of r for which

$$r < \frac{\sqrt{2}-1}{\sqrt{3}-1}R$$

CHAPTER 4.3.

RESULTS AND DISCUSSION

Experimental calibration curves were obtained for the two porous silica packings: Hypersil (Shandon Southern Products Ltd.) and SG60F (an experimental batch supplied by Materials Preparation Unit AERE, Harwell), specified in Table 3.1. These calibration curves were obtained by eluting narrow distribution polystyrene standards (Waters Associates) in the molecular weight range 2,700,000 to 2000 and benzene which was taken to be a totally permeating solute. Sample loads were 1ul of 0.1% solutions of each solute in dichloromethane (the eluent).

Reduced calibration curves (log (M.W) v K) were obtained from the calibration curves (log (M.W) v V_r) by assuming that the exclusion coefficient, K, was 1.0 for benzene and zero for the polystyrene sample of molecular weight 2,700,000. Calibration curves were found to be independent of flow rate. From equations (4.8. - 4.12) the exclusion coefficients for molecules of radius 0 - R were found for each of the pore models. To convert the molecular radii to molecular weight equation (4.13.) was used (75).

$$\log(M.W) = \log C + \frac{\log r}{0.588} \qquad (4.13.)$$

where C is a constant for any particular polymer-solvent combination. The theoretical curves (in the form log (M.W) v K) may then be fitted to the experimental data by translation until the best fit is achieved. These curves are shown in Figures 19-23 along with the experimental data. All five pore models give calibration curves which have the basic shape expected and give good agreement over the linear section. However, at the high molecular

weight end of the calibration curves (K = 0) there is little deviation from linearity compared to the experimental curves. The explanation of this is that in the pore structures considered here, the pores are all the same size and there is therefore a fixed maximum molecular size which will fit into the pores, whereas in a real porous network there will be many more large pores. Deviations between theoretical and experimental curves at the low molecular weight end (K - 1.0) are probably due to the assumption that K = 1.00 for benzene (101).

Recently in this laboratory (102), random packings of spheres have been generated by computer and exclusion curves calculated from these models give excellent agreement with experimental data (Figure 24). More work is to be carried out in this field to make the pore model more realistic but the results available indicate that to a very good approximation using realistic pore geometries and spherical molecules, calibration curves may be predicted by using the theory of steric exclusion.

CHAPTER 5.

BAND DISPERSION OF POLYMERS IN EXCLUSION CHROMATOGRAPHY

CHAPTER 5.1.

INTRODUCTION

In exclusion chromatography, dispersion of a sharply injected polymer sample arises from the kinetic processes occurring within the column but there will also be a contribution from the polydispersity, P , of the sample.

As outlined in Chapter 2.5., the kinetic dispersion of any sample of a pure compound (in the case of a polymer, a monodisperse sample for which P = unity) eluted from a column of length, L, is related to the plate height, H, and the number of theoretical plates N, by equations (5.1.) and (5.2.) respectively (3).

$$H = L\left(\frac{\sigma_v}{V_r}\right)^2 \qquad (5.1.)$$

$$N = \frac{L}{H} = \left(\frac{V_r}{\sigma_v}\right)^2 \qquad (5.2.)$$

where σ_v is the standard deviation of the peak in volume units and V_r the elution volume. The effect of polydispersity will be to increase the peak width and so lead to an apparent increase in H and a decrease in N.

Since variances from independent sources are additive we can obtain the total peak variance from

$$\sigma_v^2(\text{total}) = \sigma_v^2(\text{kinetic}) + \sigma_v^2(\text{poly}) \qquad (5.3.)$$

or in terms of the plate height

$$H_{(\text{total})} = H_{(\text{kinetic})} + H_{(\text{poly})} \qquad (5.4.)$$

In order to compare the theories (outlined in Chapter 2.5.) for kinetic peak broadening in exclusion chromatography, it is necessary to be able to calculate $\sigma^2_{v(\text{poly})}$ in order to obtain $\sigma^2_{v(\text{kinetic})}$

and $H_{(kinetic)}$ on which these theories are based. Various methods have been used to separate $\sigma^2_{(poly)}$ from the observed $\sigma^2_{(total)}$ but no attempt has been made to measure the variation of $H_{(kinetic)}$ with velocity to test the various theories.

Waters (103) used recycle exclusion chromatography. In the recycle mode (30, 104) the total chromatographic peak width is $\sigma^2_{v(kinetic\ total)}$ where

$$\sigma^2_{v(kinetic\ total)} = \sum \sigma^2_{v(kinetic)} = n\sigma^2_{v(kinetic)} \quad (5.5.)$$

and n is the number of cycles through the system. The total peak width due to polydispersity is $\sigma^2_{v(poly\ total)}$ where

$$\sigma^2_{v(poly\ total)} = \sum \sigma_{v(poly)}{}^2 = n^2\sigma^2_{v(poly)} \quad (5.6.)$$

In these equations $\sigma^2_{v(kinetic)}$ and $\sigma^2_{v(poly)}$ are the single-pass peak width and $\sigma^2_{v(kinetic\ total)}$ and $\sigma^2_{v(poly\ total)}$ are the multiple pass widths.

The measured peak width $\sigma^2_{v(total)}$ is therefore given by

$$\sigma^2_{v(total)} = n\sigma^2_{v(kinetic)} + n^2\sigma^2_{v(poly)} \quad (5.7.)$$

or

$$\frac{\sigma^2_{v(total)}}{n^2} = \frac{\sigma^2_{v(kinetic)}}{n} + \sigma^2_{v(poly)} \quad (5.8.)$$

By plotting $\sigma^2_{v(total)}/n^2$ versus $1/n$, a straight line is obtained with slope $\sigma^2_{v(kinetic)}$ and intercept $\sigma^2_{v(poly)}$. Waters

used this method to calculate the polydispersity of narrow distribution polystyrene standards.

Tung et al (105) introduced the concept of reverse-flow technique. Subsequently this has been used (100) to obtain the chromatographic broadening. In this method, the samples in solution are allowed to penetrate halfway down the column, and then the flow is reversed. Thus dispersion due to polydispersity is eliminated and the initial sample band is subjected to kinetic broadening only. The other half of the column can similarly be used to obtain the kinetic broadening for the whole column.

Bly (106, 107) proposed the use of equations (5.9.) and (5.10.) to calculate the true values of H and N and correct for this effect of polydispersity.

$$H = \frac{H_{app}}{P^2} \qquad (5.9.)$$

$$N = N_{app} \times P^2 \qquad (5.10.)$$

These equations, however, were empirically derived and are highly inaccurate for efficient columns (108).

It will be shown in Chapter 5.2. that the major factor in determining peak widths in most published exclusion chromatograms of polymer standards has almost certainly been the polydispersity of the standard rather than the kinetic broadening of the column. Chapter 5.3. deals with experimental evidence to support the theory, correction for the polydispersity contribution to the plate height and a comparison of $H_{(kinetic)}$ with the theories outlined in Chapter 2.5.

CHAPTER 5.2.

ALLOWANCE FOR POLYDISPERSITY IN THE DETERMINATION OF THE TRUE PLATE HEIGHT IN EXCLUSION CHROMATOGRAPHY

The polydispersity, P, of a polymer sample is defined by equation (5.11.).

$$P = \frac{M_w}{M_n} \qquad (5.11.)$$

where M_w and M_n are weight-and number- averaged relative molecular masses of the polymer samples. M_w and M_n are defined by equations (5.12.) and (5.13.).

$$M_n = \int M\, f\,(M)\, d\, M \qquad (5.12.)$$

$$M_w = \frac{\int M^2\, f\,(M)\, d\, M}{\int M\, f\,(M)\, d\,(M)} \qquad (5.13.)$$

where f (M) d M is the number fraction of polymer molecules having relative molecular masses in the range M to M + dM. A typical distribution showing M_n and M_w is given in Figure 25. The polydispersity of this particular distribution is 1.09.

The second moment or variance of the distribution about this mean is given by equation (5.14.).

$$\sigma_M^2 = \int (M-M_n)^2\, f\,(M)\, d\, M \qquad (5.14.)$$

On expansion

$$\sigma_M^2 = \int M^2\, f\,(M)\, d\, M - 2 \int M_n M\, f\,(M)\, d\, M + \int M_n^2\, f\,(M)\, d\, M$$

$$= \int M^2\, f\,(M)\, d\, M - 2\, M_n^2 + M_n^{\,2}$$

$$= M_w\, M_n - M_n^{\,2} \qquad (5.15.)$$

Equation (5.15) may be rearranged to give

$$\left(\frac{\sigma_M}{M_n}\right)^2 = \left(\frac{M_w}{M_n}\right) - 1 = P - 1 \qquad (5.16.)$$

which holds whatever the form of f (M).

Equation (5.16.) and Figure 25 show that σ_M is a substantial fraction of M_n even for a polymer sample with a polydispersity as low as 1.09. Figure 26 shows a corresponding case where P = 1.01 and the distribution function is Gaussian. It is qualitatively clear that the polydispersity of even a relatively narrow polymer fraction will contribute substantially to the total width of the eluted peak in exclusion chromatography. To obtain a quantitative measure it is necessary to consider the calibration curve relating relative molecular mass to elution volume, an example of which is shown in Figure 27. V_o is the void volume of the packing (volume outside the particles); V_t is the void volume plus the volume of all pores accessible to a small molecule. M_u and M_l are the upper and lower relative molecular mass limits corresponding to the elution volumes V_o and V_t respectively and obtained from the extrapolation of the linear portion of the calibration curve. M^* is any intermediate relative molecular mass on the linear portion of the curve corresponding to an elution volume V^*. The relative molecular mass selectivity of a packing material is conveniently denoted by S, the reciprocal of the gradient of the linear portion of the calibration curve, that is

$$\frac{1}{S} = -\frac{d \ln M}{dV} \qquad (5.17.)$$

We thus have

$$V_t = V_o + S \ln \left(\frac{M_u}{M_l}\right) \qquad (5.18.)$$

and for any intermediate relative molecular mass close to M^*.

$$V_M = V^* + S \ln \left(\frac{M^*}{M}\right) \qquad (5.19.)$$

Writing $M = M^* + \delta M$ then gives

$$V_M = V^* + S \ln \left(\frac{M^*}{M^* + \delta M}\right)$$

$$= V^* - S \ln \left(1 + \frac{\delta M}{M^*}\right) \qquad (5.20.)$$

$$= V^* - \delta V$$

Equation (5.20.) can be applied to a polymer sample where number average molecular weight is $M_n = M^*$. The elution peak will then be centred on V^* and the second moment of the peak on a volume basis will be

$$\sigma^2_{v(poly)} = \int_{-\infty}^{\infty} (\delta V)^2 f (M_n + \delta M) \, d (\delta M)$$

$$= S^2 \int_{-\infty}^{\infty} \left[\ln \left(1 + \frac{\delta M}{M_n}\right)\right]^2 f (M_n + \delta M) \, d (\delta M) \qquad (5.21.)$$

For a polymer of narrow relative molecular mass range (i.e. low polydispersity) we may assume to a first approximation that f (M) is Gaussian, that is

$$f(M) = f(M_n + \delta M) = \frac{\exp\left(-\frac{\delta M^2}{2\sigma_M^2}\right)}{(2\pi\sigma_M^2)^{\frac{1}{2}}} \qquad (5.22)$$

σ_M being the standard deviation of the distribution. Figure 26 illustrates equation (5.22) where P = 1.01 and therefore $\sigma_M/M_n = 0.1$. The width of the distribution is again noticeable even for this very low value of P.

Insertion of f (M) from equation (5.22) into equation (5.21.) gives

$$I = \frac{\sigma_{v\,(poly)}^2}{S^2} = \int_{-\infty}^{\infty} \left[\ln\left(1 + \frac{\delta M}{M_n}\right)\right]^2 \frac{\exp\left(-\frac{\delta M^2}{2\sigma_M^2}\right)}{(2\pi\sigma_M^2)^{\frac{1}{2}}}\, d(\delta M)$$

Replacing $\delta M/M_n$ by y and $M_n^2/2\sigma_M^2$ by a gives

$$I = (\ln(1 + y))^2 \exp(-ay^2) \left(\frac{a}{\pi}\right)^{\frac{1}{2}} dy$$

expanding the logarithm to several terms for $y < 1$ gives

$$\ln(1 + y) = y\left(1 - \frac{y}{2} + \frac{y^2}{3} - \frac{y^4}{4} + \ldots\ldots\right)$$

$$(\ln(1 + y))^2 = y^2\left(1 - y + \frac{11}{12}y^2 - \frac{5}{6}y^3 + \frac{137}{180}y^4 + \ldots\ldots\right)$$

Noting that

$$\int_{-\infty}^{\infty} y^{2n+1} \exp(-ay^2)\, dy = 0$$ for integral values of n we can write

$$I = \int_{-\infty}^{\infty} (y^2 + \frac{11}{12} y^4 + \frac{137}{180} y^6) \exp(-ay^2) (\frac{a}{\pi})^{\frac{1}{2}}\, dy$$

In general

$$\int_{-\infty}^{\infty} y^{2n} \exp(-ay^2)\, dy = \frac{1.3.5....(2n-1)}{2^n a^n} (\frac{\pi}{a})^{\frac{1}{2}}$$

Thus

$$I = \frac{1}{2a} + \frac{11}{4} \cdot \frac{1}{4a^2} + \frac{137}{12} \cdot \frac{1}{8a^3} + \ldots.$$

$$= (\frac{\sigma_M}{M_n})^2 + \frac{11}{4} (\frac{\sigma_M}{M_n})^4 + \frac{137}{12} (\frac{\sigma_M}{M_n})^6$$

Since $(\frac{\sigma_M}{M_n})^2 = (P - 1)$ we obtain finally

$$I = (P-1) \left[1 + \frac{11}{4} (P-1) + \frac{137}{12} (P-1)^2 \ldots.. \right]$$

$$= (P-1)(1 + \alpha)$$

Thus we have that

$$\sigma^2_{v(poly)} = S^2 (P-1)(1+\alpha) \qquad (5.23.)$$

where $\alpha = \frac{11}{4}(P - 1) + \frac{137}{12}(P - 1)^2 + \ldots .$ (5.24.)

Values of α as a function of P are shown in Figure 28. Since variances from independent sources are additive we obtain for the total peak variance

$$\sigma^2_{v(total)} = \sigma^2_{v(kinetic)} + \sigma^2_{v(poly)} \quad (5.25.)$$

Using equation (5.1.) for $\sigma^2_{v(kinetic)}$ and equation (5.23.) gives

$$\sigma^2_{v(total)} = \frac{H}{L} V_r^2 + S^2(P - 1)(1 + \alpha) \quad (5.26.)$$

The apparent plate height and apparent plate number are conveniently defined by analogy with equations (5.1.) and (5.2.) as

$$H_{app} = L\left(\frac{\sigma_{v(total)}}{V_r}\right)^2 \quad (5.27.)$$

$$N_{app} = \left(\frac{V_r}{\sigma_{v(total)}}\right)^2 \quad (5.28.)$$

We thus obtain

$$H_{app} = H + L(P - 1)(1 + \alpha)\left(\frac{S}{V_r}\right)^2 \quad (5.29.)$$

$$\frac{1}{N_{app}} = \frac{1}{N} + (P - 1)(1 + \alpha)\left(\frac{S}{V_r}\right)^2 \quad (5.30.)$$

The ratio V_r/S is the hypothetical range of relative molecular mass measured in powers of e which would be eluted over a volume V_r. This ratio, denoted by x is generally within the range 4 -12 for an exclusion chromatography support material of uniform pore size and is readily found from the calibration curve.

Replacing V_r/S by x and rearranging gives finally

$$H = H_{app} - \frac{L(P - 1)(1 + \alpha)}{x^2} \qquad (5.31.)$$

$$\frac{1}{N} = \frac{1}{N_{app}} - \frac{(P - 1)(1 + \alpha)}{x^2} \qquad (5.32.)$$

It is readily seen from equation (5.32.) that for a monodisperse polymer (P = unity), $N = N_{app}$, while for a polydisperse polymer sample eluted from a column of infinite plate efficiency, N_{app} has a maximum value given by

$$N_{app(max)} = \frac{x^2}{(P - 1)(1 + \alpha)} \qquad (5.33.)$$

Typical values for $N_{app(max)}$ are shown in Table 5.1. for different values of x and P. The contribution of polydispersity to peak dispersion in a moderately efficient column of $N \approx 1000$ will be relatively unimportant for entries above the stepped line but substantial for entries below the line. Table 5.2. shows the combined effects of polydispersity and kinetic dispersion on N_{app} for the case where x = 8. For entries above the stepped line the error in assuming $N = N_{app}$ is less than 15%. It is seen that even

for the least efficient column with N = 300 it is necessary to use a sample with a polydispersity of not more than 1.03, while if N = 1000 the polydispersity must be below 1.01.

It becomes clear that the true plate number or plate height cannot generally be determined by elution of commercially available polymer standards whose polydispersities are rarely below 1.03 and in any case are not known with high enough precision to allow the precise calculation of the second terms in equations (5.31.) and (5.32.).

From equation (5.31.) it is readily seen that the contribution of polydispersity to the apparent plate height depends only upon the column length, the polydispersity of the sample, P, and x. For a particular sample, all these factors are independent of flow rate and therefore at all flow velocities, the contribution to the plate height due to polydispersity should be constant. Thus correction for this contribution to the apparent plate height should merely require a translation of the absicca. Recently, Giddings et al (109) have studied the effect of polydispersity in the peak broadening in thermal field-flow fractionation. They arrive at a result using the mass variance rather than the number variance which is analagous to equation (5.31.).

CHAPTER 5.3.

EXPERIMENTAL PROCEDURE, RESULTS AND DISCUSSION

In retentive chromatography, the plate height dependence on velocity may be written in the form

$$H = \frac{B}{u} + Au^n + Cu \qquad (5.34.)$$

or in terms of reduced parameters as

$$h = \frac{B'}{\nu} + A'\nu^n + C'\nu \qquad (5.35.)$$

where u is the linear velocity of the mobile phase, ν is the reduced velocity, B and B' describe the dispersion due to molecular diffusion, A and A' describe the dispersion due to the interparticle space (flow effects) and C and C' represent the dispersion due to mass transfer phenomena. From the non-equilibrium theory of chromatography, outlined in Chapter 2.5. and Appendix 1, the stationary phase mass transfer terms are given by

$$C_s = (q_s \frac{D_M}{D_s})(\frac{d_p^2}{D_M}) \frac{k''}{(1+k'')^2} \qquad (5.36.)$$

and

$$C_s' = (q_s \frac{D_M}{D_s}) \frac{k''}{(1+k'')^2} \qquad (5.37.)$$

where q_s is a geometrical factor, k'' is the zone capacity ratio, d_p is the particle diameter (for particles of uneven size, d_p is given by the volume weighted average value) and D_M and D_s are the diffusion coefficients in the mobile and stationary phases respectively.

The aim in this section of the work was to see if band dispersion in exclusion chromatography obeys the same rules as it does in the retentive forms of chromatography.

5.3.1. Correction of Plate Height for Polydispersity

From Chapter 5.2. it is seen (ignoring extra-column effects) that the plate height arising from kinetic processes within the column may be written in the form

$$H = H_{app} - \frac{L(P-1)(1+\alpha)}{x^2} \qquad (5.38.)$$

$$\text{or} \quad h = h_{app} - \frac{L(P-1)(1+\alpha)}{x^2 d_p} \qquad (5.39.)$$

where H_{app} and h_{app} are the measured plate height and reduced plate height respectively, L is the column length, P is the polydispersity of the polymer, α is a function of (P-1), x is the range of molecular weight resolvable by the packing material in powers of e and d_p is the particle diameter.

Using columns of different lengths (257mm, 101mm and 55mm), packed with 6um Hypersil as described in Chapter 3.2., H_{app} and h_{app} were determined over a range of velocities for several polystyrene standards of molecular weights from 2,000 to 33,000 for a totally permeating solute (benzene) and a retained solute (m-dinitrobenzene). Figure 29 shows a typical chromatogram of PS 2700K, (a totally excluded solute used to calculate the mobile phase linear velocity) two partially excluded solutes, an unretained solute (benzene) and two retained solutes (m-dinitrobenzene and acetophenone).

The variation of plate height with velocity for the five polystyrene samples, the totally permeating and retained solutes are given in Tables 5.3(a) - 5.9(c). Figures 30-34 show graphically the effect of column length on the plate height versus velocity curves for each of the five polystyrenes. For each of these figures the three curves are more or less parallel but displaced from each other with the longer columns giving higher values of H_{app} at any particular velocity as predicted by equation (5.38.). Figures 35 and 36 show the plate height versus velocity curves for the totally permeating and retained solutes. These curves are essentially invarient with column length, since P is equal to unity the polydispersity contribution is zero, and $H = H_{app}$. The only variation is due to the irreproducibility of packing, i.e. the A term in equation (5.34.).

For each of the polystyrene samples, H_{app} was interpolated for selected velocities and plotted for each velocity against the column length (Figures 37-41). Straight lines were obtained from which, by equation (5.38.) the true plate height was given by the intercept and the polydispersity of the sample from the gradient.

When the chosen velocity corresponded to an optimum reduced velocity (bottom lines in Figures 37-41), true reduced plate heights (intercepts) of around two were obtained for all the polymer standards and for the totally permeating and retained solute. These optimum velocities were taken to be $u = 0$ for polystyrenes of molecular weight 4000 - 33,000; for the polystyrene of molecular weight 2000, the totally permeating and the retained solutes, the actual minima in the curves were used.

Thus if we correct for the effect of polydispersity (or use monodisperse polymers) and work at around the optimum velocity, similar efficiencies may be obtained in exclusion chromatography as are currently obtained in retentive chromatography ($h \approx 2$). The wide peaks observed in exclusion chromatography are not therefore due to low rates of equilibration, but almost entirely to the polydispersity of the samples.

From equation (5.38.), the gradient of the lines in Figures 37-41 are given by

$$\text{Gradient} = \frac{(P-1)(1+\alpha)}{x^2} \qquad (5.40.)$$

The H_{app} versus column length curves for any sample but at different velocities are parallel as predicted by equation (5.40.). Table 5.10. lists the gradient of these lines, the value of x for each of the samples calculated from the calibration curve for Hypersil (Figure 42) and the calculated polydispersity of each sample. These standards have very low values of polydispersity (1.007 - 1.06) but it is important to note that even for a sample whose polydispersity is as low as 1.06, the ratio of peak width due to polydispersity versus peak width due to kinetic effects on a 257mm long column at the optimum velocity is around 6.

These experiments go a long way to verifying the validity of the theoretically derived result (equation (5.31.)) which allows the calculation of the plate height due to kinetic effects occurring within the column for a solute of known polydispersity. They also give a relatively simple method of calculating exact values of

polydispersity. The method used here is similar to that used by Waters (103) to calculate the polydispersity of polymer standards except that he used recycling to change the effective length of the column.

5.3.2. Variation of Plate Height with Velocity and Calculation of the Stationary Phase Mass Transfer Term for Partially and Totally Permeating Solutes

Figures 43 and 44 show the variation of the apparent plate height with linear velocity (H_{app} versus u) and with reduced velocity (H_{app} versus ν) for the seven solutes under study on a column, packed with 6um Hypersil, of length 101mm. Figure 44 particularly shows up the effect of polydispersity since the influence of the diffusion coefficients has been eliminated. Correcting for the effect of polydispersity may be carried out as shown in Chapter 5.3.1. by plotting the apparent plate height, H_{app}, versus column length for a number of velocities and the corrected curve is given by the plate height at the intercept (L = 0), $H_{intercept}$ versus velocity. However, since the effect of polydispersity is a thermodynamic effect and $H_{intercept}$ for a polymer and the minimum plate height, H_{min}, for a totally permeating solute are approximately equal when measured at their respective optimum velocities, correcting for the effect of polydispersity may be carried out by redrawing the plate height scales in Figures 30-34 so that the plate height for a polymer sample at the optimum velocity is equal to H_{min} for a totally permeating solute. As will be shown later, there is no need to carry out this correction since over the range of velocities studied for the polystyrene samples, the plate height is dominated by the stationary phase mass

transfer term (which is given by the gradient of H versus u curves and will be the same in both corrected and uncorrected curves) and this is the only section of the plate height curve which may be studied.

The plate height curves for the totally permeating and retained solutes show the well known trend for retentive chromatography. At very low velocities, the plate height is dominated by molecular diffusion (the B term). As the velocity increases, the effect of molecular diffusion decreases and the dispersion due to flow effects and mass transfer begin to predominate. The curves show a minimum plate height of approximately two particle diameters at a linear velocity of approximately 0.2 cm s^{-1} which corresponds to a reduced velocity of around three. As the velocity increases further, the plate height eventually becomes completely dominated by the stationary phase mass transfer term and equations (5.34.) and (5.35.) may be approximated by

$$H = C_s u \qquad (5.41.)$$

$$h = C_s' \nu \qquad (5.42.)$$

where C_s and C_s' are given by equations (5.36.) and (5.37.) respectively.

The partially permeating solutes (polystyrene standards) should also give minima in their plate height versus velocity curves but it is only for the polystyrene of molecular weight 2000 that we were able to work at low enough flow velocities actually to observe the minimum. Over the range of velocity studied, plots of H versus u for the partially permeating solutes (Figures 30-34)

were linear and the relationship may be approximated by equation (5.41.)

Table 5.11. lists values of C_s (calculated from Figures 30-34) for each solute and each column, the average C_s for each solute, the zone capacity ration k" values of D_M calculated from the Wilke-Chang equation (99) and the computed values of $(q_s \frac{D_M}{D_s})$.

On theoretical grounds (see Appendix 1), q_s is expected, for the spherical material used in this work, to be 0.033 which leads to the conclusion from our data that $\frac{D_M}{D_s}$ falls in the region 7-17 with a slight indication that $\frac{D_M}{D_s}$ increases with the degree of exclusion of the solute.

In a recent publication, Van Kreveld and Van den Hoed (97) found ratios of $\frac{D_M}{D_s}$ to lie in the range 1.5 - 9 with a steady increase with the degree of exclusion.

In gas chromatography, Knox and McLaren (110) found that $\frac{D_M}{D_s}$ was around 1.5 increasing with the degree of constriction of the pore network. Therefore if the pore network is invarient one would expect that as the solute size increases this would effectively increase the degree of constriction within the network leading to higher values of $\frac{D_M}{D_s}$. Thus the diffusion coefficient is lower in the stationary phase than in the mobile phase because of simple obstruction. However, this decrease in diffusion coefficient is not large enough to drastically affect the near-equilibrium assumption and therefore the retention volume may still be predicted using an equilibrium model. This explanation would account for the observed results of both this and Van Kreveld's work. However,

the fundamental difference between the two sets of results lies in what value of $\frac{D_M}{D_s}$ they predict for a totally permeating solute. Van Kreveld finds that $\frac{D_M}{D_s}$ is around 1.5 for a totally permeating solute which is in good agreement with other experimentally derived results (110,111). This work, on the above assumptions, gives values which are around 8. To account for this discrepancy I would like to put forward and discuss several possible explanations.

a) Because of the narrowness of the pores it could be envisaged that close to the pore walls the liquid is strongly bound to the surface leading to a fairly structured region of liquid within the pores which would result in D_s being lower than D_M. The extent of this structuring would depend on the pore size, decreasing as the pore size increases. However, on repeating the above experiments for a totally permeating solute and a slightly excluded solute (Table 5.12. and Figures 45 and 46) on a material with pore diameter 600Å (SG 60 F), similar values of $\frac{D_M}{D_s}$ were obtained. Extrapolating data from the literature (25) also gave similar values of $\frac{D_M}{D_s}$ for a slightly excluded solute using a material whose pore diameter was around 50Å (Table 5.12.). Further evidence against this proposal is that mass transfer coefficients measured for both liquid chromatography and gas chromatography on the same support (90) are approximately equal whereas it would be expected that C_s in gas chromatography would be lower than C_s in liquid chromatography if structuring of the stationary phase was a major factor.

b) The lowest values of C_s so far achieved (101) were carried out by using porous particles with a very narrow size distribution

(37-44um), whereas this work was carried out with particles in the size range 2-10um. Theory suggests that in calculating C_s the value of d_p to be used is the volume weighted average value. The size distribution of the particles used in this work (measured from electron micrographs) was approximately Gaussian with d_p = 5.9um and $(d_p^3)^{\frac{1}{3}}$ = 6.2um. Since I used d_p = 6um in the calculations this should not be a large source of error.

c) It has been assumed in the calculation of C_s that, since plots of plate height versus velocity are linear in the high velocity region, then the slope of this part of the curve is given by C_s. However, this slope may not be due to C_s alone but may contain a contribution from the A-term since

$$H = Au^{0.33} + C_s u \qquad (5.43.)$$

This dependence may appear to be linear over the small range of velocities studied here. To account for the effect of the A term (and the B term which could affect the results for the totally permeating and retained solutes), a corrected reduced plate height, h_c, was calculated for each of the h_{app} values in Tables 5.3(a) - 5.9(c) by use of equation (5.44.)

$$h_c = h_{app} - \frac{B'}{\nu} - A'\nu^{0.33} \qquad (5.44.)$$

using values of B' = 2, A' = 1 (112).

Plots of h_c versus reduced velocity (Figures 47-50) again appeared to be linear for PS 33K, PS 20K, PS 10K and PS 4K and the computed values of $\frac{D_M}{D_{s(corrected)}}$ are given in Table 5.13. along with the uncorrected values for these four solutes.

It is evident that the correction factor increases as the molecular weight of the sample decreases due to the fact that $A'\nu^{0.33}$ is larger relative to $C\nu$ for the plate height data of PS 4K (ν = 1-100) than for the plate height data of PS 33K (ν = 10-300). It is also obvious from Table 5.13. that there is an increase in $\frac{D_M}{D_s}$ with the size of the molecule in good agreement with the work of Van Kreveld (97). The h_c values for PS 2K, the totally permeating solute and the retained solute are meaningless because at the reduced velocities used in this work $C'_s\nu$ is very low and the error in h_c (i.e. $C'_s\nu$) is larger than h_c itself. However, one would expect from the trend in Table 5.13. that $\frac{D_M}{D_s}$ would continue to decrease for PS 2K and the totally permeating solute.

Unfortunately, it is not possible to calculate C_s for a totally permeating solute using 6um particles because, due to pressure limitations, we cannot work at high enough reduced velocities in order to eliminate the effects of the A and B terms and if we restrict ourselves to the range of velocities used in this work, A and B are not known accurately enough to calculate C_s.

5.3.3. Variation of Plate Height with Velocity for Monodisperse Polymers

Chapter 5.3.1. showed that by correcting for the effect of polydispersity, efficiencies comparable with those obtained in retentive chromatography, may be achieved in exclusion chromatography. In order to prove this beyond doubt, attempts were made to produce monodisperse polymers from the narrow fraction polystyrene samples and to see how this affected the plate height.

a) Cuts of exclusion chromatography peak: Using PS 3K the plate height was measured against velocity as in Chapter 5.3.1. Cuts of the sample were then taken as the sample eluted from the column. These cuts were then reinjected into the column and the variation of plate height with velocity is shown in Figure 51 for both the initial sample and the cuts. This figure shows that while we have reduced the plate height by a factor of two we have not reduced it to the value predicted for a monodisperse sample. This is because in taking a cut we are reducing the polydispersity but within the cut there is still a number of oligomers which give rise to the higher values of plate height than expected. To reduce the effect of polydispersity further we could repeatedly take cuts of cuts, but unfortunately, if the initial sample is kept below 10ug to avoid overloading, we go beyond the detection limit after taking two cuts.

b) Fractionation by adsorption chromatography: The polystyrene standard PS 3K may be well fractionated by adsorption chromatography using a less polar eluent (80:20; pentane:dichloromethane) on the same columns as were used for exclusion chromatography. A typical adsorption chromatogram for this sample is shown in Figure 52. Each peak on the chromatogram corresponds to an oligomer. Cuts of one of these oligomers were taken and injected into the column in the exclusion mode and the variation of plate height with velocity for these cuts is shown in Figure 51. Values of H of around three to four particle diameters were obtained.

Figure 53 shows a plot of reduced plate height versus reduced velocity for this oligomer and for a totally permeating solute and it is clearly seen that both curves correspond closely.

Thus by using monodisperse samples, as predicted by Chapter 5.3.1., efficiencies comparable with those in retentive chromatography may be obtained in exclusion chromatography. Note that in Figure 51 the plate height curves are parallel as would be expected since polydispersity is a thermodynamic effect.

Using higher molecular weight samples, it was necessary to use a slightly more polar eluent for the sample to have k" values in the same range as above. For PS 10K the eluent was 70:30; pentane:dichloromethane, but there was not the same degree of resolution and the best that could be obtained was a broad envelope: the oligomers could not be separated. Cuts of this envelope were obtained and reinjected into the column in the exclusion mode and the variation of plate height with velocity is shown in Figure 54. These cuts give plate height values which are much reduced but do not represent values for monodisperse solutes for the same reason as in Chapter 5.3.3.(a).

It is clear from the plate height data of the cuts of PS 3K obtained by adsorption chromatography that similar efficiencies may be obtained (when working around the optimum velocity) for monodisperse polymers in exclusion chromatography as are obtained in retentive chromatography.

5.3.4. Variation of Plate Height with Velocity for Totally Excluded Solutes

The variation of plate height with velocity for totally excluded solutes (Figures 55-57) is anomalous. Since these materials are completely excluded from the pores of the packing material, there should be no polydispersity contribution to the

plate height since $x \rightarrow \infty$ There should also be no stationary phase mass transfer contribution to the plate height and therefore equation (5.34.) should be approximated by

$$H = \frac{B}{u} + Au^n \qquad (5.45.)$$

Since these polymers have very low diffusion coefficients, the contribution of longitudinal moleular diffusion should be negligible over the velocity range studied and the plate height should be given by

$$H = Au^n \qquad (5.46.)$$

PS 200K and PS 470K follow this type of pattern over the high velocity range but at low velocities we get a very large increase in plate height for the longer columns. These samples give "minima" in the plate height curves of around 3-4 particle diameters at a linear velocity of around 0.1cm s^{-1} which corresponds to a reduced velocity of around 300. PS 2700K gives curves similar to those for the other two excluded solutes except that the linear section occurs at higher values of H and increases with column length. One possible explanation of this higher value of H is that this very large molecule is being excluded from part of the volume outside the particles and that this extra plate height value is the polydispersity contribution arising from this secondary exclusion. However, this explanation is inconsistent because on the basis of molecular size versus "pore diameter", the degree of this secondary exclusion for a molecule of this size would be so small that x, in equation (5.39.), would be very large and hence the polydispersity contribution negligible.

Kaizuma et al (113) obtained plate height curves using glass beads over a very wide velocity range and observed maxima in these curves. These experiments are analagous to those carried out here since if conditions are ideal the only contribution to the plate height should arise from flow effects, i.e. the A term in the Knox equation or Giddings' coupled term. This does not, however, appear to be the explanation of the phenomenon observed in these results since the maximum in Kaizuma's work were found at much higher reduced velocities ($\nu \approx 3000$) and much lower reduced plate heights ($h \approx 10$).

The most satisfactory explanation, however, is that the observed results are caused by the interference of non-equilibrium processes or processes in which at high velocities only a very small fraction of the molecules may actually take part in the process, whereas at lower velocities a higher percentage of the solute molecules take part in the process. The influence of this non-equilibrium process(es) should lead to poorly shaped peaks as well as to an increase in the plate height as the velocity decreases. Figure 58 shows the variation of peak shape with velocity for PS 2700K. These shapes should not be compared quantitatively (since they were not all obtained at the same recorder chart speed) but it is seen that, in general, the peak shape deteriorates as velocity decreases in line with the above argument. The peak shapes for the other two excluded solutes did not show significant variation with velocity.

TABLE 5.1.

Values of $N_{app(max)}$ for various values of P and x

P	$(1+\alpha)$	$N_{app(max)}$ x = 4	x = 8	x = 12
1.001	1.003	16000	64000	144000
1.003	1.008	5400	21200	48000
1.010	1.029	1550	6200	14000
1.030	1.093	490	1950	4400
1.10	1.39	115	460	1040

TABLE 5.2.

Values of N_{app} for various values of P and N when x = 8

P	$(1+\alpha)$	N = 300	1000	3000	10,000	(a)	(b)
1.001	1.003	298	985	2870	8650	64000	
1.003	1.008	296	955	2630	6800	21200	
1.010	1.029	286	861	2025	3835	6200	
1.030	1.093	260	661	1225	1635	1950	
1.10	1.39	182	315	400	440	460	

Notes: a: values in this column are $N_{app(max)}$

b: values in this row are true plate numbers N.

Table 5.3.(a)

Plate Height versus Velocity data PS 33K 55 x 7mm column

$\frac{H_{app}}{10^{-4}\ cm}$	h_{app}	$\frac{u}{cm\ s^{-1}}$	ν
18.0	3.0	0.014	9
22.8	3.8	0.02	13
31.2	5.2	0.047	30
37.8	6.3	0.077	50
40.8	6.8	0.11	71
44.4	7.4	0.15	97
61.2	10.2	0.205	132
72.0	12.0	0.26	168

Table 5.3.(b)

Plate Height versus Velocity data PS 33K 101 x 7mm column

$\frac{H_{app}}{10^{-4}\ cm}$	h_{app}	$\frac{u}{cm\ s^{-1}}$	ν
27.5	4.6	0.0045	3
27.5	4.6	0.019	12
48.5	8.1	0.115	74
70.5	11.7	0.27	174
117.0	19.5	0.42	271
134.5	22.4	0.55	355

Table 5.3.(c)

Plate Height versus Velocity data PS 33K 257 x 7mm column

$\frac{H_{app}}{10^{-4}\ cm}$	h_{app}	$\frac{u}{cm\ s^{-1}}$	ν
73.0	12.2	0.045	29
76.0	12.7	0.07	46
81.0	13.5	0.10	65
79.0	13.2	0.13	84
93.5	15.6	0.16	103
104.0	17.3	0.19	122
103.5	17.3	0.215	139
104.5	17.4	0.24	155
129.5	21.6	0.26	168
143.0	23.8	0.30	193
143.0	23.8	0.35	226
141.5	23.6	0.40	258
172.5	28.7	0.44	284

Table 5.4.(a)

Plate height versus velocity data PS 20K 55 x 7mm column

$\frac{H_{app}}{10^{-4}\ cm}$	h_{app}	$\frac{u}{cm\ s^{-1}}$	ν
34.5	5.8	0.014	7
37.5	6.3	0.02	10
45.5	7.6	0.047	23
46.0	7.7	0.077	37
53.0	8.8	0.11	54
57.0	9.5	0.15	73
57.5	9.6	0.205	100
71.0	11.8	0.26	127
86.0	14.3	0.31	151
100.5	16.8	0.43	210
119.5	19.9	0.55	269

Table 5.4.(b)

Plate height versus velocity data PS 20K 101 x 7mm column

$\frac{H_{app}}{10^{-4}\ cm}$	h_{app}	$\frac{u}{cm\ s^{-1}}$	ν
56.5	9.4	0.0045	2
51.5	8.6	0.019	10
66.5	11.1	0.045	22
65.0	10.8	0.11	54
74.5	12.4	0.205	100
88.5	14.7	0.29	142
107.5	17.9	0.43	210
140.5	23.4	0.55	269
157.0	26.2	0.64	312
180.0	30.0	0.77	376

Table 5.4.(c)

Plate height versus velocity data PS 20K 257 x 7mm column

$\frac{H_{app}}{10^{-4}cm}$	h_{app}	$\frac{u}{cm\ s^{-1}}$	ν
103.5	17.2	0.011	5
116.0	19.3	0.045	22
117.0	19.5	0.07	34
119.0	19.8	0.10	49
122.0	20.3	0.13	64
128.0	21.3	0.16	78
139.0	23.2	0.19	92
139.5	23.2	0.215	104
142.5	23.7	0.24	118
150.0	25.0	0.26	127
152.5	25.3	0.30	146
169.0	28.2	0.35	170
182.0	30.3	0.40	196
182.0	30.3	0.44	215

Table 5.5.(a)

Plate height versus velocity data PS 10K 55 x 7mm column

$\frac{H_{app}}{10^{-4}\ cm}$	h_{app}	$\frac{u}{cm\ s^{-1}}$	ν
72.0	12.0	0.014	5
69.5	11.6	0.02	6
87.0	14.5	0.047	14
81.0	13.5	0.077	24
90.5	15.1	0.11	35
90.0	15.0	0.15	47
91.5	15.2	0.205	65
96.0	16.0	0.26	82
107.5	17.9	0.31	98
124.5	20.7	0.43	136
130.5	21.7	0.55	174

Table 5.5.(b)

Plate height versus velocity data PS 10K 101 x 7mm column

$\frac{H_{app}}{10^{-4}\ cm}$	h_{app}	$\frac{u}{cm\ s^{-1}}$	ν
147.0	24.5	0.0045	1.5
137.0	22.8	0.019	6
154.0	25.7	0.12	38
154.5	25.7	0.18	56
161.0	26.8	0.27	85
191.0	31.8	0.44	139
194.5	32.4	0.57	180
222.5	37.1	0.77	244

Table 5.5.(c)

Plate height versus velocity data PS 10K 257 x 7mm col

$\frac{H_{app}}{10^{-4}\ cm}$	h_{app}	$\frac{u}{cm\ s^{-1}}$	ν
328	54.7	0.011	4
365	60.8	0.045	14
335	55.9	0.07	22
341	56.8	0.10	31
324	54.0	0.13	41
340	56.7	0.16	50
336	56.0	0.19	60
338	56.3	0.215	68
344	57.3	0.24	76
358	59.8	0.26	82
364	60.7	0.30	95
380	63.4	0.35	110
383	63.9	0.40	126
351	58.5	0.44	139

Table 5.6.(a)

Plate height versus velocity data PS 4K 55 x 7mm column

$\frac{H_{app}}{10^{-4}\ cm}$	h_{app}	$\frac{u}{cm\ s^{-1}}$	ν
37.0	6.2	0.014	2
40.0	6.7	0.02	4
41.5	6.9	0.047	8
44.0	7.3	0.077	14
48.0	8.0	0.11	20
45.5	7.6	0.15	28
47.5	7.9	0.205	37
54.5	9.1	0.26	47
52.5	8.7	0.31	56
62.0	10.3	0.43	78
72.5	12.1	0.55	100

Table 5.6.(b)

Plate height versus velocity data PS 4K 101 x 7mm column

$\frac{H_{app}}{10^{-4}\ cm}$	h_{app}	$\frac{u}{cm\ s^{-1}}$	ν
85.0	14.2	0.0045	1
66.0	11.0	0.019	4
76.5	12.7	0.045	8
65.5	10.9	0.11	20
66.0	11.0	0.205	37
77.0	12.8	0.29	53
81.5	13.6	0.43	78
94.5	15.7	0.55	100
96.0	16.0	0.64	116
106.0	17.7	0.77	140

Table 5.6.(c)

Plate height versus velocity data PS 4K 257 x 7mm column

$\frac{H_{app}}{10^{-4}\ cm}$	h_{app}	$\frac{u}{cm\ s^{-1}}$	ν
153.5	23.8	0.011	2
140.5	23.3	0.045	8
143.5	23.8	0.07	13
141.5	23.5	0.10	18
151.5	25.2	0.13	24
147.5	24.5	0.16	29
144.5	24.0	0.19	35
145.0	24.2	0.215	40
155.0	25.8	0.24	43
171.5	28.5	0.26	47
164.0	27.3	0.30	55
152.0	25.3	0.35	64
165.5	27.5	0.40	73
171.5	28.5	0.44	80

Table 5.7.(a)

Plate height versus velocity data PS 2K 55 x 7mm column

$\frac{H_{app}}{10^{-4}\ cm}$	h_{app}	$\frac{u}{cm\ s^{-1}}$	ν
33.5	5.6	0.014	2
33.5	5.6	0.02	2
38.0	6.3	0.047	6
34.5	5.7	0.077	10
41.0	6.8	0.11	13
39.5	6.6	0.15	18
38.5	6.4	0.205	25
40.5	6.7	0.26	32
49.0	8,2	0.31	38
55.0	9.2	0.43	53
63.0	10.5	0.55	68

Table 5.7.(b)

Plate height versus velocity data PS 2K 101 x 7mm column

$\frac{H_{app}}{10^{-4}\ cm}$	h_{app}	$\frac{u}{cm\ s^{-1}}$	ν
85.0	14.2	0.0045	0.6
61.0	10.2	0.019	2.4
56.0	9.3	0.12	14
55.0	9.2	0.18	23
62.0	10.3	0.27	34
73.5	12.2	0.44	54
78.5	13.1	0.57	71
88.0	14.7	0.77	95

Table 5.7.(c)

Plate height versus velocity data PS 2K 257 x 7mm column

$\frac{H_{app}}{10^{-4}\ cm}$	h_{app}	$\frac{u}{cm\ s^{-1}}$	ν
155.5	25.8	0.011	1
140.5	23.3	0.045	6
127.5	21.2	0.07	8
129.5	21.5	0.10	12
131.0	21.8	0.13	16
127.0	21.2	0.16	19
133.0	22.2	0.19	24
138.5	23.0	0.215	26
138.5	23.0	0.24	30
128.0	21.3	0.26	32
149.5	23.2	0.30	37
143.5	23.8	0.35	43
149.0	24.8	0.40	49
143.0	23.8	0.44	54

Table 5.8.(a)

Plate height versus velocity data Benzene 55 x 7mm column

$\frac{H_{app}}{10^{-4}\ cm}$	h_{app}	$\frac{u}{cm\ s^{-1}}$	ν
95.0	15.8	0.014	0.2
62.0	10.3	0.02	0.4
32.5	5.4	0.047	0.8
24.0	4.0	0.077	1.3
19.5	3.2	0.11	1.9
16.0	2.7	0.15	2.6
13.0	2.2	0.205	3.6
13.0	2.2	0.26	4.6
13.5	2.2	0.31	5.4
16.5	2.7	0.43	7.4
22.5	3.7	0.55	9.6

Table 5.8.(b)

Plate height versus velocity data Benzene 101 x 7mm column

$\frac{H_{app}}{10^{-4}\ cm}$	h_{app}	$\frac{u}{cm\ s^{-1}}$	ν
212.5	35.4	0.0045	0.1
87.0	14.5	0.019	0.4
46.4	7.7	0.045	0.8
18.6	3.1	0.11	1.9
12.7	2.1	0.205	3.6
12.4	2.1	0.29	5.0
12.1	2.0	0.43	7.4
14.9	2.5	0.55	9.6
13.4	2.2	0.64	11.2
14.2	2.4	0.77	13.4

Table 5.8.(c)

Plate height versus velocity data Benzene 257 x 7mm column

$\frac{H_{app}}{10^{-4}\ cm}$	h_{app}	$\frac{u}{cm\ s^{-1}}$	ν
71.0	11.8	0.011	0.2
38.0	6.3	0.045	0.8
31.5	5.2	0.07	1.2
22.5	3.7	0.10	1.8
20.0	3.3	0.13	2.3
18.5	3.1	0.16	2.8
11.5	1.9	0.19	3.4
15.0	2.5	0.215	3.7
17.0	2.8	0.24	4.2
19.0	3.2	0.26	4.6
14.5	2.4	0.30	5.3
14.0	2.3	0.35	6.1
14.0	2.3	0.40	7.0
14.5	2.4	0.44	7.7

Table 5.9.(a)

Plate height versus velocity data m-dinitrobenzene 55 x 7mm column

$\frac{H_{app}}{10^{-4}\ cm}$	h_{app}	$\frac{u}{cm\ s^{-1}}$	ν
56.5	9.4	0.014	0.4
36.0	6.0	0.02	0.5
20.5	3.4	0.047	1.1
14.5	2.4	0.077	1.7
13.5	2.2	0.11	2.4
10.5	1.8	0.15	3.2
10.5	1.8	0.205	4.4
10.5	1.8	0.26	5.6
12.0	2.0	0.31	6.7
14.5	2.4	0.43	9.4
17.5	2.9	0.55	12.0

Table 5.9.(b)

Plate height versus velocity data m-dinitrobenzene 101 x 7mm column

$\frac{H_{app}}{10^{-4}\ cm}$	h_{app}	$\frac{u}{cm\ s^{-1}}$	ν
150.0	25.0	0.0045	0.1
53.5	8.9	0.019	0.5
34.5	5.7	0.045	1.0
14.9	2.5	0.11	2.4
10.2	1.7	0.205	4.4
11.6	1.9	0.29	6.4
13.3	2.2	0.43	9.4
14.1	2.3	0.55	12.0
13.8	2.3	0.64	13.9
14.5	2.4	0.77	16.7

Table 5.9.(c)

Plate height versus velocity data m-dinitrobenzene 257 x 7mm column

$\frac{H_{app}}{10^{-4}\ cm}$	h_{app}	$\frac{u}{cm\ s^{-1}}$	ν
69.5	11.6	0.011	0.2
31.5	5.2	0.045	1.0
24.5	4.1	0.07	1.6
18.5	3.1	0.10	2.2
18.0	3.0	0.13	2.9
17.5	2.9	0.16	3.5
14.0	2.3	0.19	4.1
15.0	2.5	0.215	4.7
12.0	2.0	0.24	5.2
16.5	2.7	0.26	5.6
14.0	2.3	0.30	6.5
14.0	2.3	0.35	7.6
14.5	2.4	0.40	8.6
14.5	2.4	0.44	9.6

Table 5.10.

Sample	Slope of H v $L/10^{-4}$	x	$(P-1)(1+\alpha)$	p
PS 2000	4.615	8.8	0.036	1.036
PS 4000	5.000	8.1	0.033	1.033
PS 10,000	12.5000	7.1	0.063	1.063
PS 20,800	3.635	6.4	0.015	1.015
PS 33,000	1.925	6.0	0.007	1.007

Table 5.11.

Sample	Column Length/mm	Slope of H v u Curve / 10^{-4} sec.	$\frac{\bar{C}}{10^{-4}\ \text{sec}}$	k"	$\frac{D_M}{10^{-10}\ m^2\ s^{-1}}$	$q_s \frac{D_M}{D_s}$	$\frac{D_M}{D_s}$ (q=0.033)
PS 2000	55	59.0	52	0.58	4.8	0.29	8.7
	101	53.0					
	257	54.0					
PS 4000	55	59.0	59	0.52	3.3	0.24	7.2
	101	51.0					
	257	68.0					
PS 10,000	55	111.0	101	0.35	1.9	0.26	7.8
	101	105.0					
	257	87.5					
PS 20,000	55	159.5	169	0.22	1.23	0.38	11.4
	101	162.5					
	257	185.0					
PS 33,000	55	213.0	221	0.12	0.93	0.56	16.8
	101	203.5					
	257	247.5					
BENZENE			8	0.79	34	0.29	8.7

Table 5.12.

Packing Material	Sample	qs $\frac{D_M}{D_s}$	$\frac{D_M}{D_S}$ (q = 0.033)
SG 60 F	Benzene	0.52	15
SG 60 F	PS 4K	0.51	15
PSM 40	PS 2000	0.34	10

Table 5.13.

Sample	$\frac{D_M}{D_s}$	$\frac{D_M}{D_S}$ (corrected)
PS 33K	16.8	15.8
PS 20K	11.4	7.4
PS 10K	7.8	6.3
PS 4K	7.2	3.6

CHAPTER 6.1.

INTRODUCTION

It has been mentioned several times earlier that sample loads were kept to below about 5ug in order to avoid overloading effects. Although the study of these effects was not a fundamental part of this work, it was necessary to determine at least qualitatively what these effects are, their magnitude and the factors which affect them in order that they may be eliminated or minimised so as not to interfere with the magnitude of the property being measured.

What I will say in this chapter will be more qualitative than quantitative but I believe that this is an important area of exclusion chromatography which should be pursued vigorously in the near future.

Done (114) found that in both adsorption and partition chromatography, on columns of very high efficiency, the plate height increased linearly with the sample load at loadings above as little as 1ug/g of packing material, that the effect was generally smaller for partition than for adsorption chromatography and that the effect decreases as k" decreases. Identical results have also been found by other workers (115). Most of the previous work on the effect of sample load on column efficiency has been carried out using very inefficient columns (116) leading to erroneous results. Chapter 6.3. deals with the effect of sample load on column efficiency for solutes which are totally and partially permeating on a highly efficient exclusion chromatography column.

Various authors (117, 118) have also pointed that the retention volume of partially permeating solutes in exclusion chromatography increases as sample load increases and this is studied in Chapter 6.2.

CHAPTER 6.2.

EFFECT OF SAMPLE LOAD ON RETENTION VOLUME

Very early in the development of exclusion chromatography, it was observed that overloading caused samples to elute later, thus appearing to be of lower molecular weight.

The retention volumes for various concentrations and injection volumes are given in Table 6.1. These results were obtained for PS 33K on a 100 x 7mm column packed with SG60F with dichloromethane as eluent.

Table 6.1.

Concentration $g\ cm^{-3} \times 10^2$	Injection volume		
	1ul	2.5ul	5ul
	V_r		
0.1	209	209	208
0.2	209	209	209
0.5	209	209	209
1.0	213	213	213
2.5	219	219	220
5.0	226	226	226
10.0	226	-	-

Two explanations have been put forward to account for this effect: a) viscous fingering (117) and b) macromolecular crowding effect (118). Viscous fingering occurs during elution at the rear boundary of a polymer sample, especially with a sample solution of appreciably higher viscosity than the eluent. Such a boundary is unstable as the eluent finds the easiest pathway and leaves fingers of the sample.

Macromolecular crowding effect also leads to an increase in the retention volume with concentration. As the concentration of the polymer sample increases, the individual macromolecular chains begin to be crowded and compressed compared to the sizes occupied by them at infinite dilution. This reduction of hydrodynamic volume causes the peaks to shift towards higher elution volumes.

The data in Table 6.1. indicates that the change of retention volume with sample load is a concentration effect rather than a sample size effect. There also appears to be a concentration below which there is no change in retention volume. However, in order to discuss this effect in more detail I suggest that this experiment should be repeated employing a more accurate means of measuring V_r and solutes of different molecular weight or degree of retention.

CHAPTER 6.3.

EFFECT OF SAMPLE LOAD ON COLUMN EFFICIENCY

Again, as in Chapter 6.2., a full treatment of this subject was not carried out. The only reason for looking at the effect of sample load on column efficiency was to ensure that we were working under conditions where the sample size did not interfere with the magnitude of the property being measured.

Figure 59 shows the variation of reduced plate height with sample size for three samples - PS 33K, PS 4K and benzene. This data was obtained on a 125 x 7mm column packed with SG60F with dichloromethane as eluent. Results were obtained using different injection volumes and concentrations and the only reasonable correlation obtained was between the plate height (or reduced plate height) and sample size (weight of sample injected). All these results were obtained at linear velocities around the minimum of the respective plate height versus velocity curves.

The variation of plate height with sample size was linear over the range of sample sizes used here and the slope of the reduced plate height versus sample size curves increases with the degree of exclusion.

The results are similar to those found for adsorption and partition chromatography except that in exclusion chromatography the rate of increases of plate height with sample size increases as k" decreases.

REFERENCES

1. M. TSWETT: Trav. Soc. Vat. Warsovie, 14, (1903).
2. R. KUHN, E. LEDERER and A. WINTERSTEIN: Ber. Deutsch. Chem. Gesell, 64, 1349 (1931) .
3. A.J.P. MARTIN and R.L.M. SYNGE: Biochem. J., 35, 1358 (194).
4. A.T. JAMES and A.J.P. MARTIN: Biochem. J., 50, 678 (1952).
5. J.J. KIRKLAND: J. Chromatog. Sci., 7, 7 (1969).
6. J.F.K. HUBER: J. Chromatog. Sci., 7, 85 (1969).
7. C. HOVARTH, B. PREISS and S.R. LIPSKY: Anal. Chem., 39, 1422 (1967).
8. J.N. DONE, G.J. KENNEDY and J.H. KNOX in "Gas Chromatography 1972". E. Perry, ed. Institute of Petroleum, London. 1973).
9. J.C. GIDDINGS: Anal. Chem., 39, 1027 (1967).
10. A. PRYDE: J. Chromatog. Sci., 12, 486 (1974).
11. J.W. McBAIN: Kolloid Z., 40, 1 (1926).
12. L. FRIEDMAN: J. Amer. Chem. Sco., 52, 1311 (1930).
13. J. PORATH and P. FLODIN: Nature, 183, 1657 (1959).
14. J.C. MOORE: J. Polym. Sci., 2A, 835 (1964).
15. H. FASOLD, G. GUNDLACH and F. TURBA in "Chromatography". E. Heftmann, ed. Reinhold, New York. 1966.
16. K.O. PEDERSON: Arch. Biochem. Biophys., Suppl. 1, 157 (1962).
17. R.L. STEERE and G.K. ACKERS: Nature, 194, 144 (1962).
18. S. HJERTEN and R. MOSBACH: Anal. Biochem., 3, 109 (1962).
19. H. DETERMANN: Angew. Chem., 76, 635 (1964).
20. J.F. LARGIER and A. POLSON: Biochim. Biophys. Acta., 79, 626 (1964).
21. J.A. CAMERON: J. Chromatog., 37, 331 (1968).
22. W. HALLER: J. Chromatog., 32, 676 (1968).
23. A. POLSON and W. KATZ: Biochem. J., 112, 387 (1969).
24. Recommendations on Nomenclature for Chromatography. Pure and Applied Chem., 37, 447 (1974).

25. J.J. KIRKLAND and P.E. ANTLE: J. Chromatog. Sci., 15, 137 (1977).

26. A.S.T.M. D-20.70.04. Bibliography on Liquid Exclusion Chromatography. ASTM, Philadelphia (1975).

27. W. HALLER: J. Chem. Phys., 42, 686 (1965).

28. A.J. De VRIES, M. Le PAGE, R. BEAU and C.L. GUILLEMIN: 3rd Int. G.P.C. Seminar, Geneva (1966).

29. J.H. ROSS and M.E. CASTO: J. Polym. Sci., C21, 142 (1968).

30. J. PORATH and H. BENNICK: Arch. Biochem. Biophys., Suppl. 1, 152 (1962).

31. A. KARMAN: Anal. Chem., 38, 286 (1966).

32. S.L. TERRY and F. RODRIGUEZ: J. Polym. Sci., C21, 191 (1968).

33. K.P. HUPE and E. BAYER: J. Gas Chromatog., 5, 197 (1967).

34. D. MacCALLUM: Macromol. Chem., 100, 117 (1967).

35. H. YAMAKAWA: Modern Theory of Polymer Solutions. Harper and Row, New York (1973).

36. H. BENOIT, Z. GRUBISIC, P. REMPP, C. DECKER and J.G. ZILLIOX: J. Chim. Phys., 63, 1507 (1966).

37. Z. GRUBISIC, P. REMPP and H. BENOIT: J. Polym. Sci., B5, 753 (1967).

38. A.C. OUANO: J. Polym. Sci., A1, 10, 2169 (1972).

39. A.C. OUANO: J. Polym. Sci., A1, 12, 1151 (1974).

40. A.C. OUANO: J. Chromatog., 118, 303 (1976).

41. D.M.W. ANDERSON, I.C.M. DEA and A. HENDRIE: Talanta, 18, 365 (1971).

42. W.A. DARK and R.J. LIMPERT: J. Chromatog. Sci., 11, 114 (1973).

43. W. HALLER: Nature, 206, 693 (1965).

44. H.P. HOOD and M.E. NORDBERG: U.S. Patent 2106744 (1943).

45. M.F. VAUGHAN: Nature, 188, 55 (1960).

46. H.L. MacDONELL: Nature, 189 302 (1961).

47. H.L. MacDONELL and J.P. WILLIAMS: Anal. Chem., 33, 1552 (1961).

48. M.I. DEVENTEVA, D.P. DOBYCHIN and V.E. SHEFTER: Russ. J. Phys. Chem., 36, 114 (1962).

49. J.H. KNOX and M. SALEEM: J. Chromatog. Sci., 7, 614 (1969).

50. J.F.K. HUBER: Chimia Suppl., 24, (1970).

51. J.J. KIRKLAND: J. Chromatog. Sci., 10, 593 (1972).

52. R.E. MAJORS: Anal. Chem., 44, 1722 (1972).

53. J.J. KIRKLAND in "Gas Chromatography 1972". E. Perry. ed. Institute of Petroleum, London (1973).

54. R.E. MAJORS: J. Chromatog. Sci., 11, 88 (1973).

55. J.J. KIRKLAND: J. Chromatog., 83, 149 (1973).

56. L.R. SNYDER and J.J. KIRKLAND, Introduction to Modern Liquid Modern Liquid Chromatography. Wiley-Interscience, New York (1974).

57. J.J. KIRKLAND: U.S. Patent 3782075.

58. R.K. ILER and H.J. McQUESTON: U.S. Patent 3955172.

59. K.K. UNGER: J. Chromatog., 83, 5 (1973).

60. K.K. UNGER: Colloid. Polym. Sci., 253, 658 (

61. J.J. KIRKLAND: J. Chromatog., 125, 231 (1976).

62. K.K. UNGER, R. KERN, M.C. NINOU and K.F. KREBS: J. Chromatog., 99, 435 (1974).

63. J.J. KIRKLAND: Chromatographia, 8, 661 (1975).

64. K.K. UNGER and P. RINGE: J. Chromatog. Sci., 9, 463 (1971).

65. F.E. REGNIER and R. NOEL: J. Chromatog. Sci., 14, 316 (1976).

66. S.H. CHANG, K.M. GOODING and F.E. REGNIER: J. Chromatog., 125, 103, (1976).

67. H. ENGELHARDT and D. MATHES: J. Chromatog., 142, 311 (1977).

68. W.W. YAU, C.R. GINNARD and J.J. KIRKLAND: J. Chromatog., 149, 465 (1978).

69. J.C. GIDDINGS, E. KUCERA, C.P. RUSSELL and M.N. MYERS: J. Phys. Chem., 72, 4397 (1968).

70. R.L. PECSOK and D. SAUNDERS: Sep. Sci., 1, 613 (1966).

71. T.C. LAURENT and J. KILLANDER: J. Chromatog., 14, 317 (1964).

72. E.F. CASSASSA: J. Polym. Sci., B5, 773 (1967).

73. J.C. MOORE and M.C. ARRINGTON: Int. Symp. on Macrom. Chem., Tokyo, Kyoto (1966).

74. E.F. CASSASSA and Y. TAGAMI: Macromol., 2, 14 (1969).

75. M.E. Van KREVELD and N. VAN DEN HOED: J. Chromatog., 83, 11 (1973).

76. G.K. ACKERS: Biochemistry, 3, 724 (1964).

77. E.M. RENKIN: J. Gen. Physiol., 38, 225 (1955).

78. W.W. YAU and C.P. MALONE: J. Polym. Sci., B5, 663 (1967).

79. W.W. YAU, C.P. MALONE and S.W. FLEMING: J. Polym. Sci., B6, 803 (1968).

80. W.W. YAU: J. Polym. Sci., A-2, 7, 483 (1969).

81. E.A. DiMARZIO and C.M. GUTTMAN: J. Polym. Sci., B7, 267 (1969).

82. E.A. DiMARZIO and C.M. GUTTMAN: Macromol., 3, 131 (1970).

83. E.A. DiMARZIO and C.M. GUTTMAN: Macromol., 3, 681 (1970).

84. E.F. CASSASSA: J. Phys. Chem., 75, 3929 (1971).

85. J.J. Van DEEMTER, F.J. ZUIDERWEG and A. KLINKENBERG: Chem. Eng. Sci., 5, 271 (1956).

86. J.C. GIDDINGS: Dynamics of Chromatography., Part 1., Dekker, New York. (1965).

87. J.C. GIDDINGS and K.L. MALLIK: Anal. Chem., 38, 997 (1966).

88. J.C. GIDDINGS: J. Chromatog., 13, 301 (1964).

89. J.N. DONE and J.H. KNOX: J. Chromatog. Sci., 10, 606 (1972).

90. J.H. KNOX and M. SALEEM: J. Chromatog. Sci., 7, 745 (1969).

91. G.J. KENNEDY and J.H. KNOX: J. Chromatog. Sci., 10, 549 (1972).

92. L.R. SNYDER: J. Chromatog. Sci., 7, 352 (1969).

93. F.W. BILLMEYER, G.W. JOHNSON and R.N. KELLEY: J. Chromatog., 34, 316 (1968).

94. R.N. KELLEY, F.W. BILLMEYER: Anal Chem., 41, 874 (1969).

95. R.N. KELLEY, F.W. BILLMEYER: Anal Chem., 42, 399 (1970).

96. G.I. TAYLOR: Proc. Roy. Soc., A219, 186 (1953).

97. M.E. Van KREVELD and N. VAN DEN HOED: J. Chromatog., 149 71 (1978).

98. P.A. BRISTOW, P.N. BRITTAIN, C.M. RILEY and B.F. WILLIAMSON: J. Chromatog., 113 57 (1977).

99. C.R. WILKE and P. CHANG: Amer. Inst. Chem. Engr. J., 264 (1955).

100. J.G. HENDRICKSON: J. Polym. Sci., A-2 6, 1903 (1968).

101. G.J. KENNEDY: Ph.D. Thesis, Univ. of Edinburgh (1973).

102. H. SCOTT, J.H. KNOX: Unpublished Work.

103. J.L. WATERS: J. Polym. Sci., A-2, 8, 411 (1970).

104. K. BOMBAUGH, W. DARK and R. LEVANGIE: J. Chrom. Sci., 7, 43 (1969).

105. L.H. TUNG, J.C. MOORE and G.W. KNIGHT: J. App. Polym. Sci., 10, 1261 (1966).

106. D.D. BLY: J. Polym. Sci., A-1, 6, 2085 (1968).

107. D.D. BLY: Anal. Chem., 41, 477 (1969).

108. J.H. KNOX and F. McLENNAN: Chromatographia, 10, 75 (1977).

109. L.K. SMITH, M.N. MYERS and J.C. GIDDINGS: Anal. Chem., 49, 1750 (1977).

110. J.H. KNOX and L. McLAREN: Anal. Chem., 36, 1477 (1964).

111. S.B. HOROWITZ and I.R. FENICHEL: J. Phys. Chem., 68 , 3378 (1964).

112. J.N. DONE, J.H. KNOX and J. LOHEAC: Applications of High Speed Liquid Chromatography. John Wiley. London, 1974.

113. H. KAIZUMA, M.N. MYERS and J.C. GIDDINGS: J. Chromatogr. Sci., 8, 630 (1970).

114. J.N. DONE: J. Chromatogr., 125, 43 (1976).

115. R.P.W. SCOTT and P. KUCERA: J. Chromatogr., 119, 467 (1976).

116. J. CHUANG and J.F. JOHNSON: Sep. Sci., 10, 161 (1975).

117. J.C. MOORE: Sep. Sci., 5, 723 (1970).

118. A. RUDIN: J. Polym. Sci., A1, 9, 2587 (1971).

APPENDIX 1

The Generalized Non- Equilibrium Theory of Chromatography Applied to the Calculation of the Stationary Phase Mass Transfer Term

This discussion will be restricted to the stationary phase mass transfer term since this is the most significant part of the total plate height expression under normal operating conditions in exclusion chromatography.

As was pointed out earlier, solute in a chromatographic zone is slightly out of equilibrium due to the moving concentration gradients and the inability of equilibration to keep up with this and it is this departure from equilibrium which is responsible for zone spreading.

The procedure used is to derive a general expression for the plate height in terms of departure from equilibrium, concentration gardients, velocities, physical dimensions and the equilibrium fractions in the system. The departure from equilibrium terms are then calculated for the particular phase under study and this leads to an explicit expression for the plate height in terms of the physical parameters and dimensions.

Before developing the theory a few important parameters must be defined. The solute concentration, c, the number of moles per unit volume of column, may be divided into two parts, c_m and c_s, the mobile and stationary phase contributions. At equilibrium these terms will be designated by c_m^* and c_s^* so that

$$c = c_m^* + c_s^* = c_m + c_s \qquad (A.1.)$$

From Chapter 1.2.1. we have that

$$\frac{c_m^*}{c_s^*} = \frac{1}{k''} = \frac{R}{1-R} \qquad (A.2.)$$

where R is the fraction of solute molecules in the mobile phase. The theory will be developed in terms of R rather than k'' since this leads to simpler equations.

We now introduce equilibrium departure terms ε_m and ε_s so that each ε term is the fractional departure from equilibrium.

$$\varepsilon_m = \frac{c_m - c_m^*}{c_m^*} \qquad (A.3.)$$

$$\varepsilon_s = \frac{c_s - c_s^*}{c_s^*} \qquad (A.4.)$$

or on rearranging

$$c_m = c_m^* (1 + \varepsilon_m) \qquad (A.5.)$$

$$c_s = c_s^* (1 + \varepsilon_s) \qquad (A.6.)$$

It is clear that the departure terms are not independent of each other since excess solute in one phase (over and above equilibrium) is accompanied by a deficit in the other. Combining equations (A.1.), (A.5.) and (A.6.) we see that this balance of non-equilibrium may be written in the form

$$c_m^* \varepsilon_m + c_s^* \varepsilon_s = 0 \qquad (A.7.)$$

so that we can write either non-equilibrium term in terms of

the other

$$\varepsilon_s = -\frac{c_m^* \varepsilon_m}{c_s^*} = -\frac{R\,\varepsilon_m}{(1-R)} \qquad (A.8.)$$

At this point it must be exphasised that these departures from equilibrium terms are small, i.e. there is rapid exchange of solute between the mobile and stationary phases. This assumption is one of the cornerstones of the theory and permits simplifications to be made where otherwise extreme difficulty would be encountered.

In order to consider the role of diffusion through the two phases it is necessary to focus our attention on the detailed processes occurring within a very small element of each phase rather than a small region of the overall column. Thus we may represent such local conditions by using primed symbols, i.e. c_i' is the <u>local concentration per unit volume of phase i</u>. At equilibrium the local concentration in phase i is denoted by $c_i^{*\prime}$ and it is important to note that this is always greater than the overall concentration by the ratio of the volumes to which they are related.

$$c_i^{*\prime} = c_i^* \times \frac{\text{total column volume}}{\text{volume of phase i in column}} \qquad (A.9.)$$

The local rate of accumulation of solute in phase i is defined by s_i' and the local downstream velocity in phase i is v_i' (note that $v_s' = 0$). Also note that the average of some local quantities, e.g. $\bar{v}_i'$ and $\bar{\varepsilon}_i$ are simply the overall quantities v_i and ε_i.

Zone spreading, as has already been mentioned, originates because at the front of the zone too much solute is transported forward and at the rear of the zone too little is transported forward. The amount of solute transported forward through a unit area normal to the flow in the unit time is given by the solute flux

$$J = \sum \int c_i' v_i' dA_i \qquad (A.10.)$$

where A_i is the fraction of cross-sectional area occupied by phase i. On writing c_i' in terms of the equilibrium departure

$$c_i' = c_i^{*\prime} (1 + \varepsilon_i')$$

equation (A.10.) becomes

$$J = \sum c_i^{*\prime} \int v_i' dA_i + \sum c_i^{*\prime} \int \varepsilon_i' v_i' dA_i \qquad (A.11.)$$

In this equation, the last term is the flux ΔJ responsible for zone spreading.

$$\Delta J = \sum c_i^{*\prime} \int \varepsilon_i' v_i' dA_i \qquad (A.12.)$$

Since $\frac{c_i^{*\prime}}{c_i^*} = \frac{1}{A_i}$ from equation (A.9.) and $c_i^* = X_i^* c$ then

$$c_i^{*\prime} = \frac{X_i^* c}{A_i} \qquad (A.13.)$$

where X_i^* is the equilibrium fraction of solute molecules in phase i. Thus

$$\Delta J = c\sum X_i^*\left(\frac{1}{A_i}\right)\int \varepsilon_i' v_i' dA_i \qquad (A.14.)$$

From Fick's first law, the flux of material during diffusion along a concentration gradient is always $-D\frac{\partial c}{\partial z}$ where D is the diffusion coefficient.

Therefore

$$\Delta J = -D\frac{\partial c}{\partial z} \qquad (A.15.)$$

where D is the apparent diffusion coefficient responsible for zone spreading.

Eliminating ΔJ between equations (A.14.) and (A.15.) gives

$$D = -\frac{\sum X_i^*\left(\frac{1}{A_i}\right)\int \varepsilon_i' v_i' dA_i}{\partial(\ln c)/\partial z} \qquad (A.16.)$$

and the plate height, $H = 2D/V$ is given by

$$H = -\frac{2\sum X_i^*\left(\frac{1}{A_i}\right)\int \varepsilon_i' v_i' dA_i}{V\,\partial(\ln c)/\partial z} \qquad (A.17.)$$

The summation in equation (A.17.) is only related to the mobile phase since $v_s' = 0$.

Therefore since $V = Rv$, $X_m^* = R$ and $\int \varepsilon_m' v_m' dA_m = \varepsilon_m v A_m$ equation (A.17.) is reduced to

$$H = \frac{-2\varepsilon_m}{\partial(\ln c)/\partial z} \qquad \text{(A.18.)}$$

This equation should not be construed to mean that H is inversely proportional to $\partial(\ln c)/\partial z$ or is independent of v since (as will be shown later) ε_m is of such a form as to cancel the former and to introduce a velocity proportional term.

We must now calculate the departure from equilibrium terms. This is done by equating mass transfer to both flow and to departure from equilibrium thus obtaining a relationship between the zones flow properties and the departure from equilibrium terms.

The rate of accumulation of solute within a phase is given by the three-dimensional form of Fick's second law.

$$s_i' = D_i \nabla^2 c_i' \qquad \text{(A.19.)}$$

where ∇^2 is the Laplacian operator.

Since $c_i^{*'}$ is a constant

$$\nabla^2 c_i' = c_i^{*'} \nabla^2 \varepsilon_i' \qquad \text{(A.20)}$$

and equation (A.19.) may be written in the form

$$s_i' = D_i c_i^{*'} \nabla^2 \varepsilon_i' \qquad \text{(A.21.)}$$

in which non-equilibrium has been related to mass transfer. Equation (A.21.) is valid if the diffusion coefficient D_i is constant which should be valid for the homogeneous phases found in chromatography.

The mass transfer rate may also be related to flow. The reason for this is that flow supplies new solute to a region and that this solute must be redistributed between the phases and the rate of this redistribution is obviously determined by the rate at which new solute is brought into the region by flow. By the conservation of mass we may write

$$\frac{\partial c_i'}{\partial t} = \left(\frac{dc_i'}{dt}\right)_{\text{mass transfer}} + \left(\frac{dc_i'}{dt}\right)_{\text{flow}} \qquad \text{(A.22.)}$$

i.e. the rate of increase in the local concentration in phase i, c_i', is equal to the increase caused by mass transfer plus the increase caused by flow in and out of the region.

The first term on the right hand side of equation (A.22.) is simply given by the mass transfer rate s_i' and the second is given by

$$\left(\frac{dc_i'}{dt}\right)_{\text{flow}} = v_i' \frac{\partial c_i'}{\partial z} \qquad \text{(A.23.)}$$

where $\frac{\partial c_i'}{\partial z}$ is the concentration gradient.

Thus

$$\frac{\partial c_i'}{\partial t} = s_i' - v_i' \frac{\partial c_i'}{\partial z} \qquad \text{(A.24.)}$$

If we now apply the near-equilibrium approximation we see that since c_i' and $c_i^{*\prime}$ are nearly equal, $\frac{\partial c_i'}{\partial t}$ and $\frac{\partial c_i'}{\partial z}$ may be replaced by $\frac{\partial c_i^{*\prime}}{\partial t}$ and $\frac{\partial c_i^{*\prime}}{\partial z}$ respectively, and equation (A.24.)

becomes on rearranging

$$s_i' \approx \frac{\partial c_i^{*'}}{\partial t} + v_i' \frac{\partial c_i^{*'}}{\partial z} \qquad (A.25.)$$

The term $\frac{\partial c_i^{*'}}{\partial t}$ may be converted to a distance derivative by noting that the entire concentration profile is advancing with a velocity of essentially V = Rv (note that there are slight departures from this at the front and back of the zone centre) and therefore

$$\frac{\partial c_i^{*'}}{\partial t} - V \frac{\partial c_i^{*'}}{\partial z} \qquad (A.26.)$$

and hence

$$s_i' = (v_i' - V) \frac{\partial c_i^{*'}}{\partial z} \qquad (A.27.)$$

By elimination of the s_i' term between equations (A.21.) and (A.27.) we see that

$$D_i c_i^{*} \nabla^2 \varepsilon_i' = (v_i' - V) \frac{\partial c_i^{*'}}{\partial z} \qquad (A.28.)$$

which links the departure from equilibrium terms with the zones flow properties. On rearrangement equation (A.28.) becomes

$$\nabla^2 \varepsilon_i' = \frac{(v_i' - V)}{D_i} \frac{\partial(\ln c)}{\partial z} \qquad (A.29.)$$

We must now obtain the stationary phase departure term through the integration of this equation and relate this to ε_m through the boundary and other conditions applicable to this differential equation. The direct integration of this equation over the whole

of the stationary phase, which would be impossible except in rather simple cases, is circumvented by the use of the general combination law.

In the application of this law it is assumed that the stationary phase can be divided into small units whose boundaries must have an open area of contact with the mobile phase but must be elsewhere impermeable to solute exchange. To a very good approximation the stationary phase lies mainly in the pores and the cavities of the support, thus fulfilling these criteria. These units are the smallest units of stationary phase which may be treated independently.

We must now define a new non-equilibrium parameter θ such that

$$\theta = \frac{(\varepsilon_s' - \varepsilon_m) D_s}{Rv \, \partial \ln c / \partial z} \qquad (A.30.)$$

At points where ε_s' is zero, θ is given by θ_o where

$$\theta_o = \frac{- \varepsilon_m D_s}{Rv \, \partial \ln c / \partial z} \qquad (A.31.)$$

Combining equations (A.18.) and (A.31.) we see that the plate height in terms of θ_o may be written

$$H = \frac{2Rv \, \theta_o}{D_s} \qquad (A.32.)$$

From equation (A.8.) we see that

$$\varepsilon_m R = - \bar{\varepsilon}_s' (1-R) \qquad (A.33.)$$

since $\bar{\varepsilon}_s' = \varepsilon_s$

and by rearranging equation (A.30.)

$$\bar{\varepsilon}_s' = \varepsilon_m + \frac{Rv}{D_s} \frac{\partial(\ln c)}{\partial z} \bar{\theta} \qquad (A.34.)$$

where $\bar{\theta}$ is the mean value of θ averaged over the total mass of the stationary phase in a small region of the column.

From equation (A.31.)

$$\varepsilon_m = - \theta_o \frac{Rv}{D_s} \frac{\partial(\ln c)}{\partial z} \qquad (A.35.)$$

and hence equations (A.33.) and (A.34.) on substitution of ε_m and rearranging become

$$\bar{\varepsilon}_s' = \frac{R\theta_o}{(1-R)} \frac{Rv}{D_s} \frac{\partial(\ln c)}{\partial z} \qquad (A.36.)$$

$$\bar{\varepsilon}_s' = (\bar{\theta} - \theta_o) \frac{Rv}{D_s} \frac{\partial(\ln c)}{\partial z} \qquad (A.37.)$$

On equating these two equations

$$\theta_o R = (\bar{\theta} - \theta_o)(1-R)$$

$$\text{or} \quad \theta_o = \bar{\theta}(1-R) \qquad (A.38.)$$

The plate height is now given by

$$H = \frac{2R(1-R)\, v}{D_s} \bar{\theta} \qquad (A.39.)$$

Since $\bar{\theta}$ is an average over the total stationary phase volume within a unit volume of the column, it may be written as

$$\bar{\theta} = \sum_j \left(\frac{V_j}{V_s}\right) \bar{\theta}_j \qquad \text{(A.40.)}$$

where V_j is the volume of unit j, V_s the stationary phase volume per unit column volume, $\bar{\theta}_j$ is the average value of θ within unit j and the summation is over all the units which the stationary phase divides itself into.

Thus

$$H = \frac{2R(1-R)v}{D_s} \sum_j \left(\frac{V_j}{V_s}\right) \bar{\theta}_j \qquad \text{(A.41.)}$$

The plate height is now made up of a sum of terms, each term being concerned only with a given unit of stationary phase.

We must now derive the $\bar{\theta}_j$'s.

The basic differential equation for the ε terms (A.29.) takes the following form for the stationary phase

$$\nabla^2 \varepsilon'_s = -\frac{Rv}{D_s} \frac{\partial(\ln c)}{\partial z} \qquad \text{(A.42.)}$$

and from equation (A.30.)

$$\nabla^2 \theta = \frac{D_s \nabla^2 \varepsilon'_s}{Rv \frac{\partial(\ln c)}{\partial z}} \qquad \text{(A.43.)}$$

Substituting $\nabla^2 \varepsilon_s'$ in this equation gives

$$\nabla^2 \theta = -1 \qquad \text{(A.44.)}$$

where the boundary conditions are

$$\frac{\partial \theta}{\partial w} = 0 \qquad \text{(A.45.)}$$

at the closed surface, and

$$\theta = 0 \qquad \text{(A.46.)}$$

at the open surface. w is normal to the bounding surface.

These equations can often usefully be expressed in terms of dimensionless parameters $\hat{x} = x/dj$ and $\hat{\theta}_j = \theta_{j/dj}^2$ where dj is the maximum depth of the unit from its open surface.

The plate height equation can now be written in terms of $\hat{\theta}_j$.

$$H = \frac{2R(1-R)v}{D_s} \sum_j \bar{\hat{\theta}}_j \frac{V_j}{V_s} d_j^s \qquad \text{(A.47.)}$$

$$\text{or} \quad H = \sum q_j \frac{V_j}{V_s} R(1-R) \frac{d_j^2 v}{D_s} \qquad \text{(A.48.)}$$

where q_j is a configuration factor and

$$q_j = 2 \bar{\hat{\theta}}_j \qquad \text{(A.49.)}$$

Equation (A.48.) may be approximated to

$$H = q\, R(1-R)\, \frac{d^2v}{D_s} \qquad (A.50.)$$

by assuming that there is only one kind of unit composing the total stationary phase. The configuration factor q can now be calculated for any solid pore structure, where the pores have a known configuration, by means of the basic θ equations.

Application to a Spherical Bead Model

This model is applicable to the porous spherical silicas used in this work. The basic differential equation for $\hat{\theta}$

$$\hat{\nabla}^2 \hat{\theta} = -1$$

becomes

$$\frac{1}{\hat{r}^2} \frac{\partial}{\partial \hat{r}} \left(\hat{r}^2 \frac{\partial \hat{\theta}}{\partial \hat{r}} \right) = -1 \qquad (A.51.)$$

in polar coordinates where $\hat{r}$ is the dimensionless radius measured from the bead centre. The integration of equation (A.51.) gives

$$\frac{\partial \hat{\theta}}{\partial \hat{r}} = -\frac{\hat{r}}{3} + \frac{c_o}{\hat{r}^2} \qquad (A.52.)$$

and

$$\hat{\theta} = -\frac{\hat{r}^2}{6} - \frac{c_o}{\hat{r}} + c_1 \qquad (A.53.)$$

where c_o and c_1 are integration constants. At the closed surface $\hat{r} = 0$ and $\frac{\partial \hat{\theta}}{\partial \hat{r}} = 0$ and therefore $c_o = 0$. At the open surface $\hat{r} = 1$ and $\hat{\theta} = 0$, therefore $c_1 = 1/6$ and

$$\hat{\theta} = -\frac{\hat{r}^2}{6} + 1/6 \qquad \text{(A.54.)}$$

The average value of $\hat{\theta}$ over the whole sphere is given by

$$\hat{\theta} = \frac{\int_0^1 4\pi\hat{\theta}\hat{r}^2 dr}{\int_0^1 4\pi\hat{r}^2 dr} = \frac{1}{15} \qquad \text{(A.55.)}$$

From equation (A.49.) q_j or q is given by $\frac{2}{15}$ and the plate height is given by

$$H = \frac{2}{15} R(1-R) \frac{r^2 v}{D_s} \qquad \text{(A.56.)}$$

or $$H = \frac{1}{30} R(1-R) \frac{d_p^2 v}{D_s} \qquad \text{(1.57.)}$$

where d_p is the bead diameter.

Since this value for the plate height is due completely to the stationary phase mass transfer, then $H = C_s v$ where

$$C_s = \frac{1}{30} R(1-R) \frac{d_p^2}{D_s} \qquad \text{(A.58.)}$$

or in terms of k"

$$C_s = \frac{1}{30} \frac{k''}{(1+k'')^2} \frac{d_p^2}{D_s} \qquad \text{(A.59.)}$$

APPENDIX 2

List of Symbols

A, A'	Coefficient of mobile phase term in plate height equations
A_i	Fraction of cross-sectional area occupied by phase i
a, a_s a_p	Mark Houwink's constants
$a_1 - a_5$	Huber's constants
B, B'	Coefficient of longitudinal diffusion term in plate height equation
C, C'	Coefficient of mass transfer terms in plate height equations
C_m, C_s	Resistances to mass transfer in the mobile and stationary phases
C_m, C_s	Equilibrium concentrations of the solute in the mobile and stationary phases
C_{mz}, C_{sz}	Equilibrium concentrations of the solute in the mobile and stationary zones
c	Number of moles of solute per unit volume of column
c_i'	Local concentration per unit volume of phase i
$c_i'^*$	Local concentration per unit volume of phase i at equilibrium
$\boldsymbol{c}_m$, $\boldsymbol{c}_s$	Number of moles of solute per unit volume of mobile and stationary phases
$\boldsymbol{c}_m^*$, $\boldsymbol{c}_s^*$	Number of moles of solute per unit volume of mobile and stationary phases at equilibrium
D	Distribution coefficient of the solute between the stationary and mobile phases
D, D'	Snyder's constants
D_m, D_s	Diffusion coefficients in the mobile and stationary phases
D_n	Overall dispersion number
$\overline{D}_r$	Average radial diffusivity
d_j	Depth of unit j of the stationary phase
d_p	Particle diameter

E_b	Energy of the bulk system
E_p	Energy of the pore system
ΔG	Free energy change
H, H.E.T.P.	Plate height. Height equivalent to a theoretical plate
ΔH	Enthalpy change
H_{app}	Plate height due to apparatus
H_{app}	Apparent plate height
H_{col}	Plate height due to column processes
$H_{intercept}$	Plate height at intercept of H_{app} versus column length curves
$H_{(kinetic)}$	Plate height due to kinetic processes within the column
H_{min}	Minimum plate height for a totally permeating monodisperse solute
$H_{(poly)}$	Plate height due to polydispersity
$H_{(total)}$	Total plate height
h	Planck's constant
h	reduced plate height
h_{app}	Apparent reduced plate height
h_c	Corrected reduced plate height
h_v	Velocity profile constant
J, ΔJ	Solute flux
K	Distribution coefficient of the solute between the stationary and mobile zones
K_m, K_{ms}, K_{mp}	Mark-Houwink's constants
k	Boltzmann's constant
k'	Phase capacity factor
k"	Zone capacity factor
$k"_{downstream}$	Zone capacity factor downstream of centre of band
$k"_{eq}$	Zone capacity factor at equilibrium (centre of band)

$k''_{upstream}$	Zone capacity factor upstream of centre of band
L	Column length
l	Step length
M, M_p, M_s	Molecular weight
M^*	Any molecular weight on linear portion of calibration curve
M_l	Lower molecular weight limit corresponding to V_t
M_n	Number average molecular weight
M_u	Upper molecular weight limit corresponding to V_o
M_w	Weight average molecular weight
M_2	Molecular weight of the solvent
δM	Infinitely small unit of molecular weight
N	Number of theoretical plates
N_{app}	Apparent number of theoretical plates
$N_{app(max)}$	Maximum value of N_{app}
n	Number of steps
n	Number of cycles in recycle chromatography
n	Number of peaks
P	Polydispersity
P(r)	Probability function
q_{bulk}	Partition function for the bulk liquid
q_j	Configuration factor
q_m, q_s	Quantities of solute in the mobile and stationary phases
q_m, q_s	Geometrical factors
q_{mz}, q_{sz}	Quantities of solute in the mobile and stationary zones
$q_{m(eq)}$, $q_{s(eq)}$	Quantities of solute in the mobile and stationary phases at equilibrium
q_{pores}	Partition function for the liquid in the pores

R	Radius of pore
R_c	Column radius
R_s	Resolution
r	Radius of polymer molecule
$\underline{r}$	Molecular position coordinate
S	Reciprocal of the gradient of the linear portion of a calibration curve
ΔS	Entropy change
s_i'	Local rate of accumulation of solute in phase i
T	Absolute temperature
t	Relaxation time for equilibration
t_o	Elution time of a totally excluded solute
u	Rate of movement of the mobile phase
u_{band}	Linear velocity of a band of solute molecules
u_{centre}	Velocity of the band centre
$u_{downstream}$	Velocity downstream of band centre
u_o	Linear velocity of mobile zone
u_{slice}	Velocity of a slice of a band
$u_{upstream}$	Velocity upstream of band centre
V_1	Molar volume of solute
V^*	Elution volume corresponding to M^*
$V_{available}$	Volume available to a molecule of radius r
V_j	Volume of unit j
V_m, V_s	Volumes of the mobile and stationary phases
V_{max}, V_{min}	Upper and lower limits of a volume period
V_{mz}, V_{sz}	Volumes of the mobile and stationary zones
V_r, $V_{r(1)}$, $V_{r(2)}$	Elution volume

V_o	Void volume of the column
V_p	Pore volume of the column
V_s	Volume of the solid of the matrix
V_s	Stationary phase volume per unit column volume
V_t	Void volume plus pore volume
V_{total}	Total volume of the pores
v_i'	Local downstream velocity of phase i
$\overline{w}$	Mean width of the peaks at the base
w_i	Geometrical factors
$w_{\frac{1}{2}}$	Half-height width of Gaussian peak
w_1, w_2	Width of peak at base
X_i^*	Equilibrium fraction of solute molecules in phase i
x	Hypothetical range of molecular weight measured in powers of e eluted over a volume V_r
δZ	Distance between adjacent peak maxima
δz	Displacement of two bands
α	A function of (P-1)
α	Geometrical factor
ε_m, ε_s	Equilibrium departure terms
η	Viscosity
$[\eta]$	Instrinsic Viscosity
θ, θ_o	Non-equilibrium parameter
$\overline{\theta}$	Mean value of θ averaged over the total stationary phase in a small region of the column
$\overline{\theta}_j$	Average value of θ within unit j
$\hat{\theta}_j$	Dimensionless non-equilibrium parameters
$\underline{\lambda}$	Molecular conformation coordinate
λ_i	Geometrical factor
ν	Reduced velocity

σ	Standard deviation of a distribution
σ_M	Standard deviation of a molecular weight distribution about the mean
σ_v	Standard deviation of a peak
σ^2	Variance of a distribution
σ_M^2	Variance of a molecular weight distribution about the mean
σ^2_{app}	Peak variance produced by the apparatus
σ^2_{col}	Peak variance produced by the column
σ^2_{total}	Total peak variance
$\sigma^2_{v(kinetic)}$	Peak variance due to kinetic processes within the column
$\sigma^2_{v(poly)}$	Peak variance due to polydispersity
$\sigma^2_{v(total)}$	Total peak variance
$\sigma^2_{v(kinetic\ total)}$	Peak variance due to kinetic processes after n cycles through the column
$\sigma^2_{v(poly\ total)}$	Peak variance due to polydispersity after n cycles through the column
Ψ	Molecular orientation coordinate
Ψ_2	Association factor

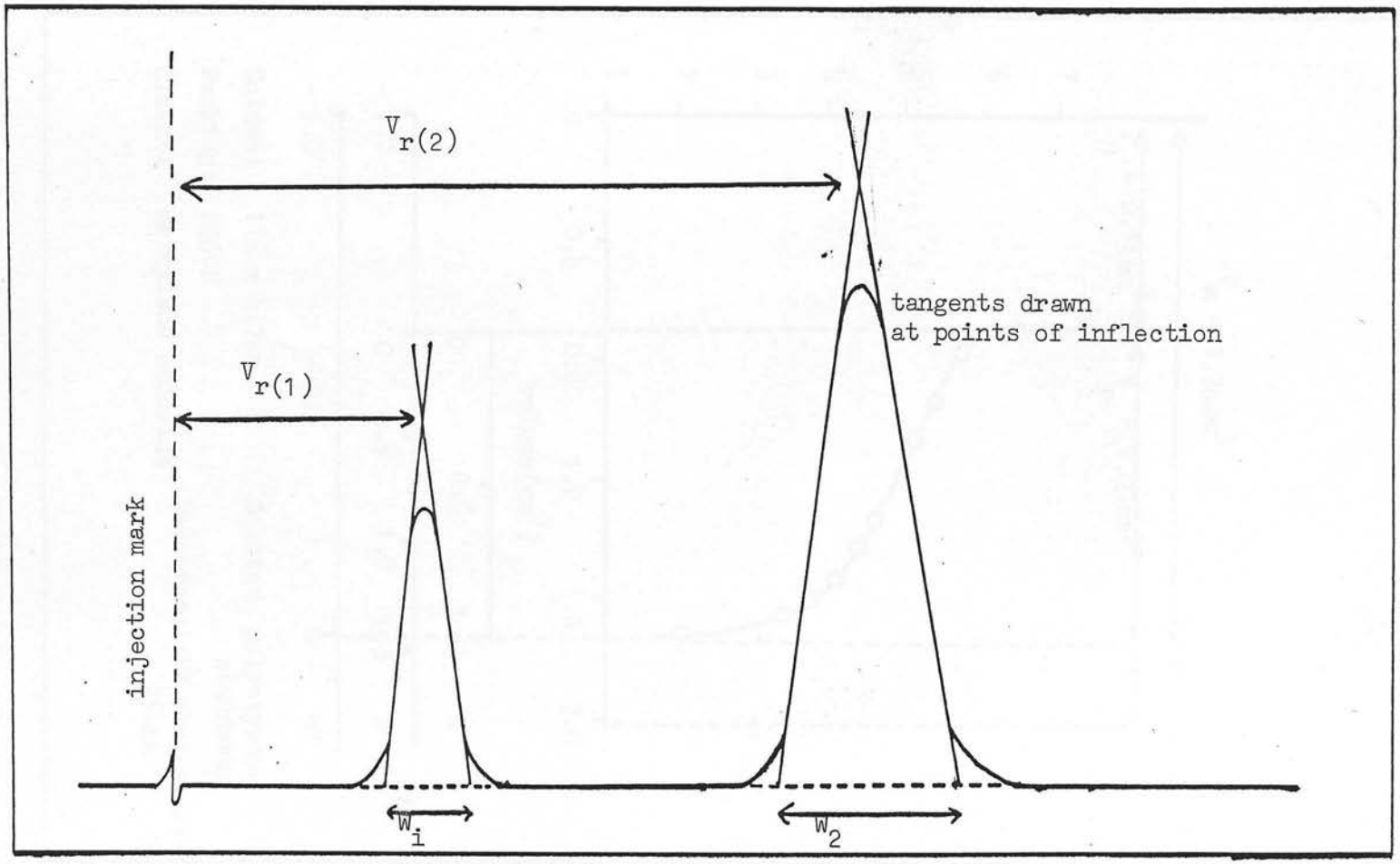

Figure 1: Elution record

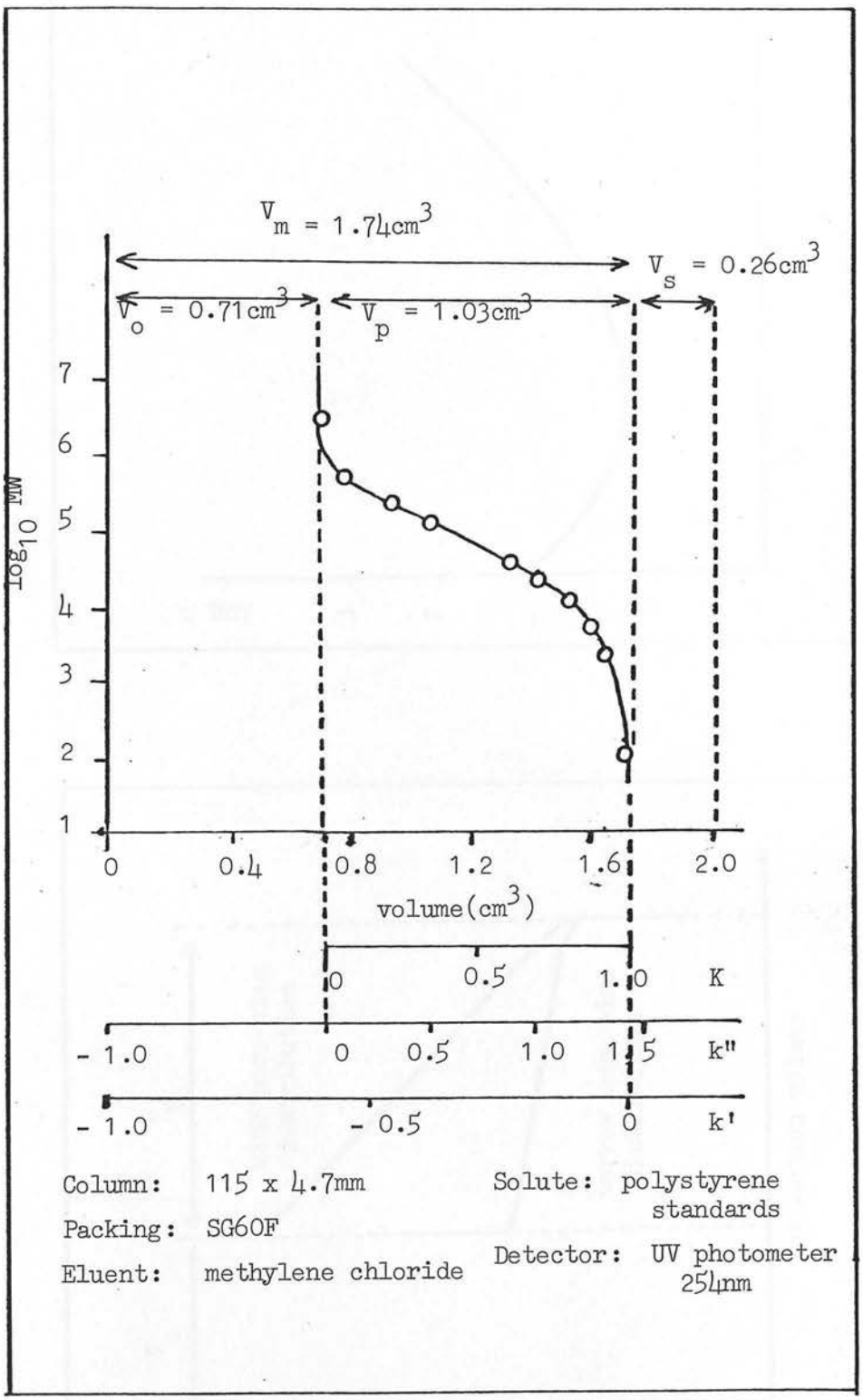

Figure 2: Calibration curve for SG60F showing the connection between the elution volume V_r and the various distribution ratios K, k" and k'.

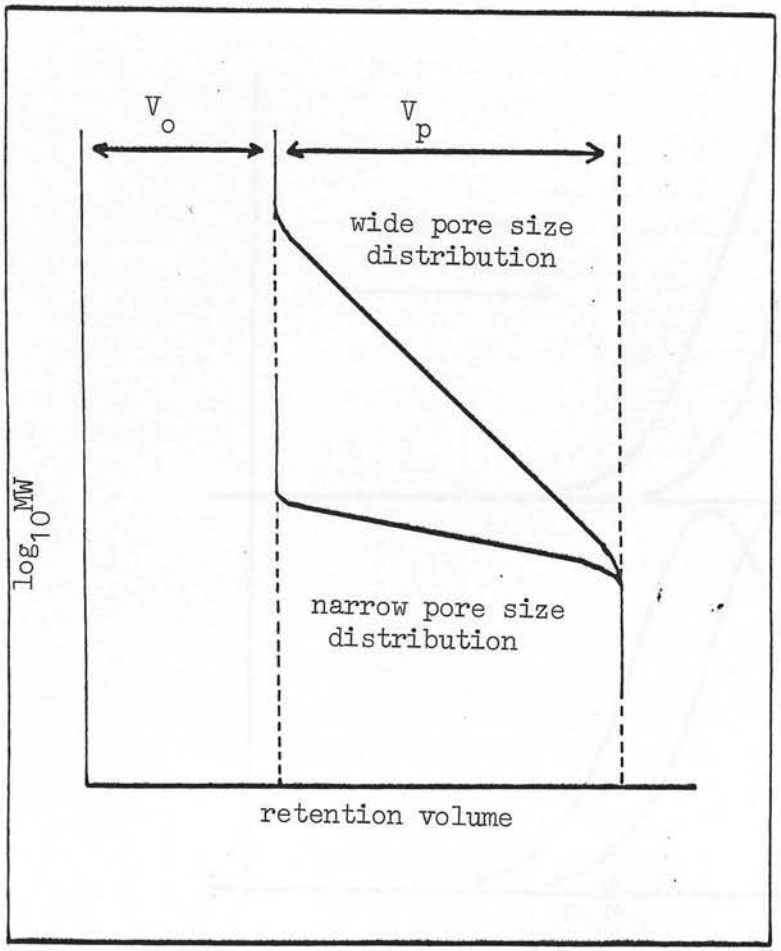

Figure 3: Hypothetical calibration curves for a narrow and a wide pore size distribution.

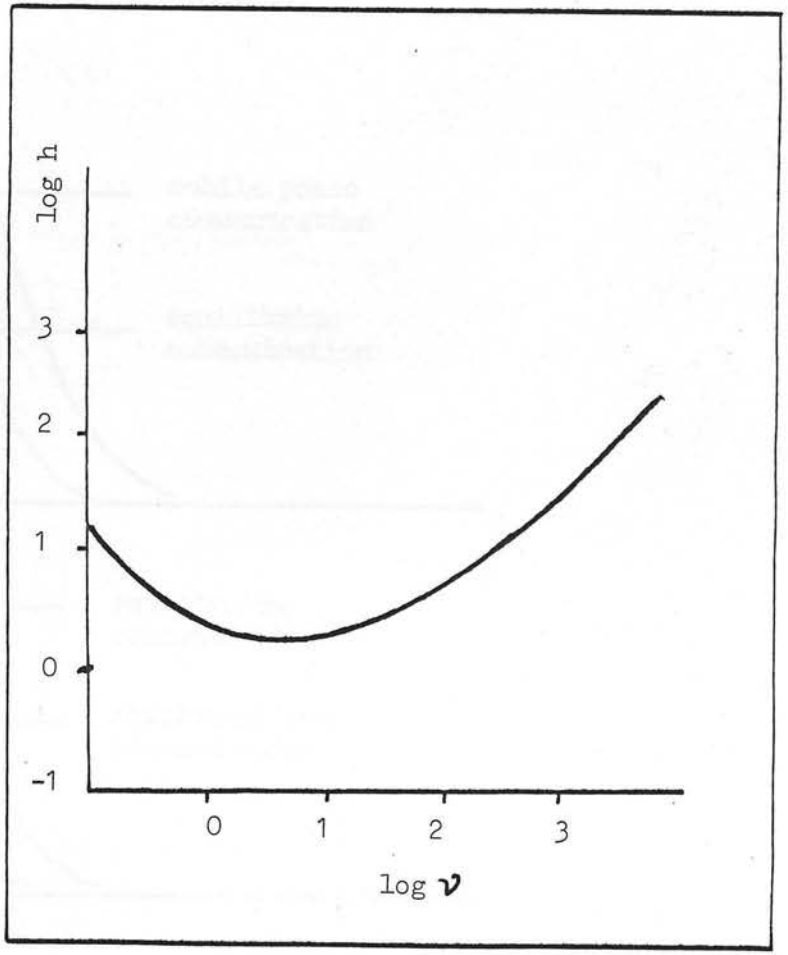

Figure 4: Dependence of reduced plate height, h, upon reduced velocity, ν.

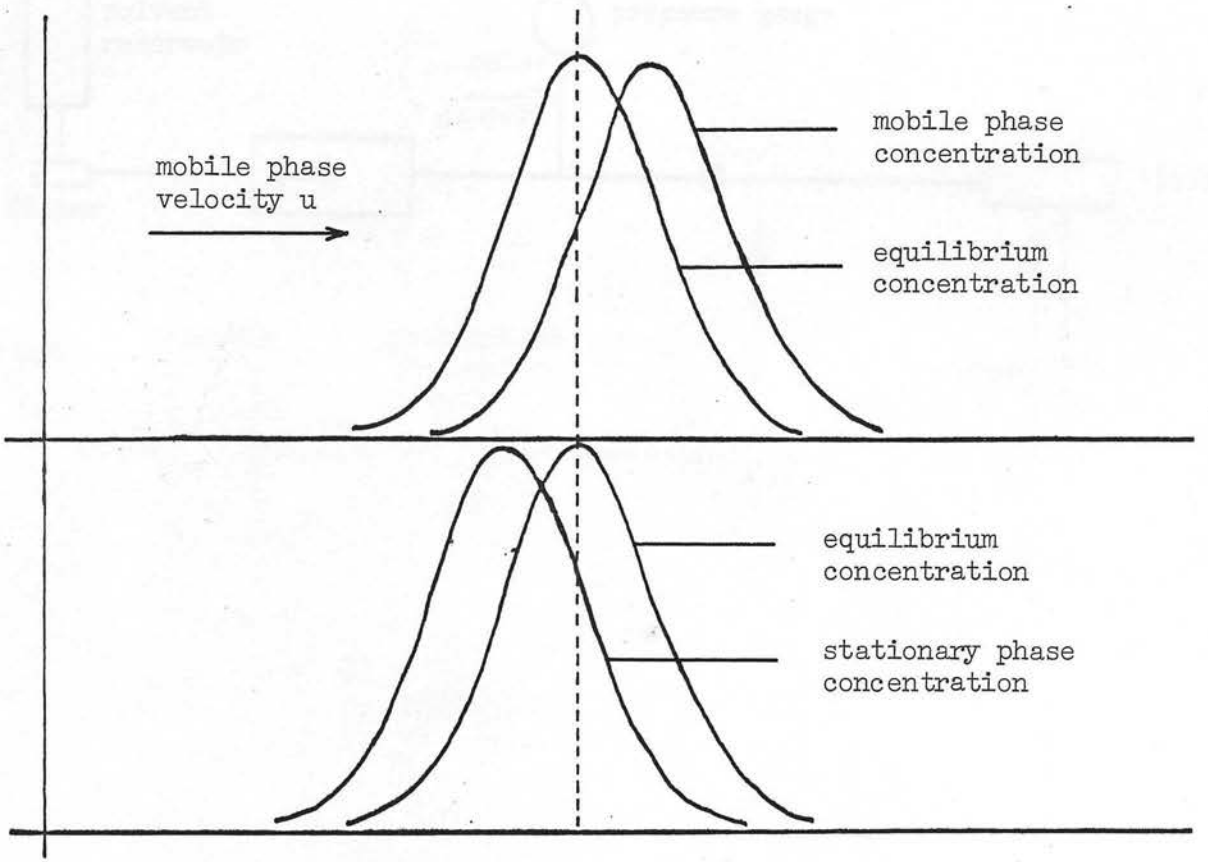

Figure 5: Relation of stationary and mobile phase concentrations profiles to the equilibrium profile

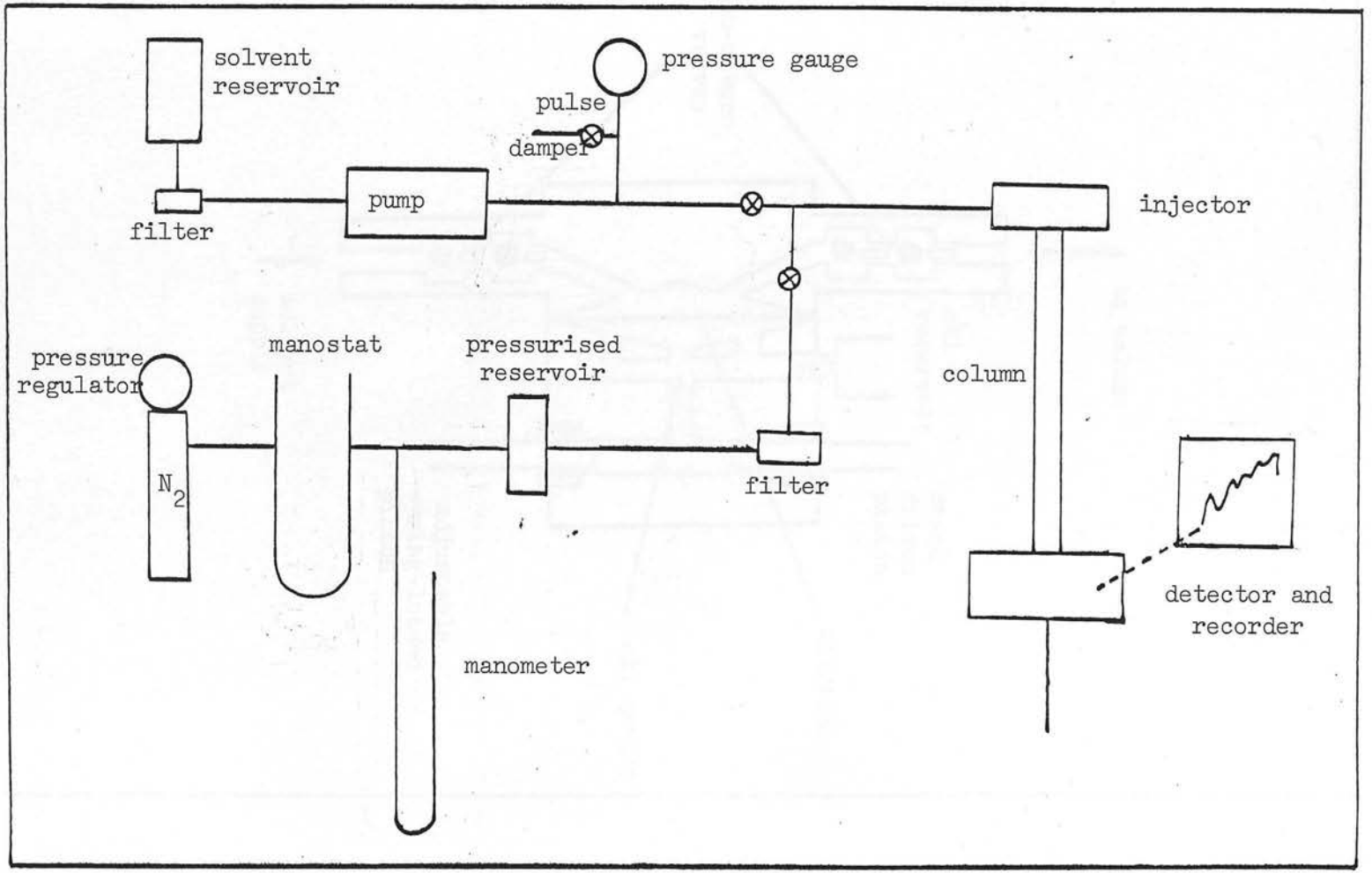

Figure 6: Schematic outline of equipment

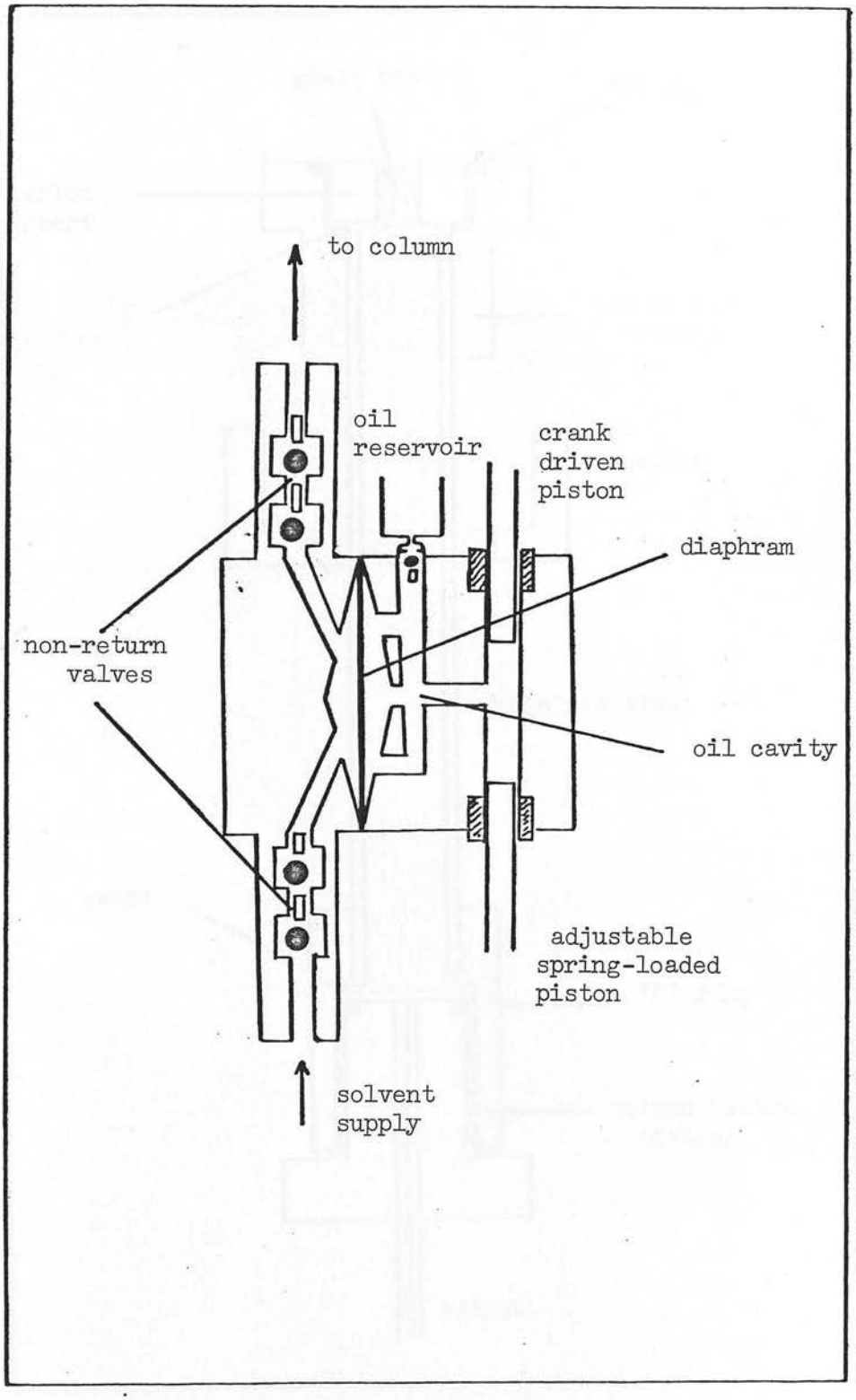

Figure 7: Orlita reciprocating pump

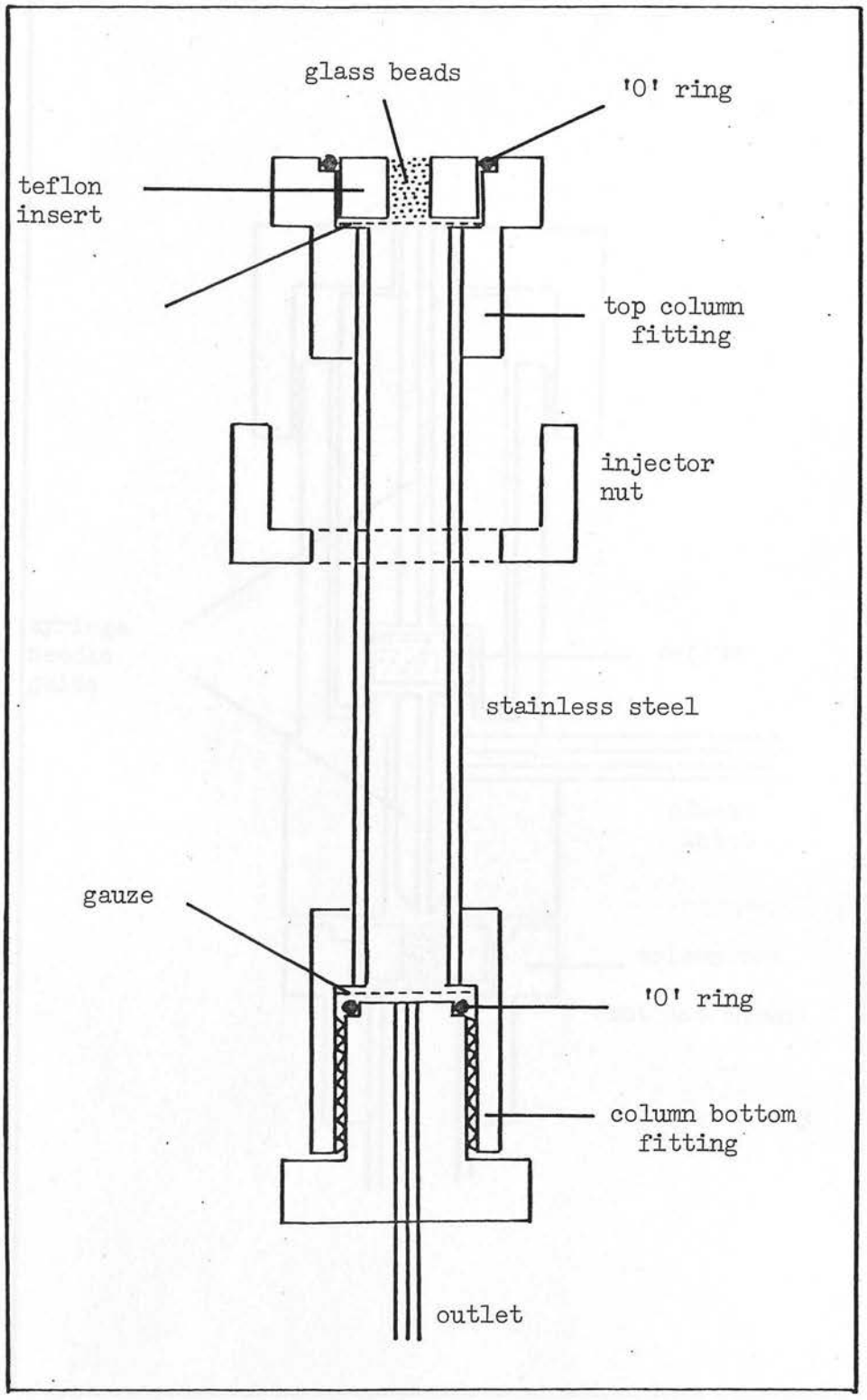

Figure 8: Column fittings

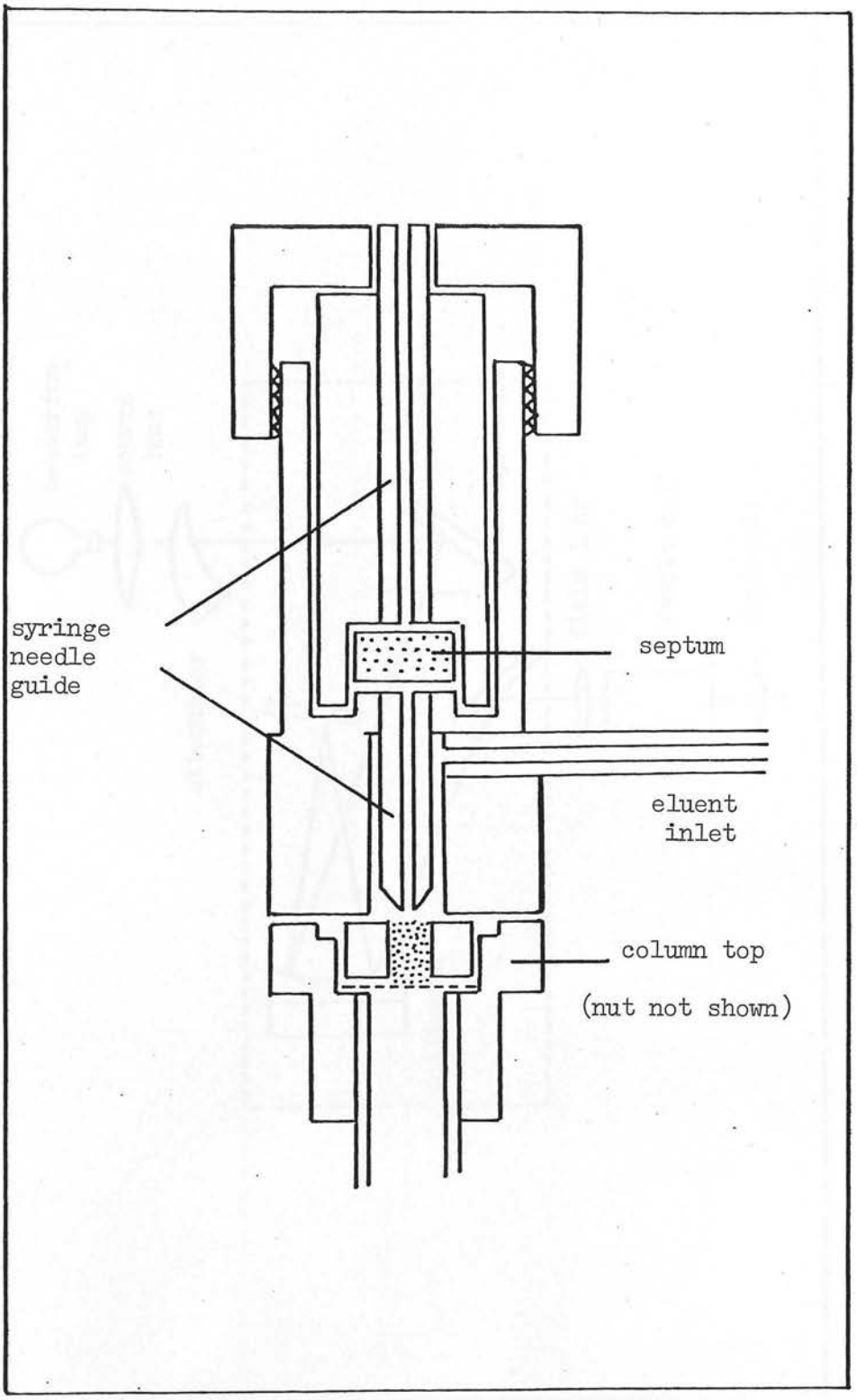

Figure 9: Column injector

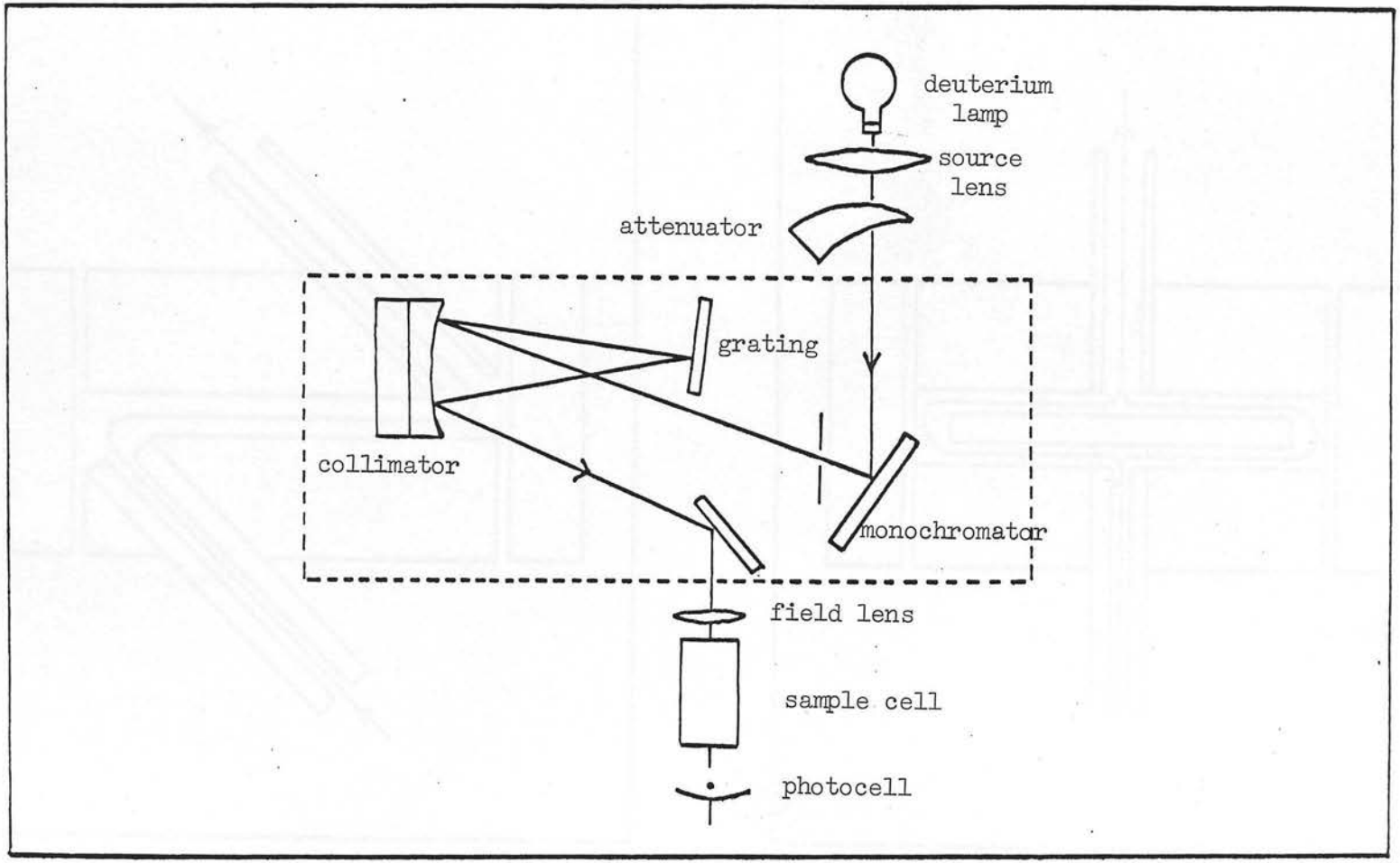

Figure 10: Cecil photometer

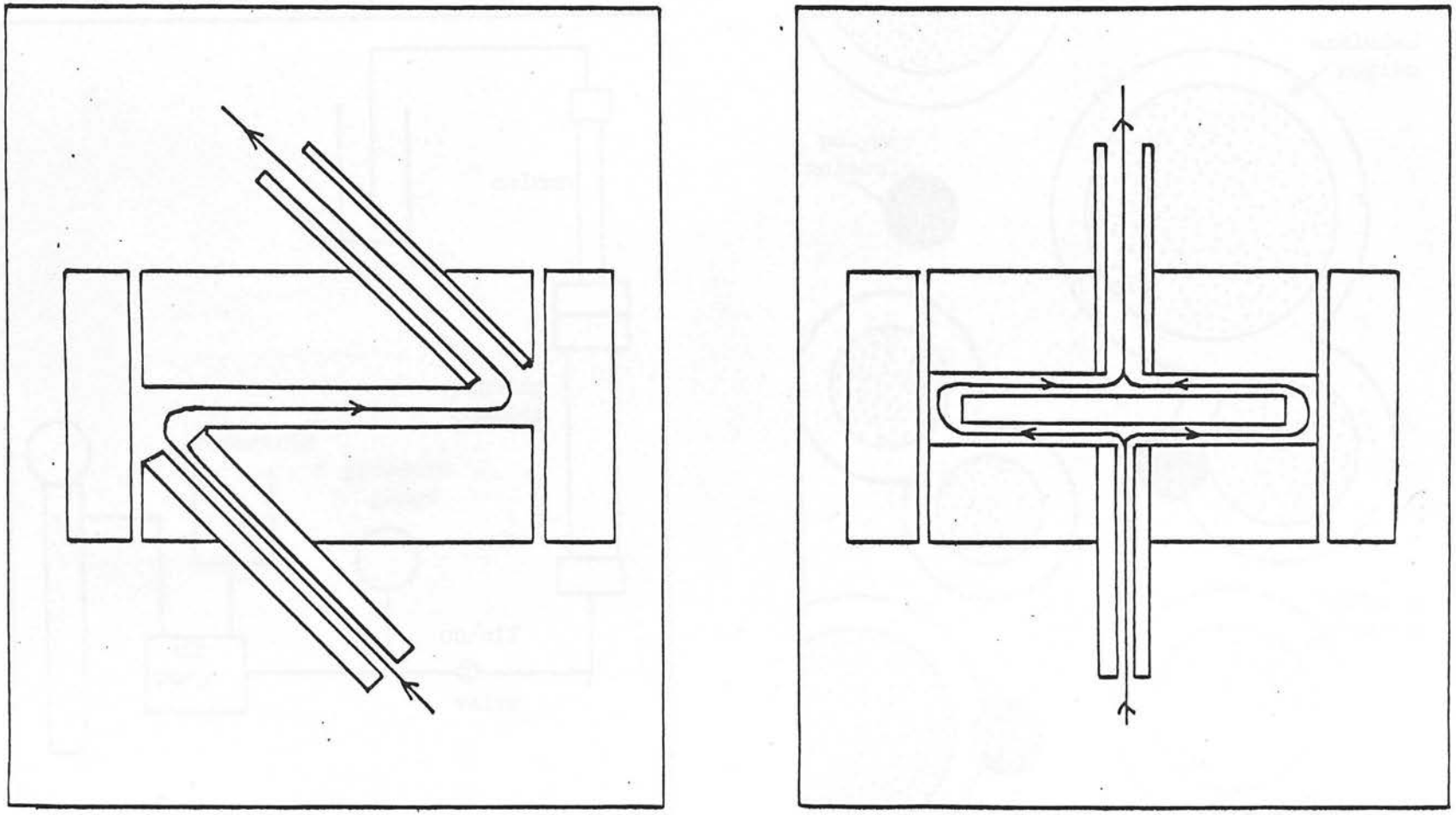

(a) (b)

Figure 11: Photometer flow-cells: (a) Z pattern (b) H pattern

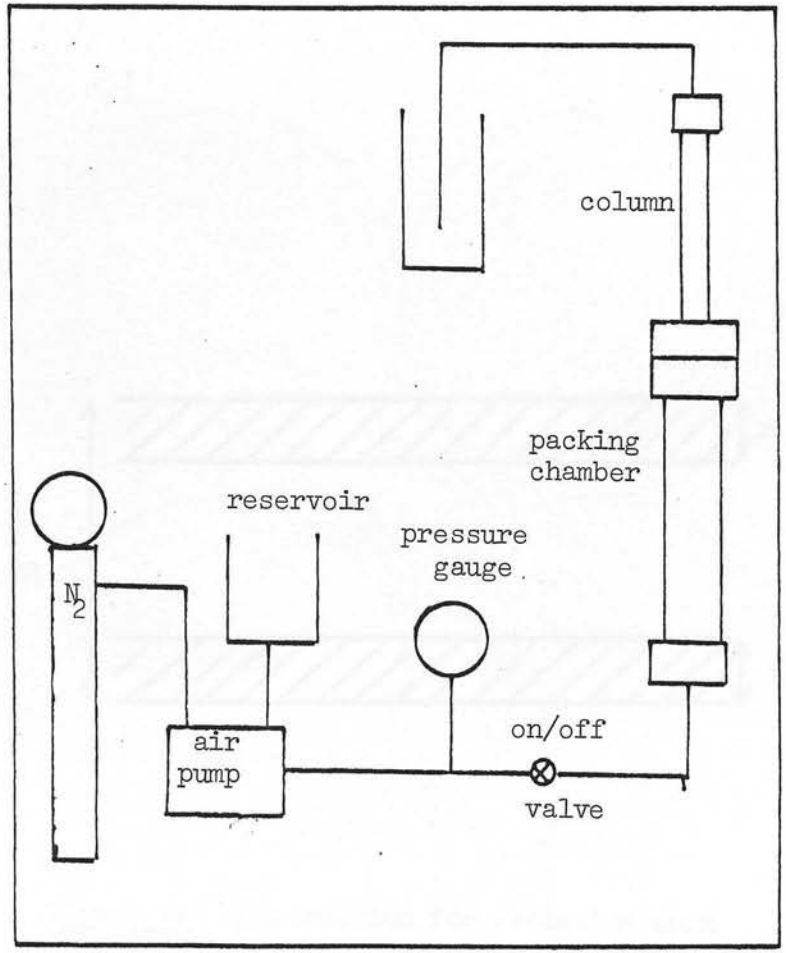

Figure 12: Slurry packing system

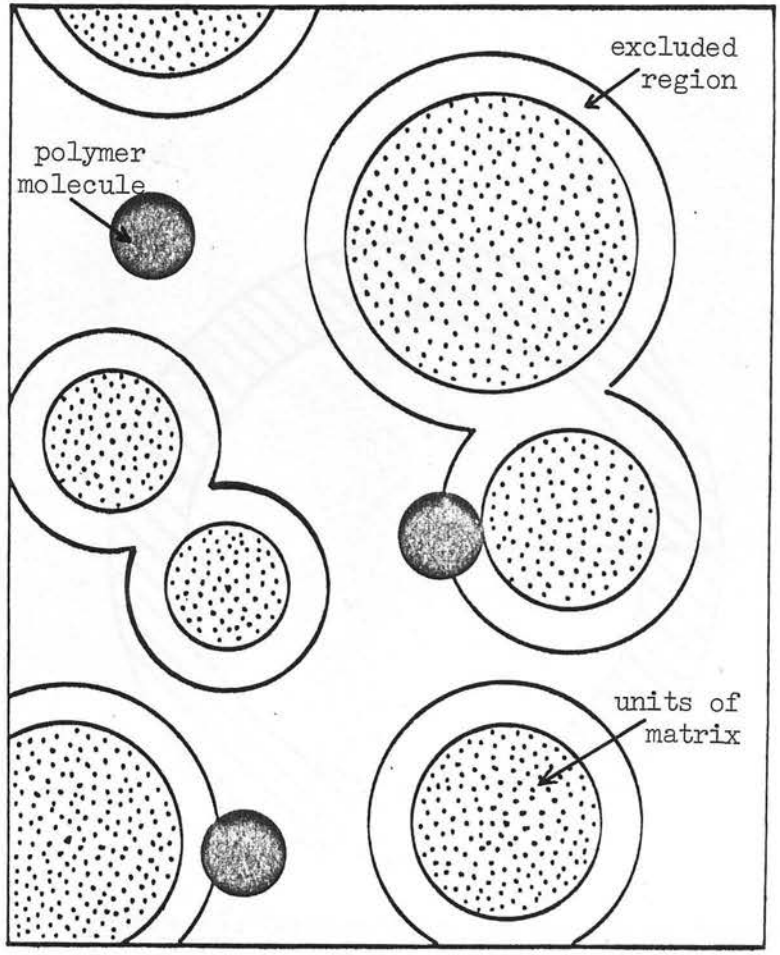

Figure 13: Principle of exclusion chromatography

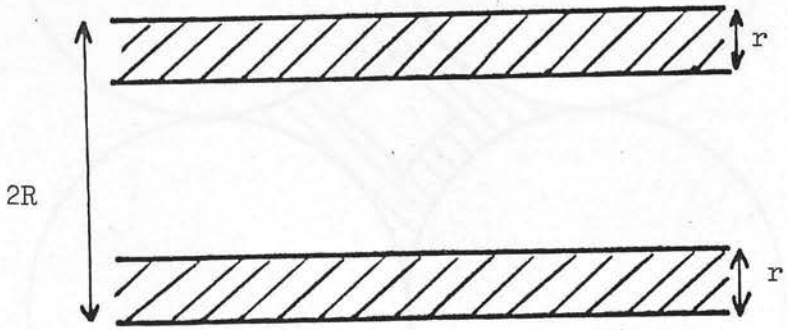

Figure 14: Construction for exclusion from infinite parallel plates

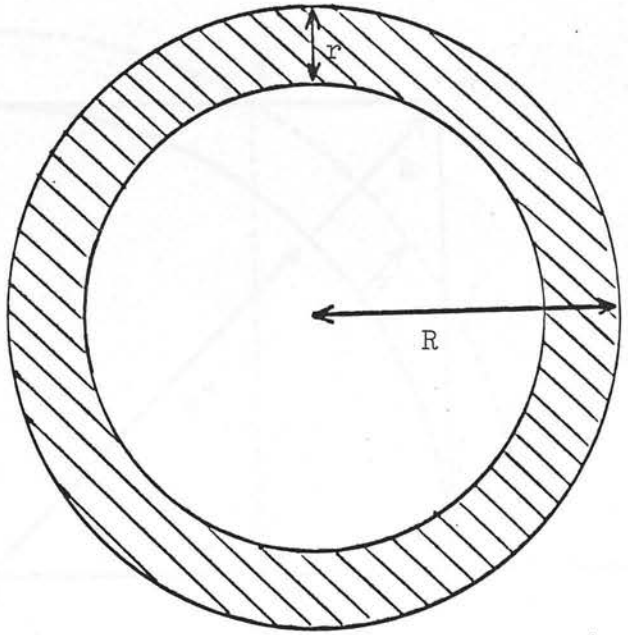

Figure 15: Construction for exclusion from an infinite cylinder

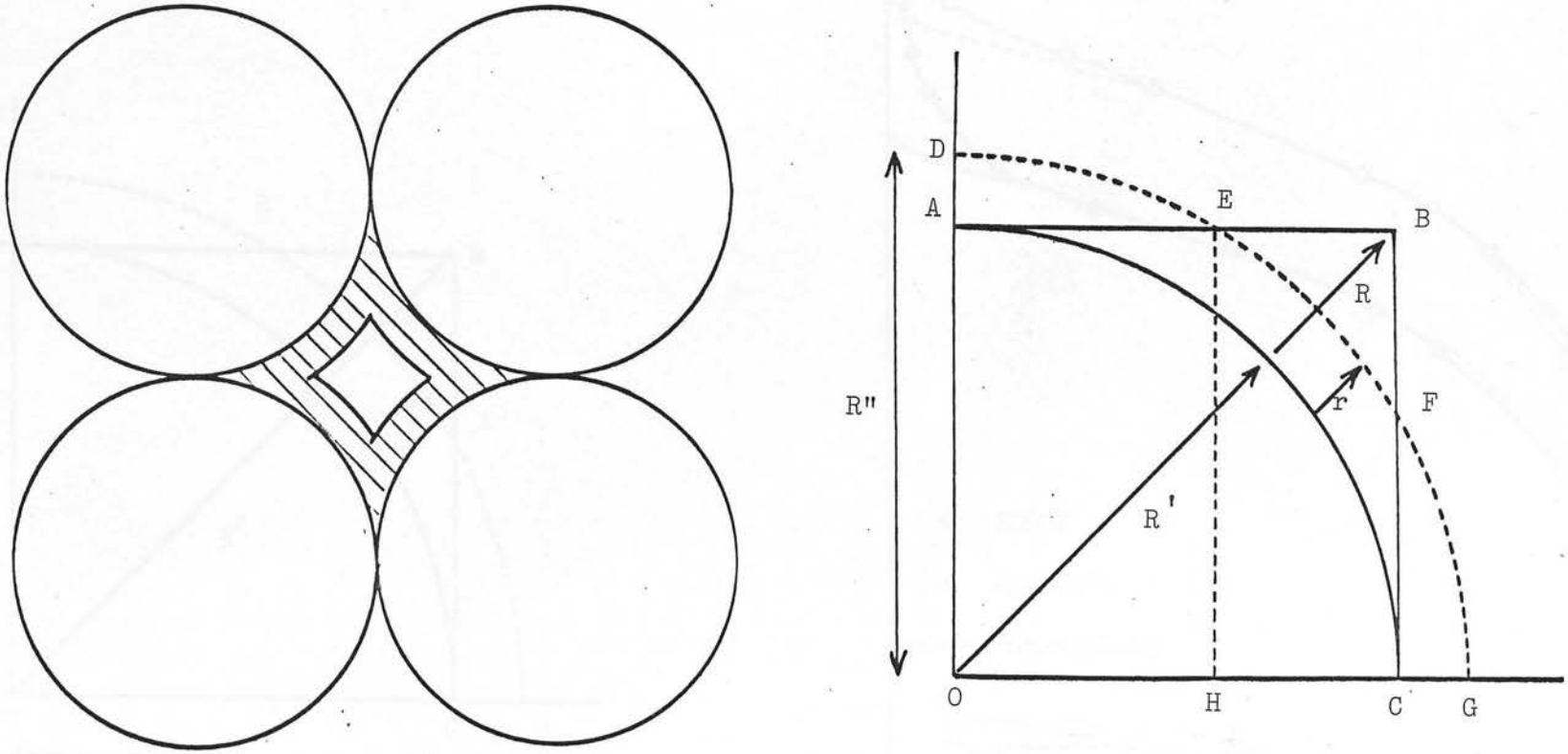

Figure 16, 17: Constructions for exclusion from an inverse cylinder

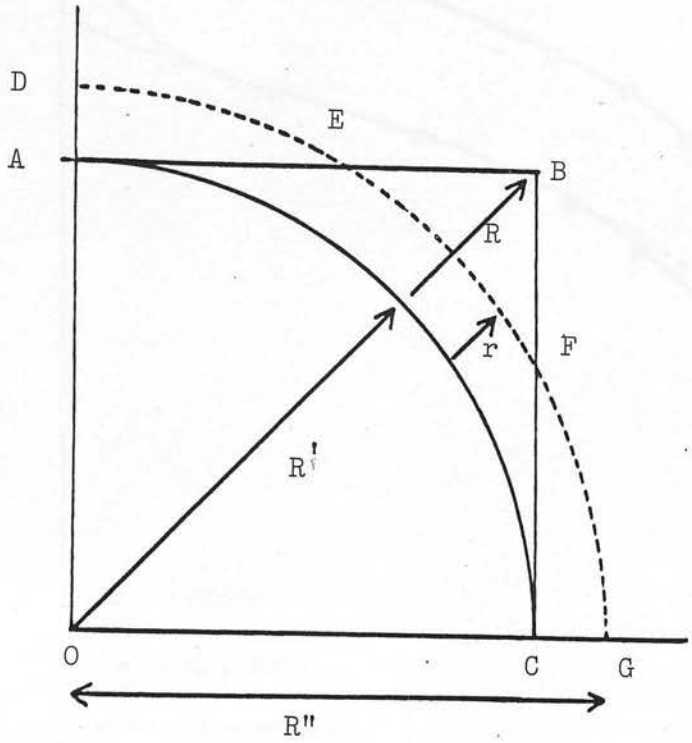

Figure 18: Construction for exclusion from an inverse sphere

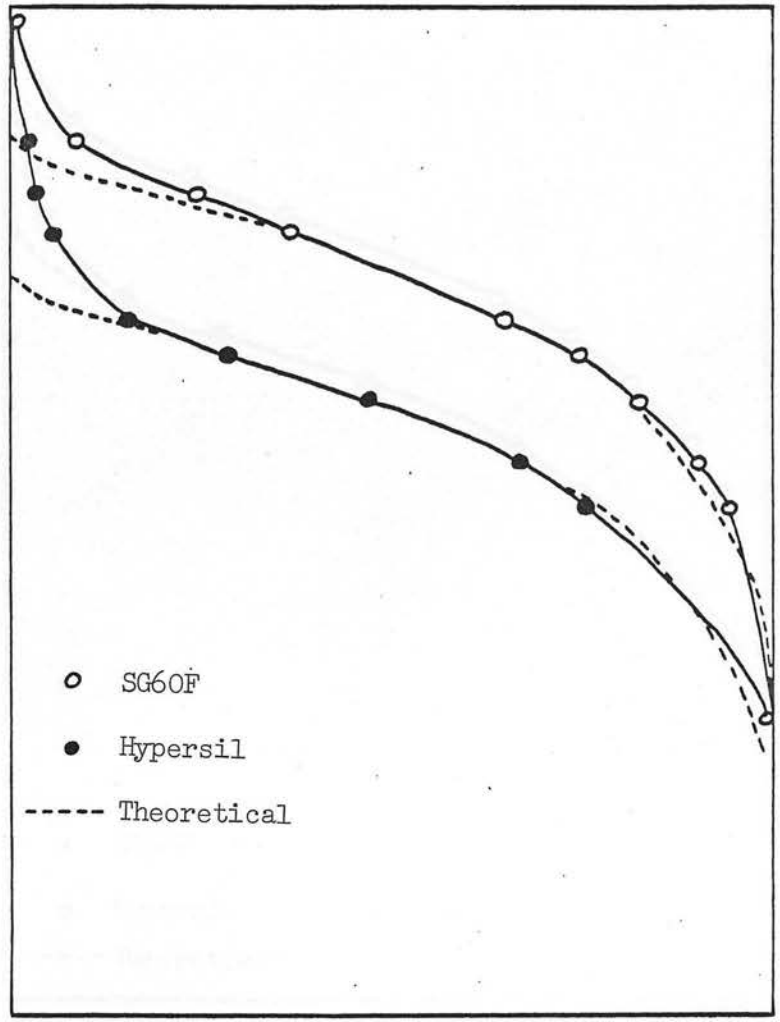

Figure 19: Experimental data and theoretical curves for infinite parallel plates

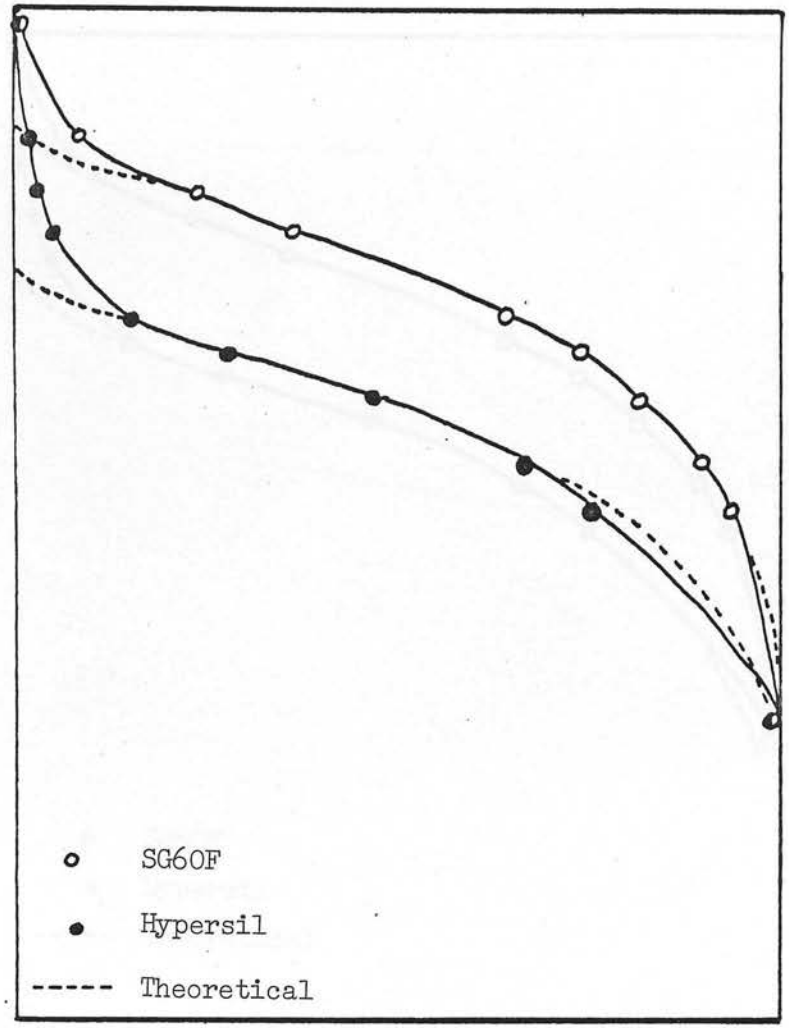

Figure 20: Experimental data and theoretical curves for an infinite cylinder

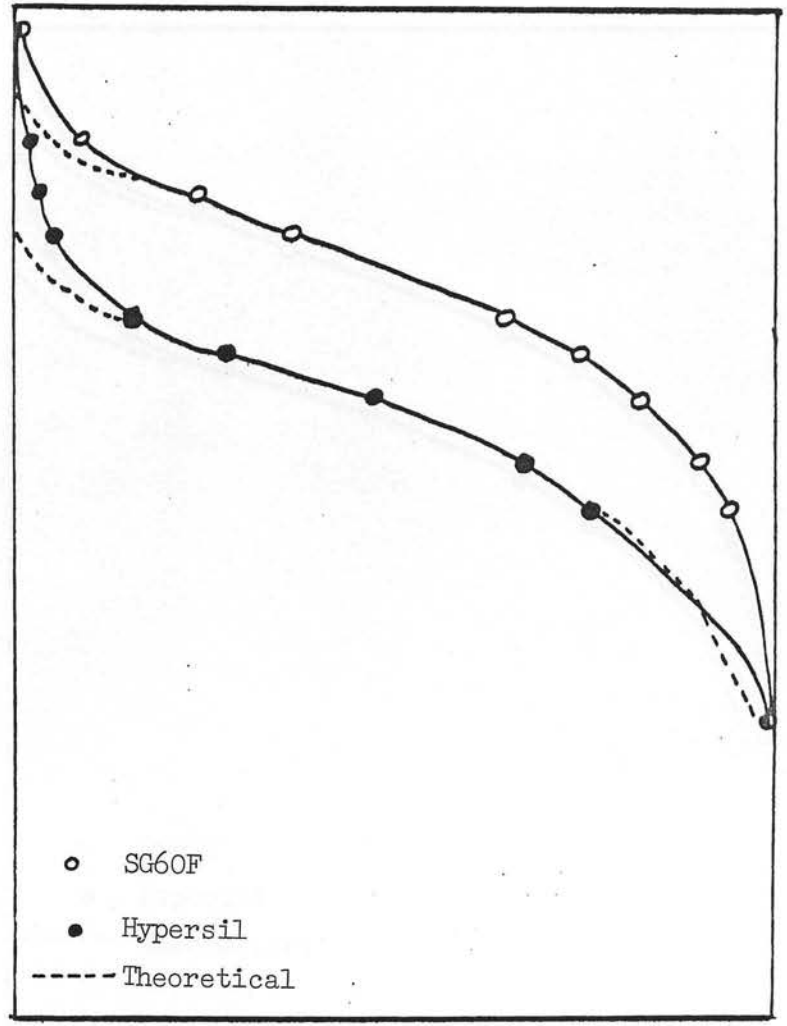

Figure 21: Experimental data and theoretical curves for a sphere

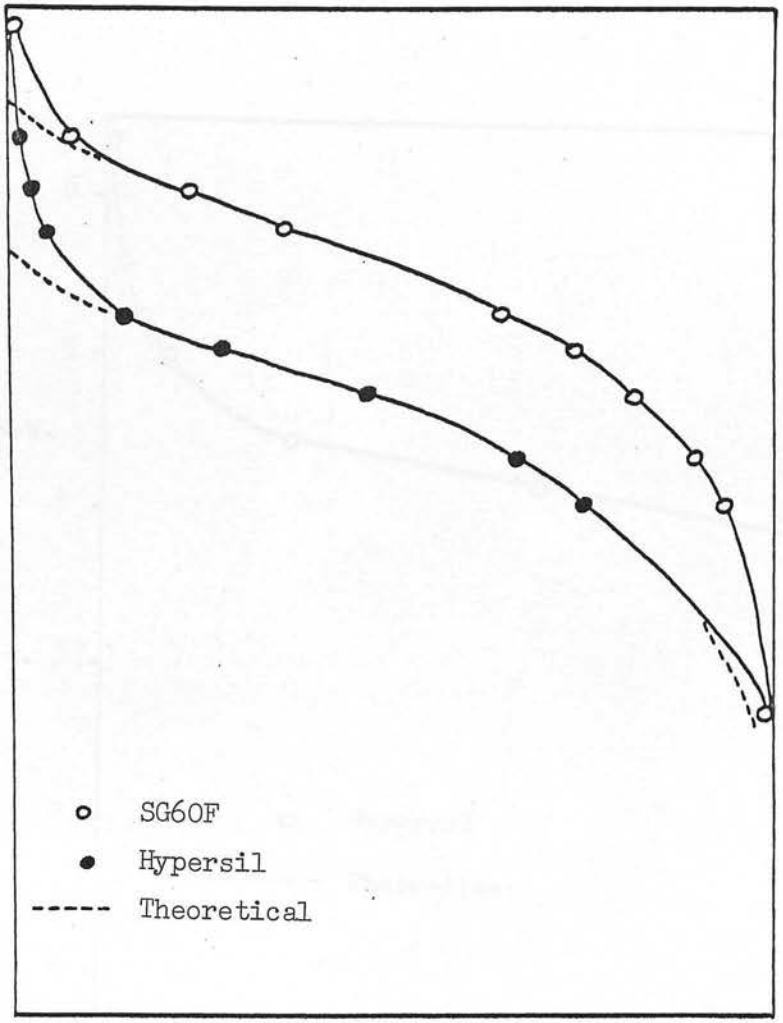

Figure 22: Experimental data and theoretical curves for an inverse cylinder

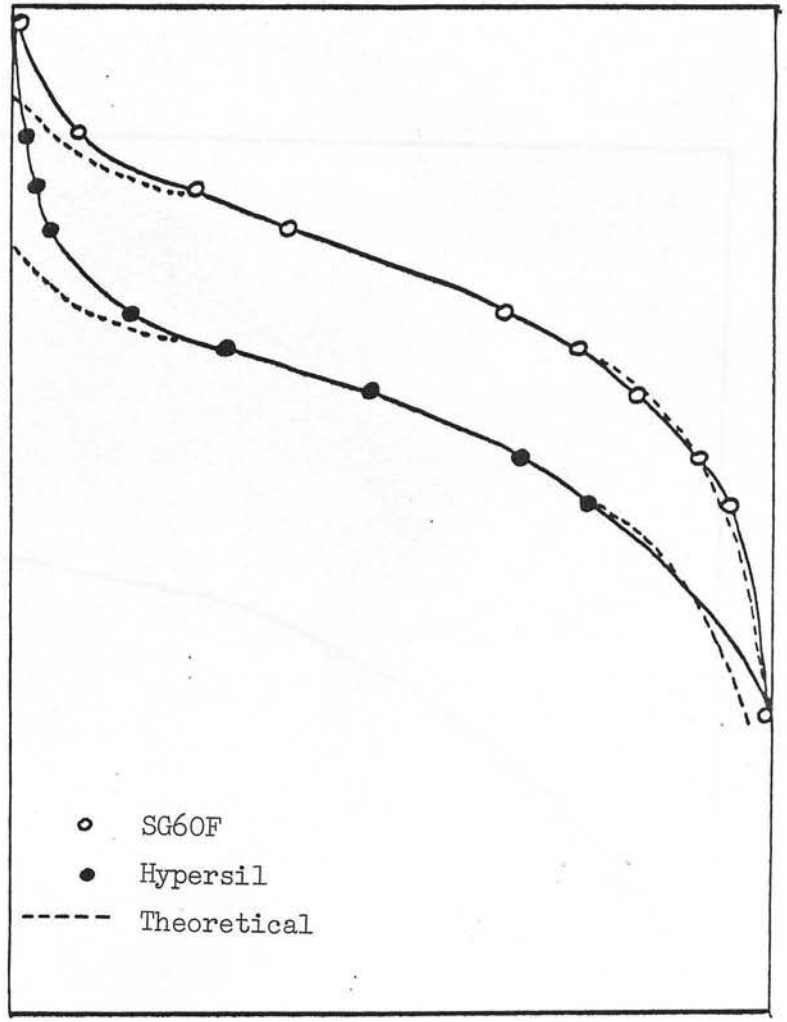

Figure 23: Experimental data and theoretical curves for an inverse sphere

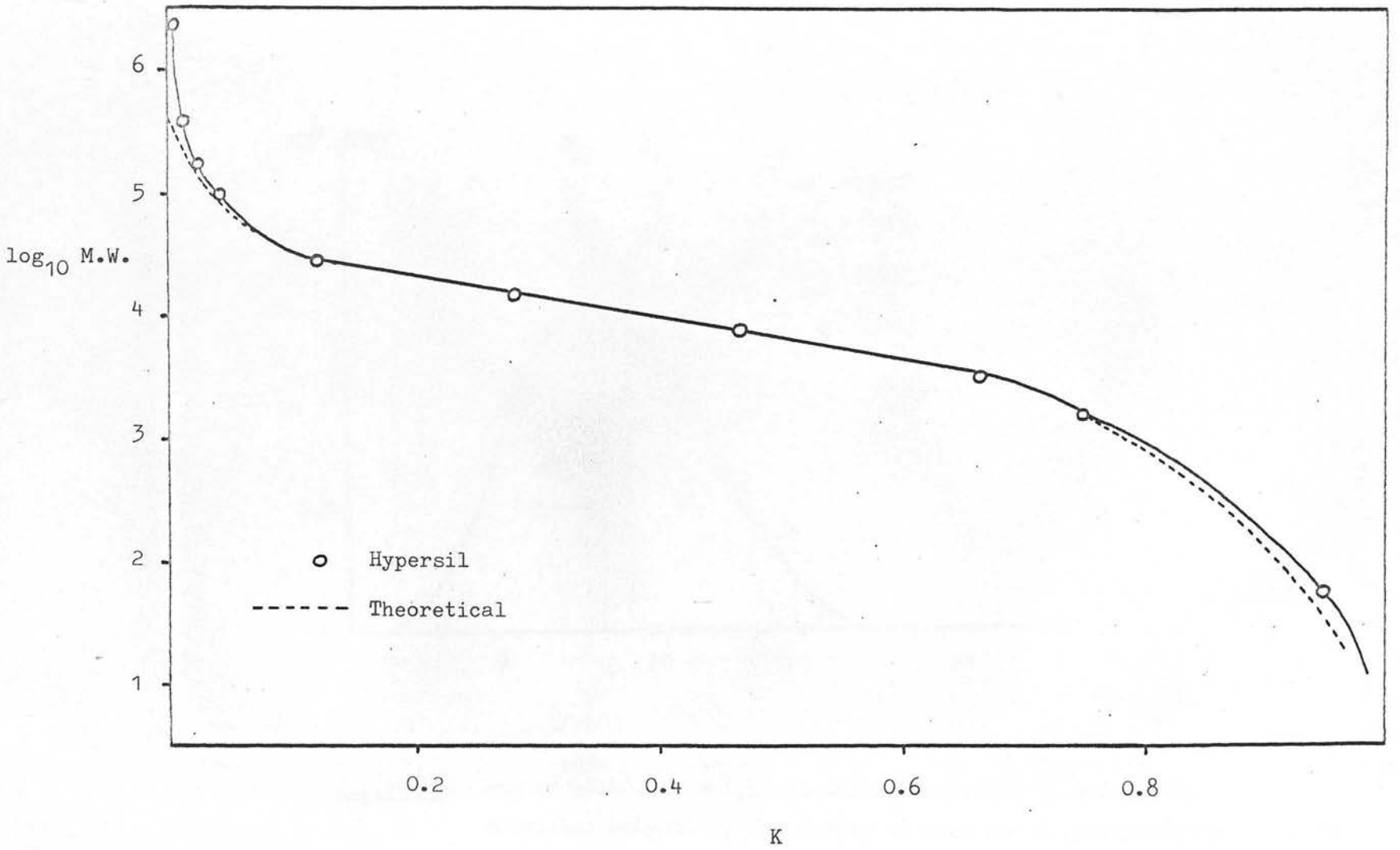

Figure 24 : Experimental data and theoretical curve for random spheres model (Ref. 102)

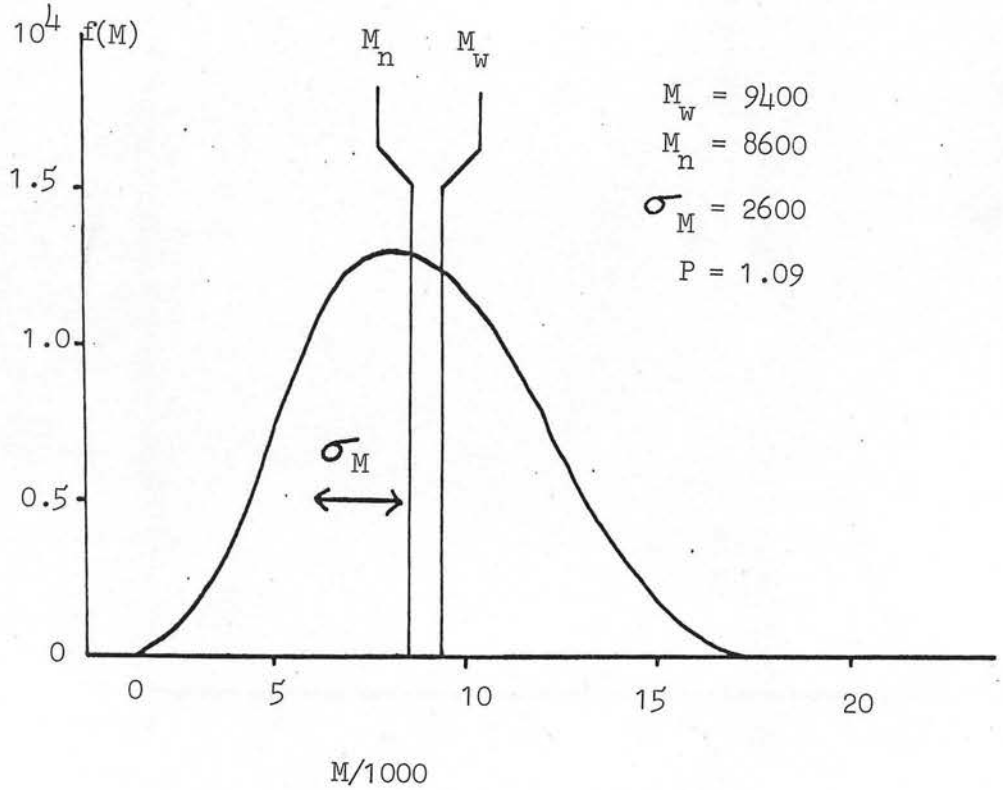

Figure 25: Number molecular weight distribution, f(M), as a function of molecular weight, M, for sample of moderate polydispersity, P = 1.09

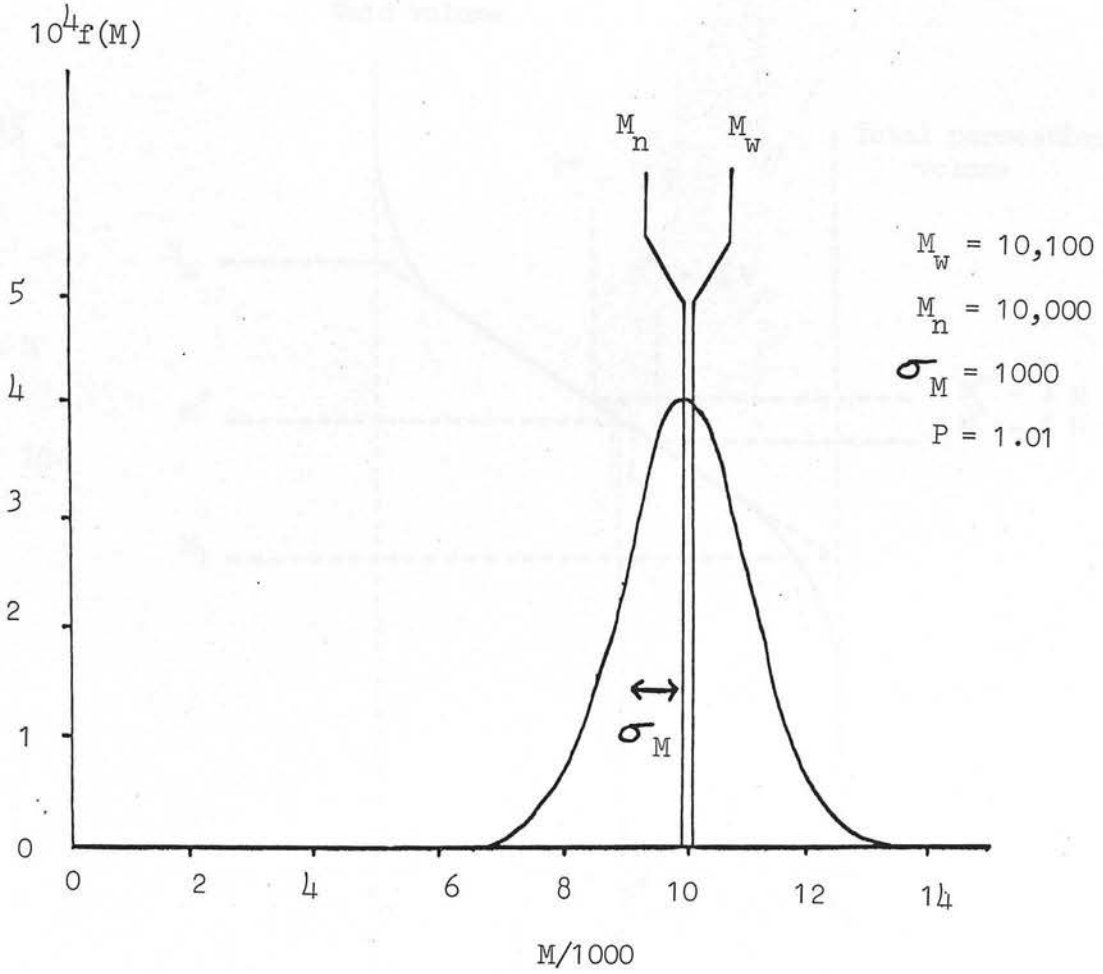

Figure 26: Gaussian molecular weight distribution for high grade polymer standard, P = 1.01

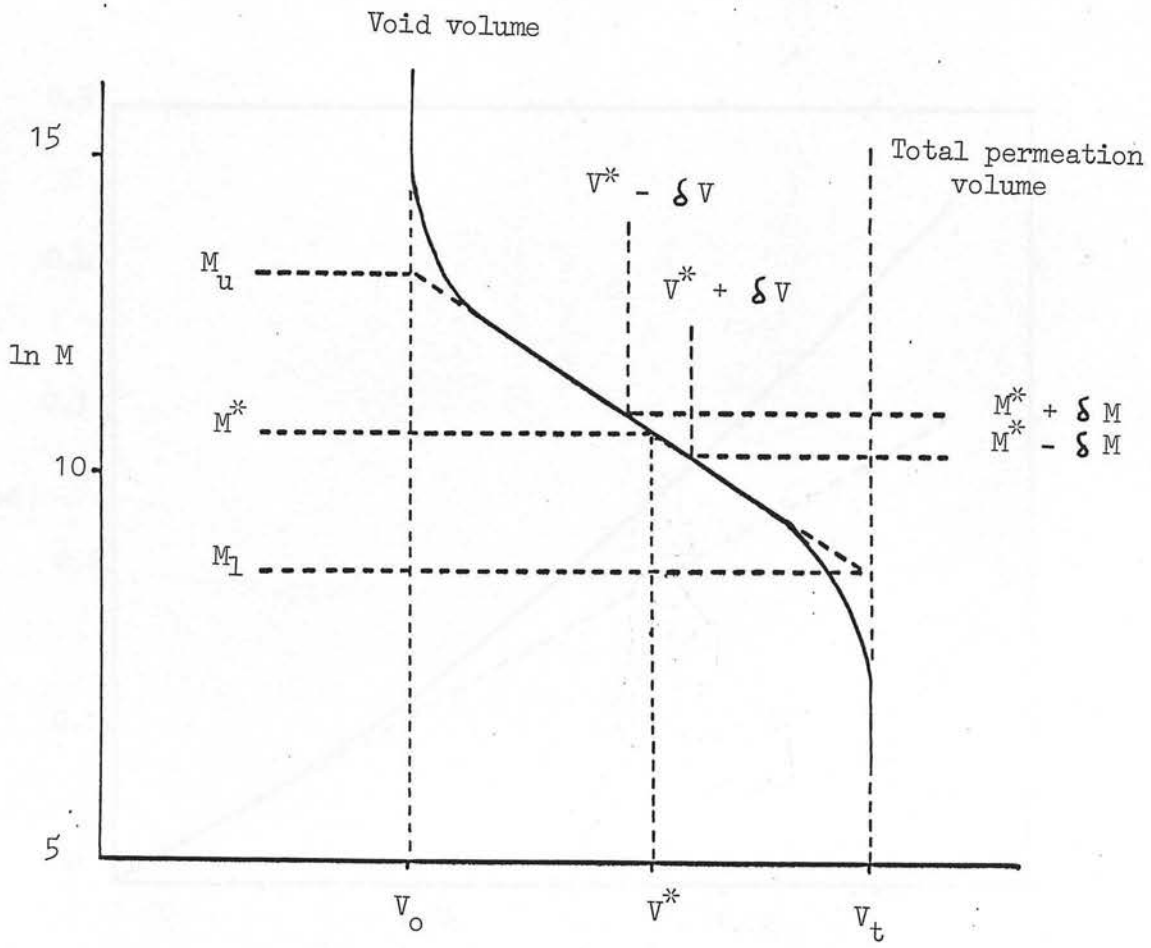

Figure 27: Illustrative calibration curve for gel permeation material showing dependence of elution volume, V, upon molecular weight, M.

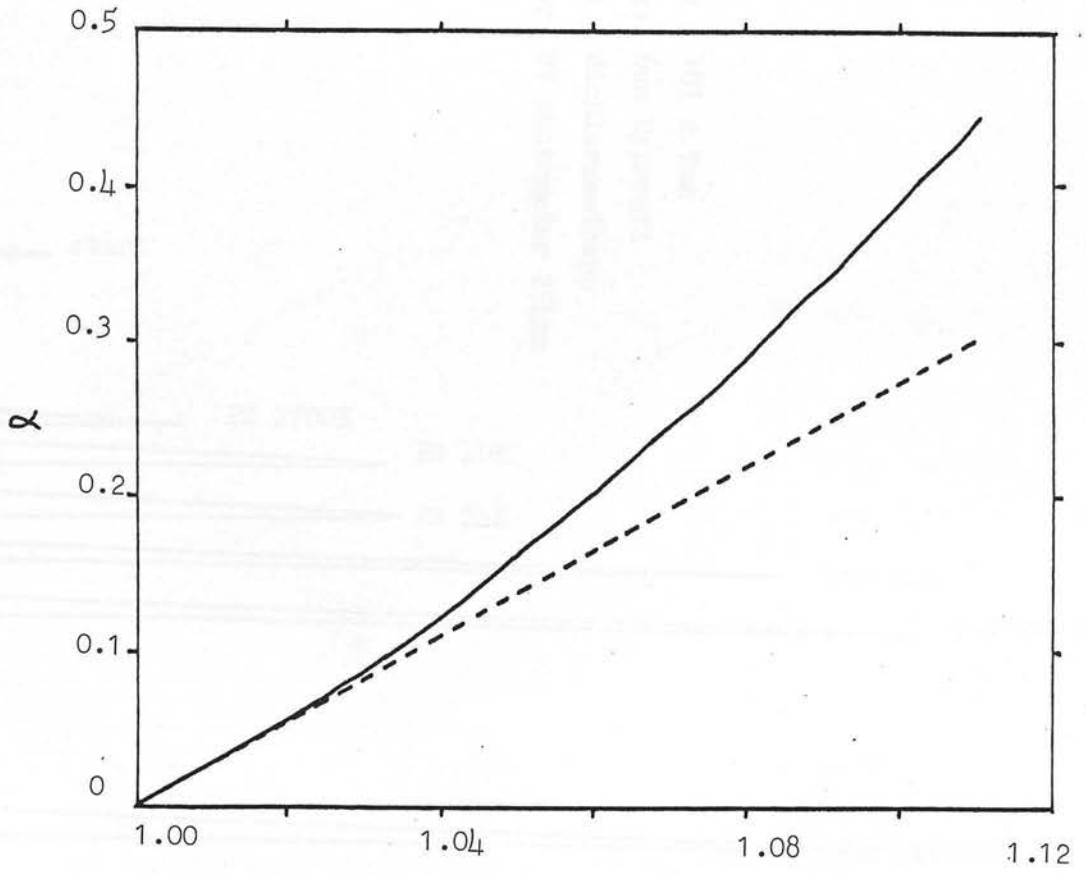

Figure 28: Dependence of α on polydispersity P. Broken line gives the asymptote for low α of $(11/4)$ (P-1)

Column: 101 x 7mm
Packing: 6um Hypersil
Eluent: dichloromethane
Detector: UV photometer 254nm

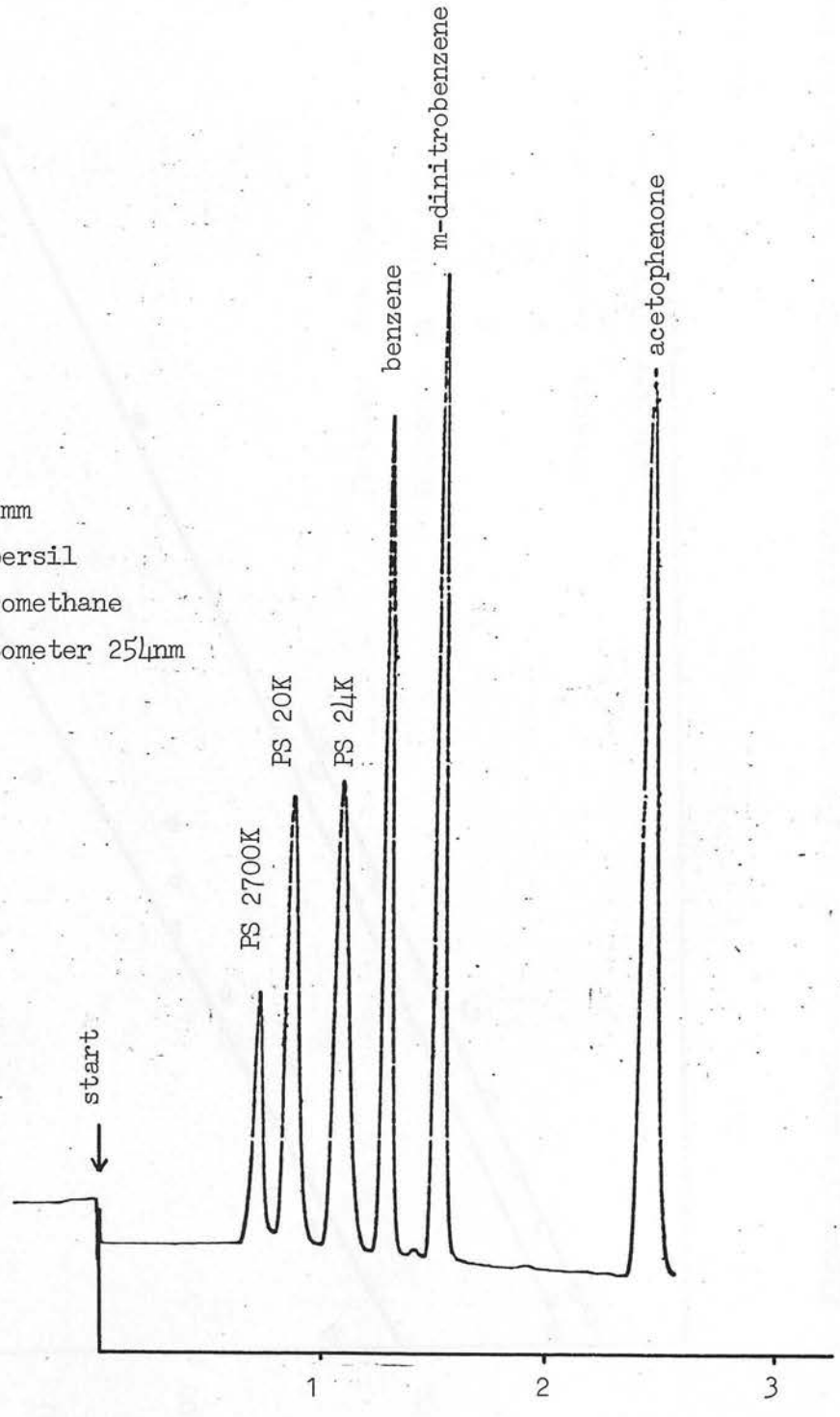

Figure 29: Typical chromatogram of excluded and retained solutes

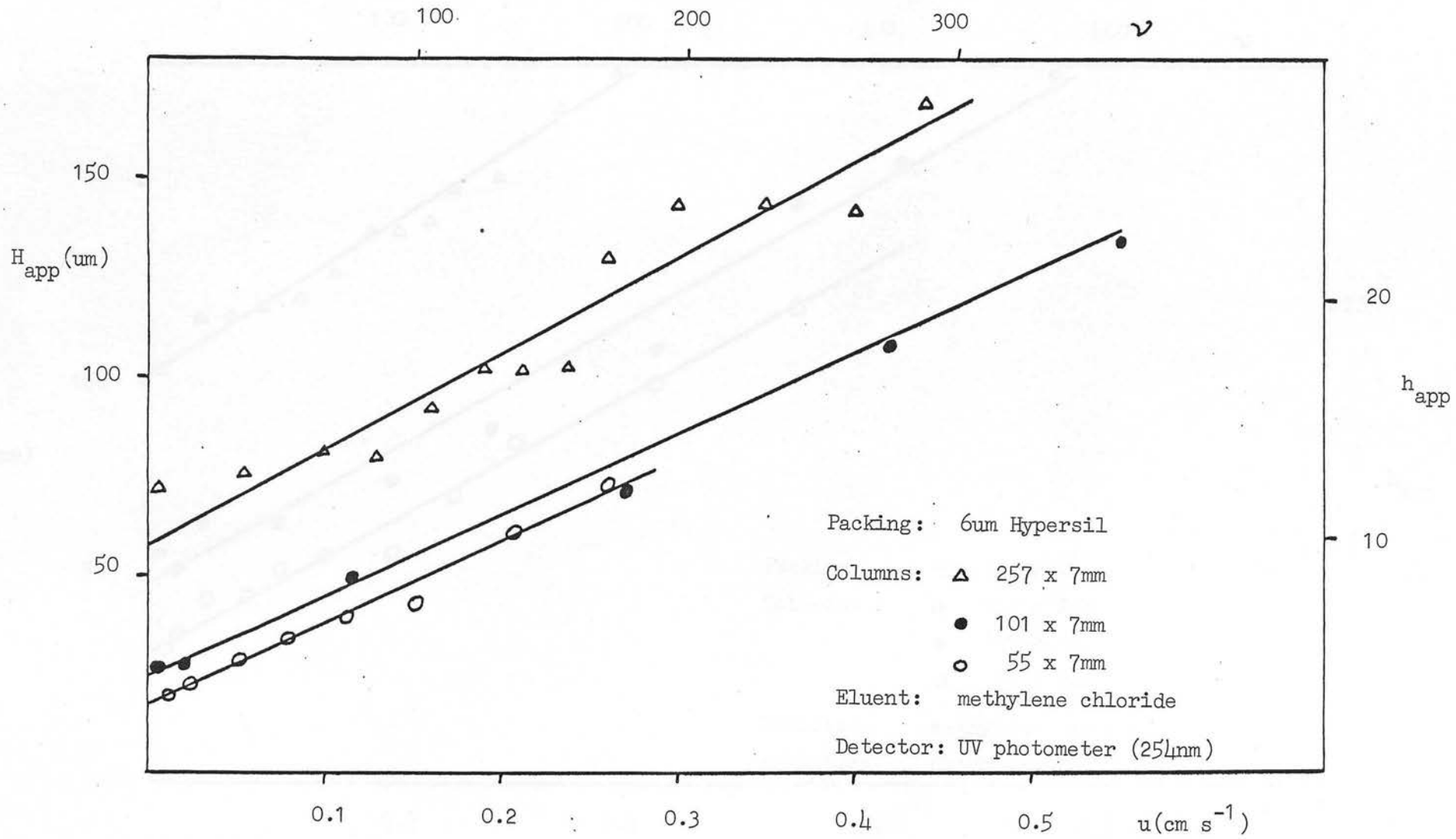

Figure 30: Effect of column length on apparent plate height versus velocity curves for PS 33K

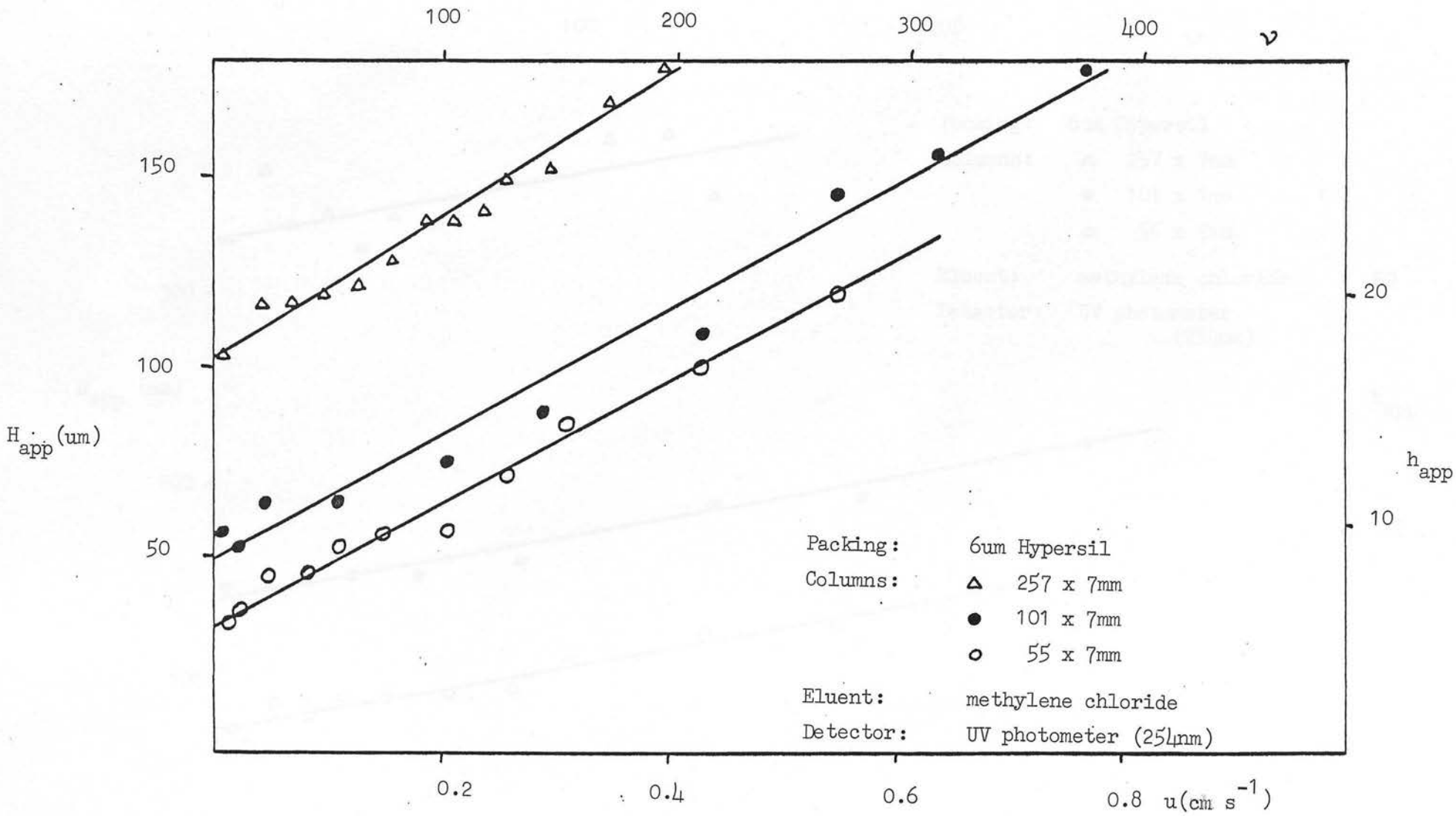

Figure 31: Effect of column length on apparent plate height versus velocity curves for PS 20K

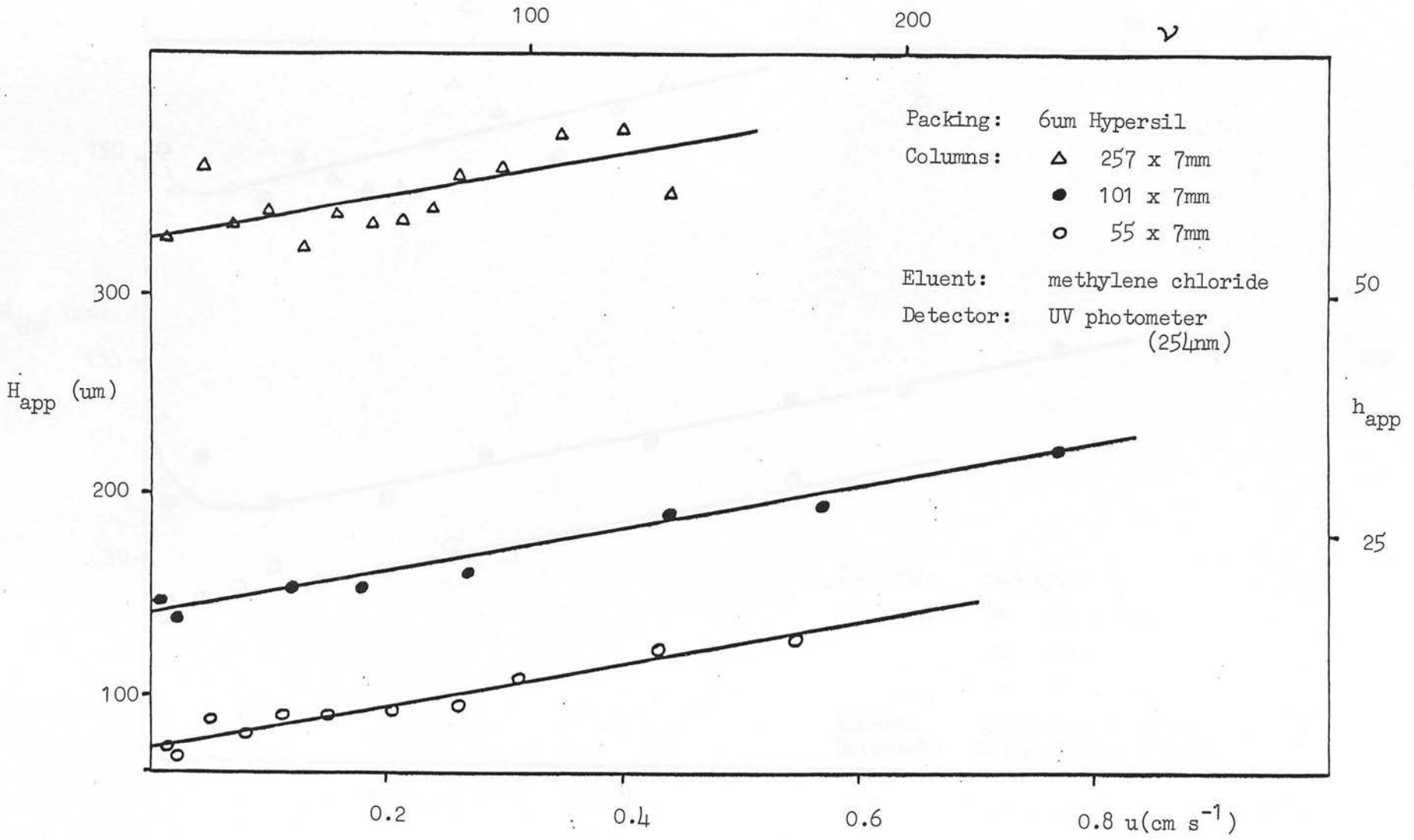

Figure 32: Effect of column length on apparent plate height versus velocity curves for PS 10K

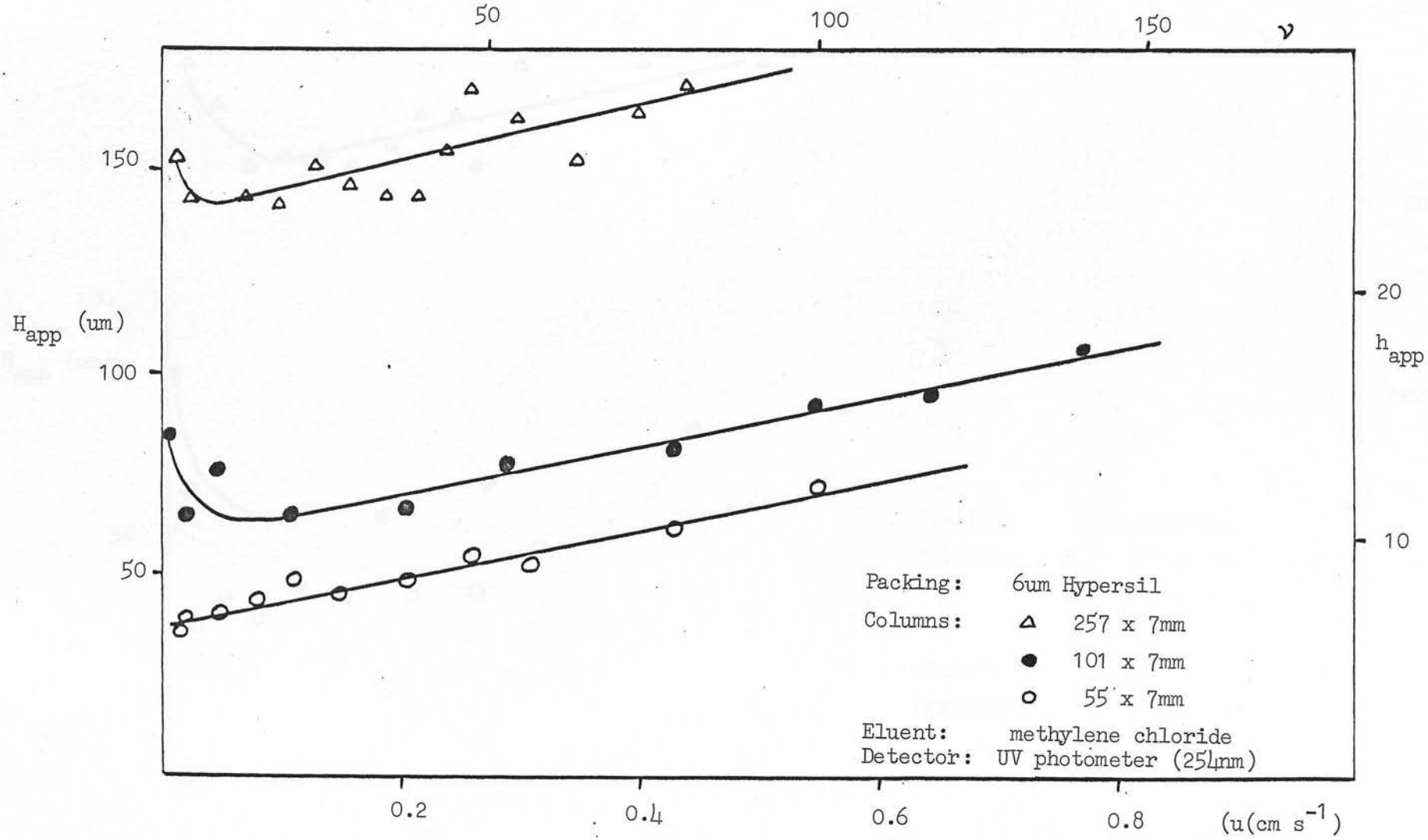

Figure 33: Effect of column length on apparent plate height versus velocity curves for PS 4K

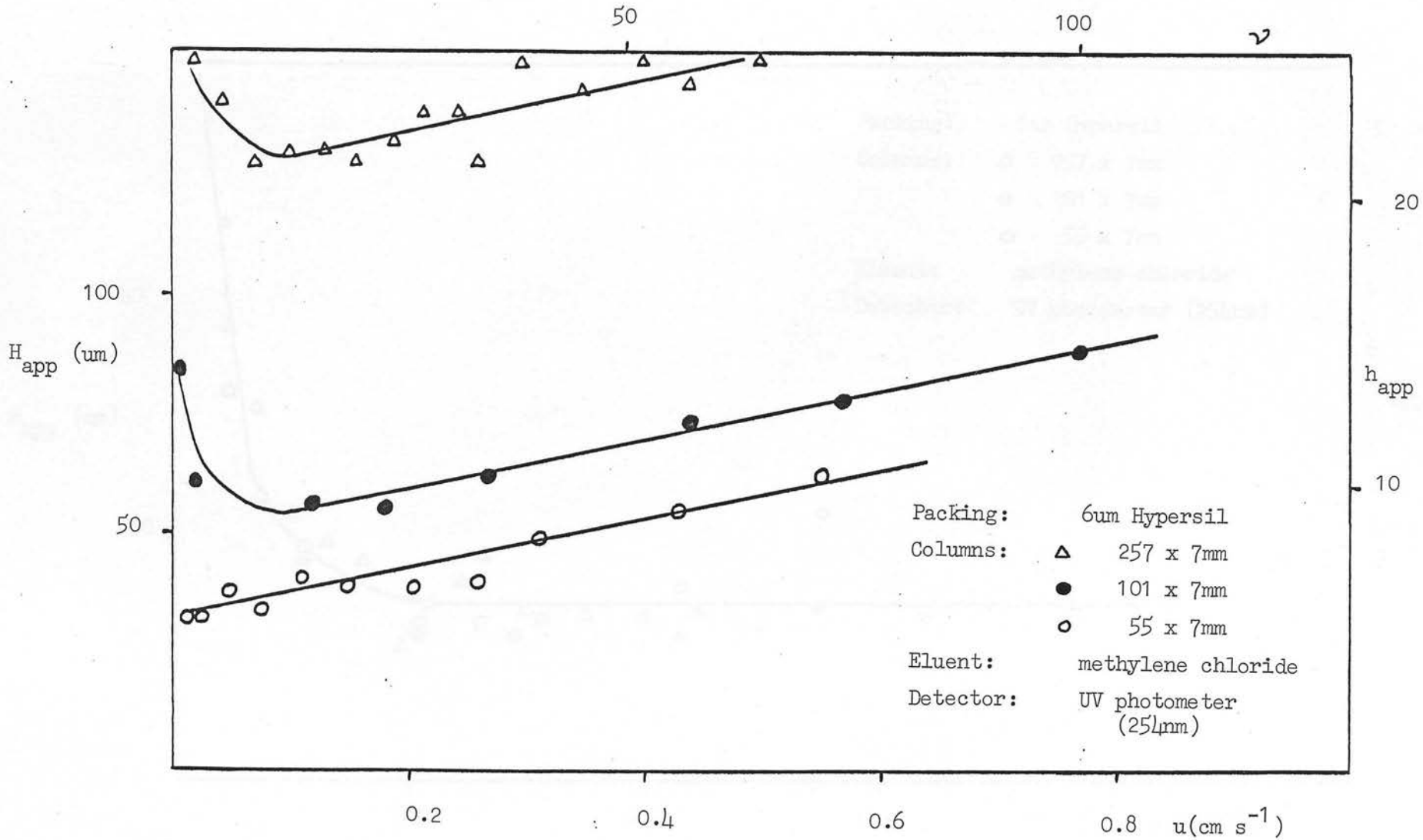

Figure 34: Effect of column length on apparent plate height versus velocity curves for PS 2K

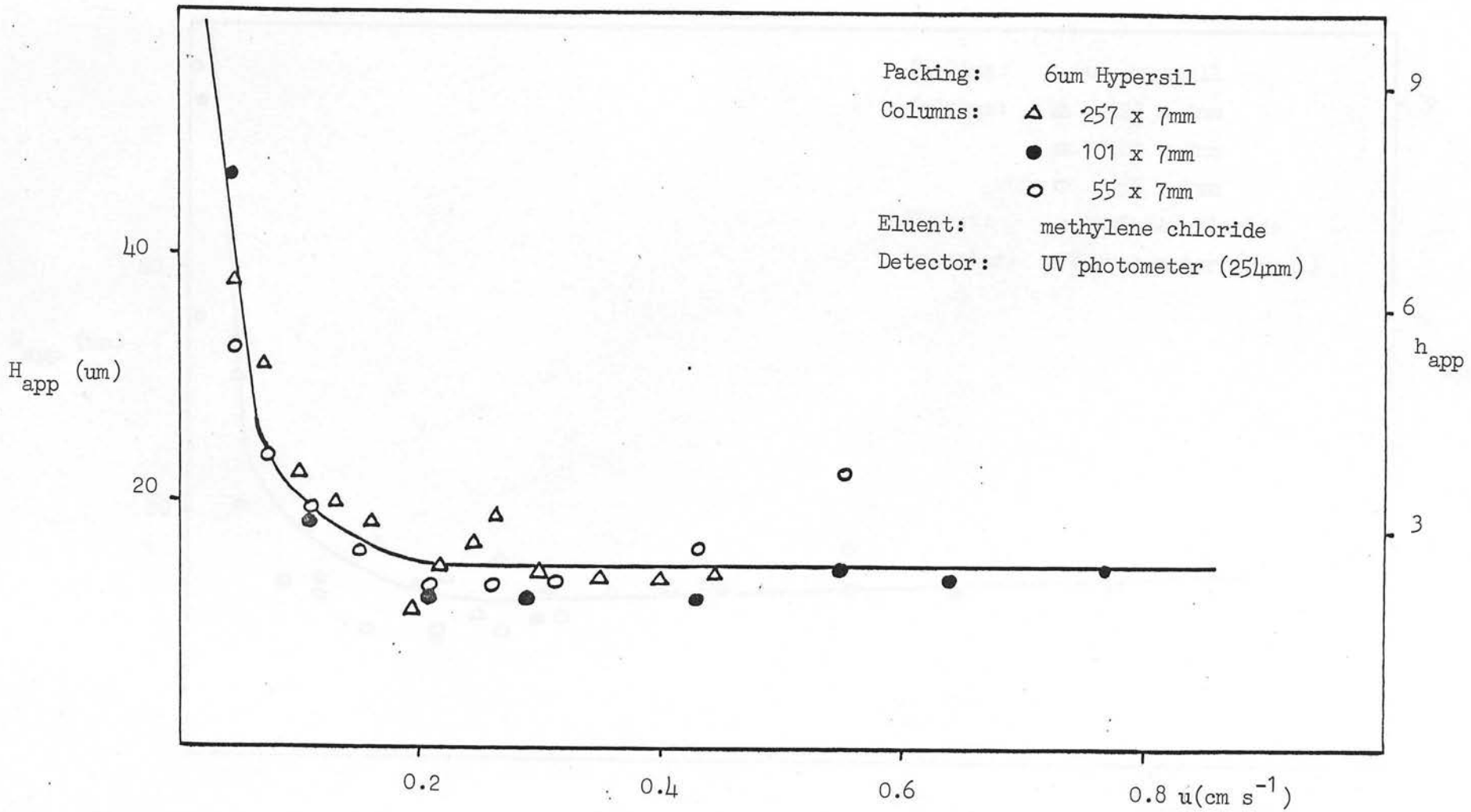

Figure 35: Effect of column length on apparent plate height versus velocity curves for Benzene

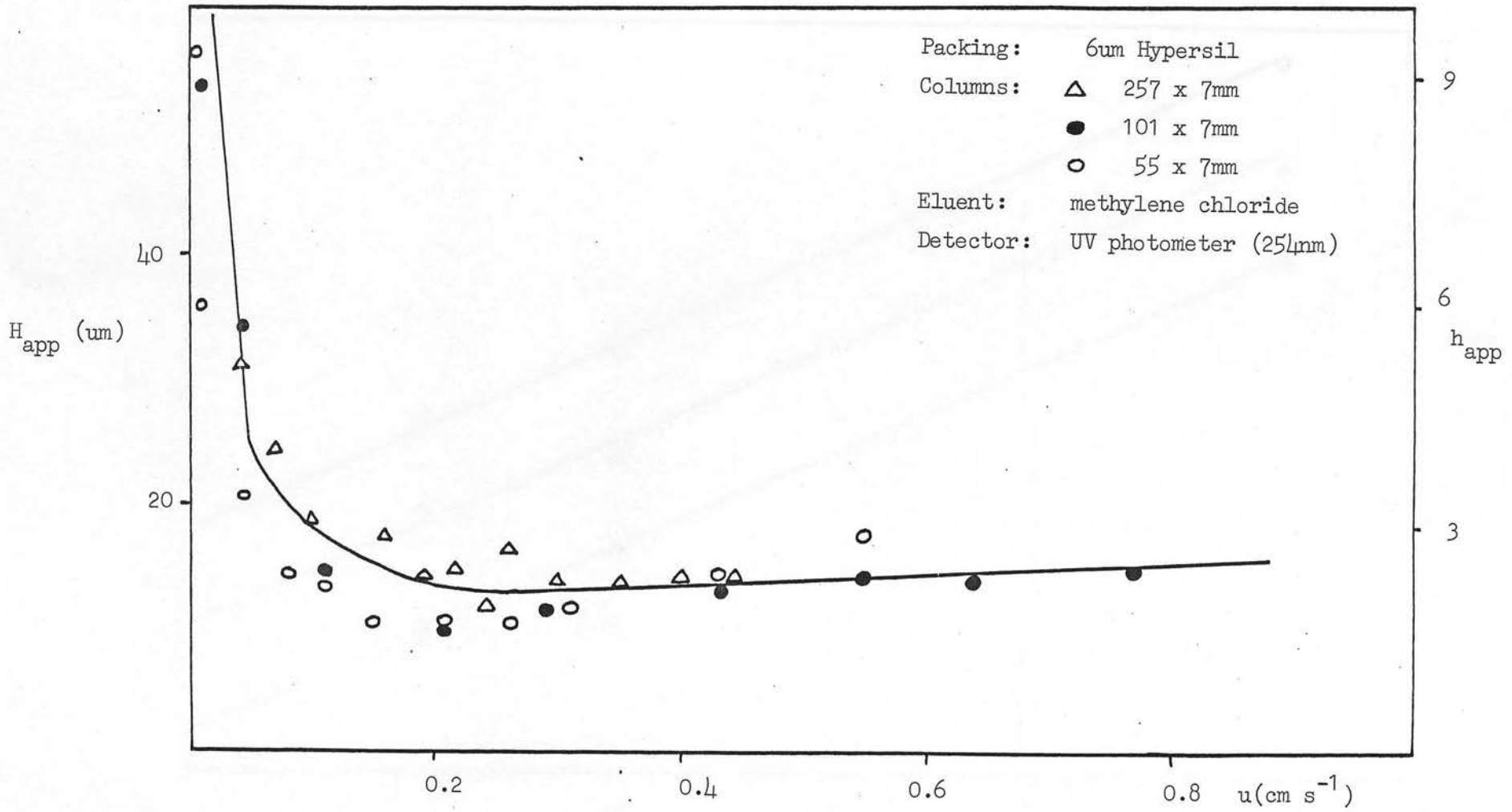

Figure 36: Effect of column length on apparent plate height versus velocity curves for m-Dinitrobenzene

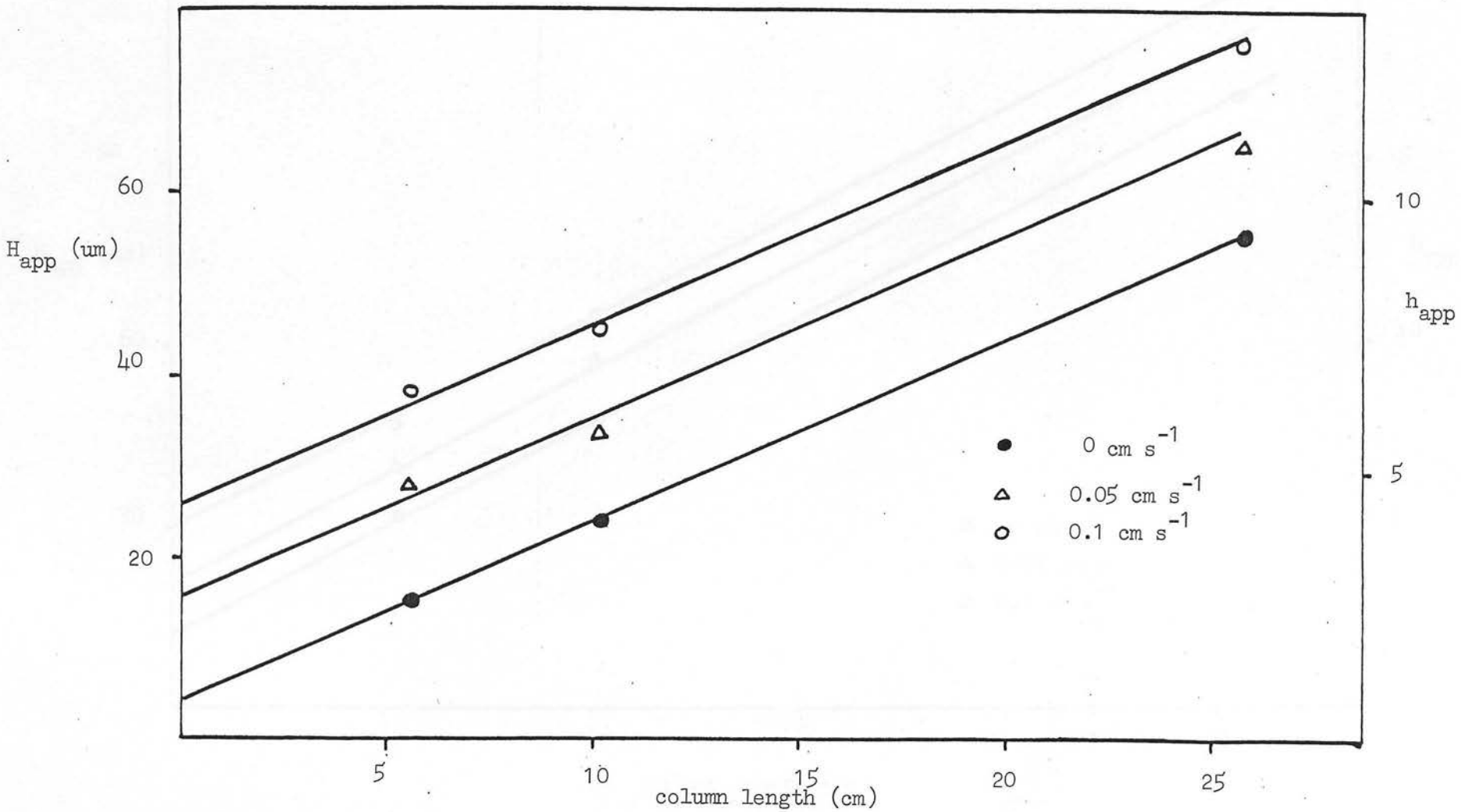

Figure 37: Apparent plate height versus column length for PS 33K at three velocities (interpolated from Figure 30).

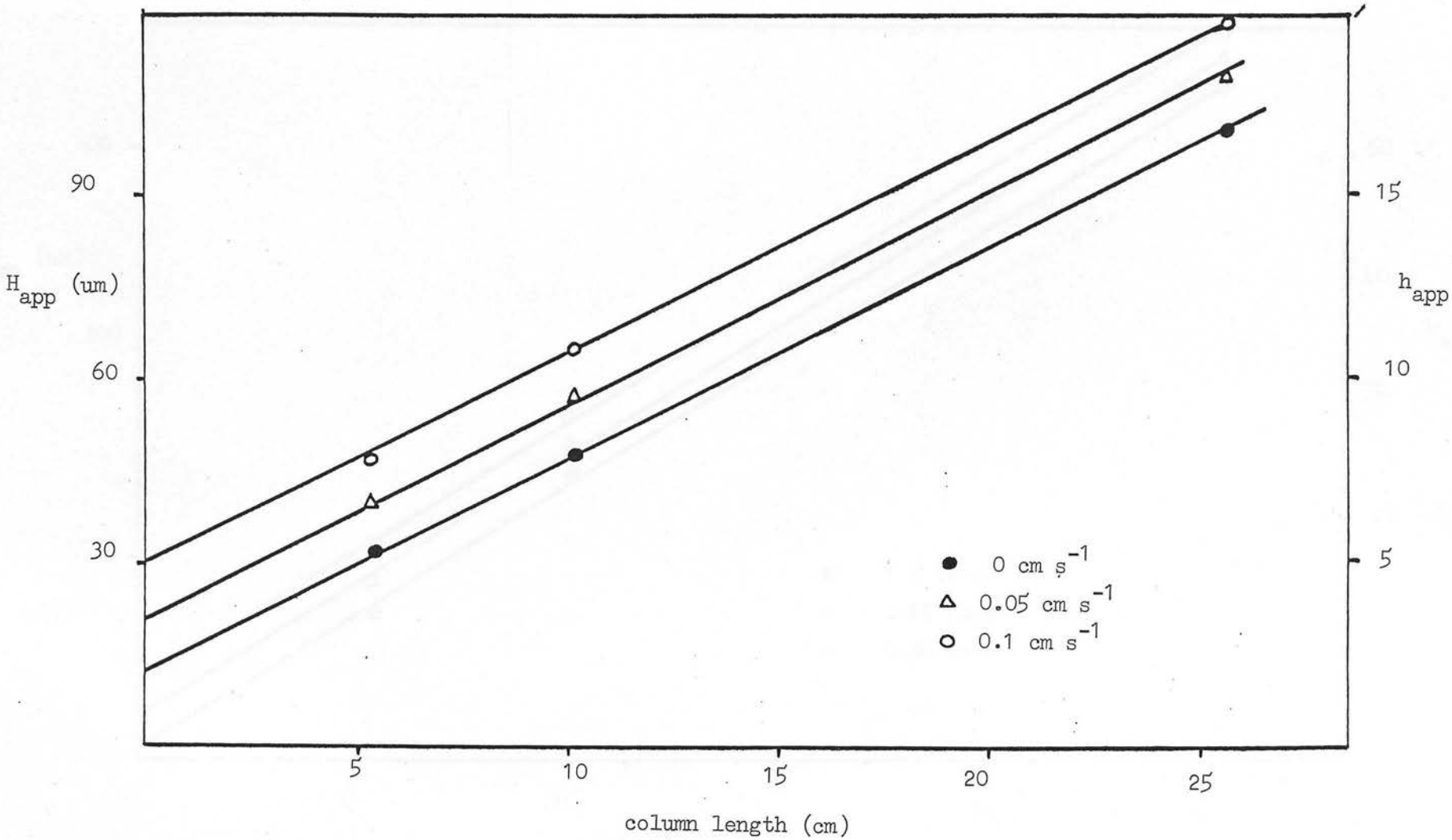

Figure 38: Apparent plate height versus column length for PS 20K at three velocities (interpolated from Figure 31).

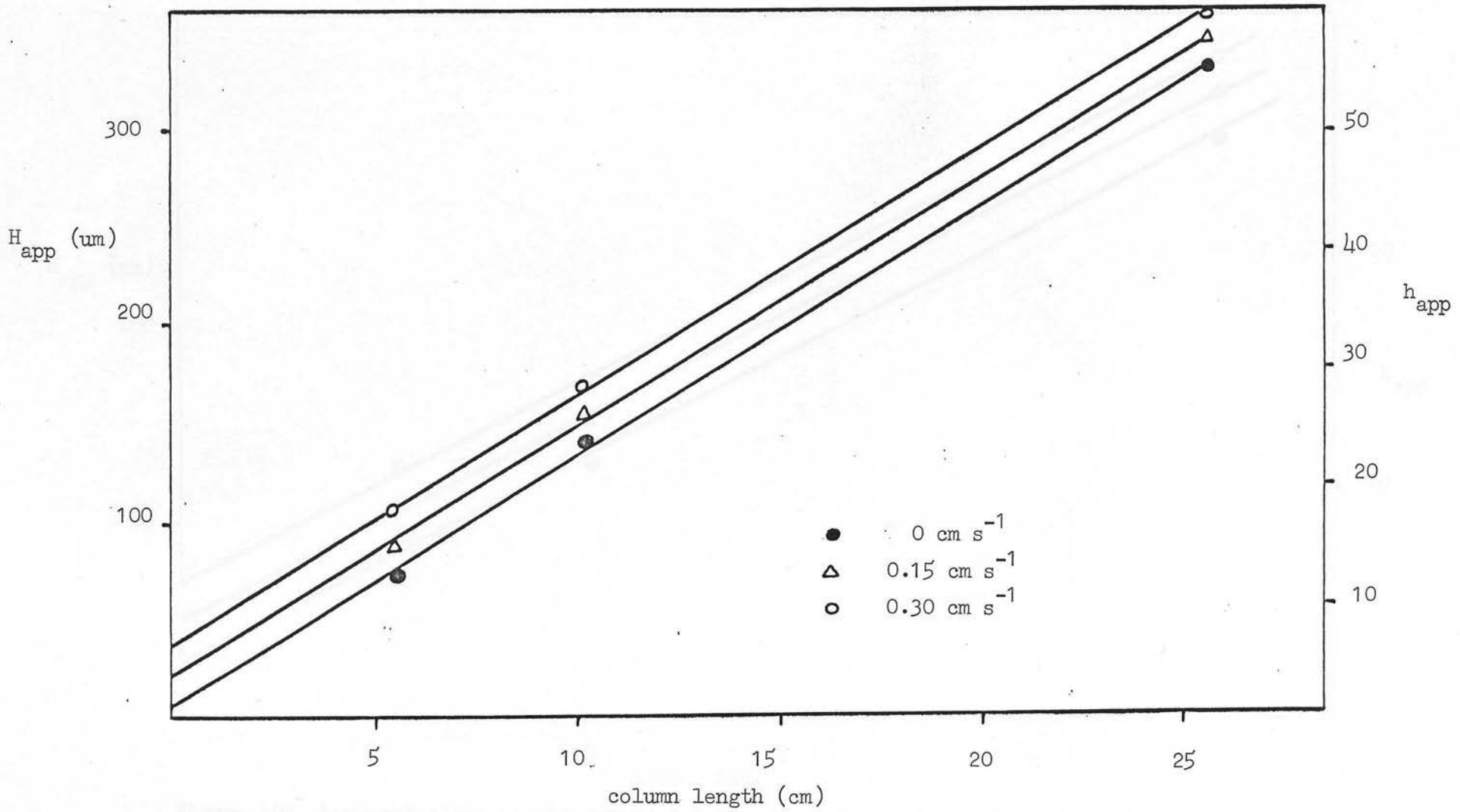

Figure 39: Apparent plate height versus column length for PS 10K at three velocities (interpolated from Figure 32).

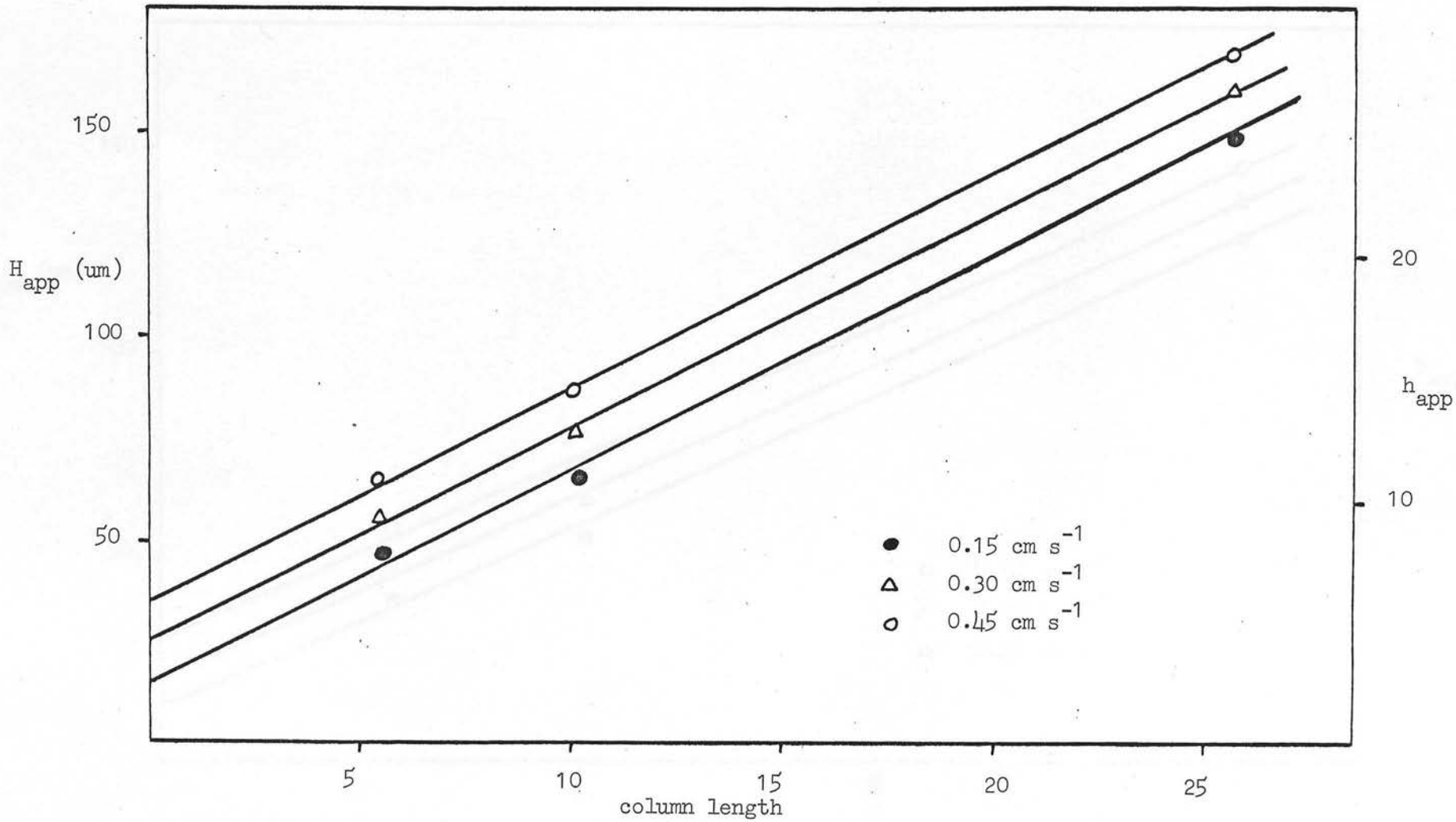

Figure 40: Apparent plate height versus column length for PS 4K at three velocities (interpolated from Figure 33).

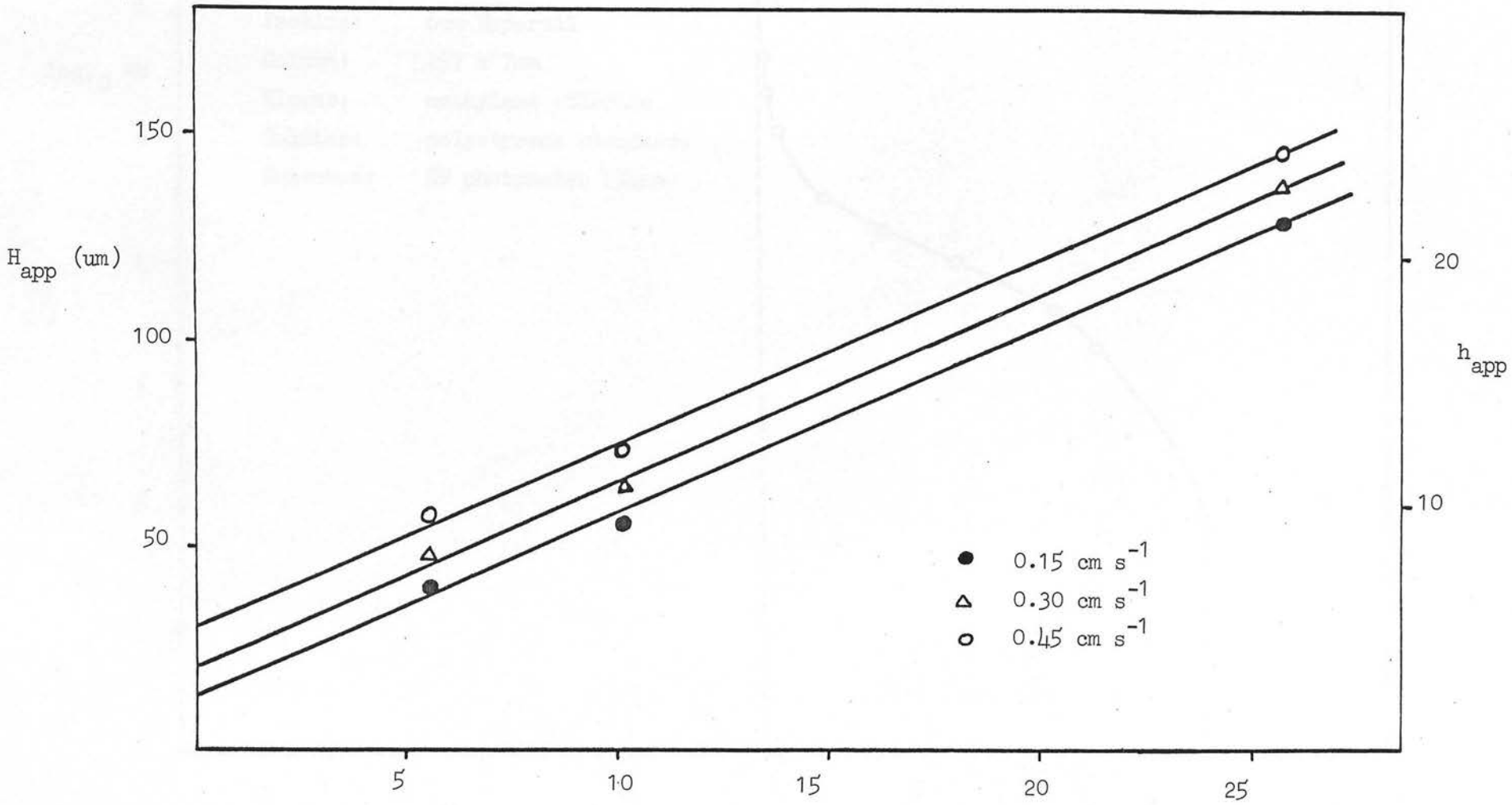

Figure 41: Apparent plate height versus column length for PS 2K at three velocities (interpolated from Figure 34).

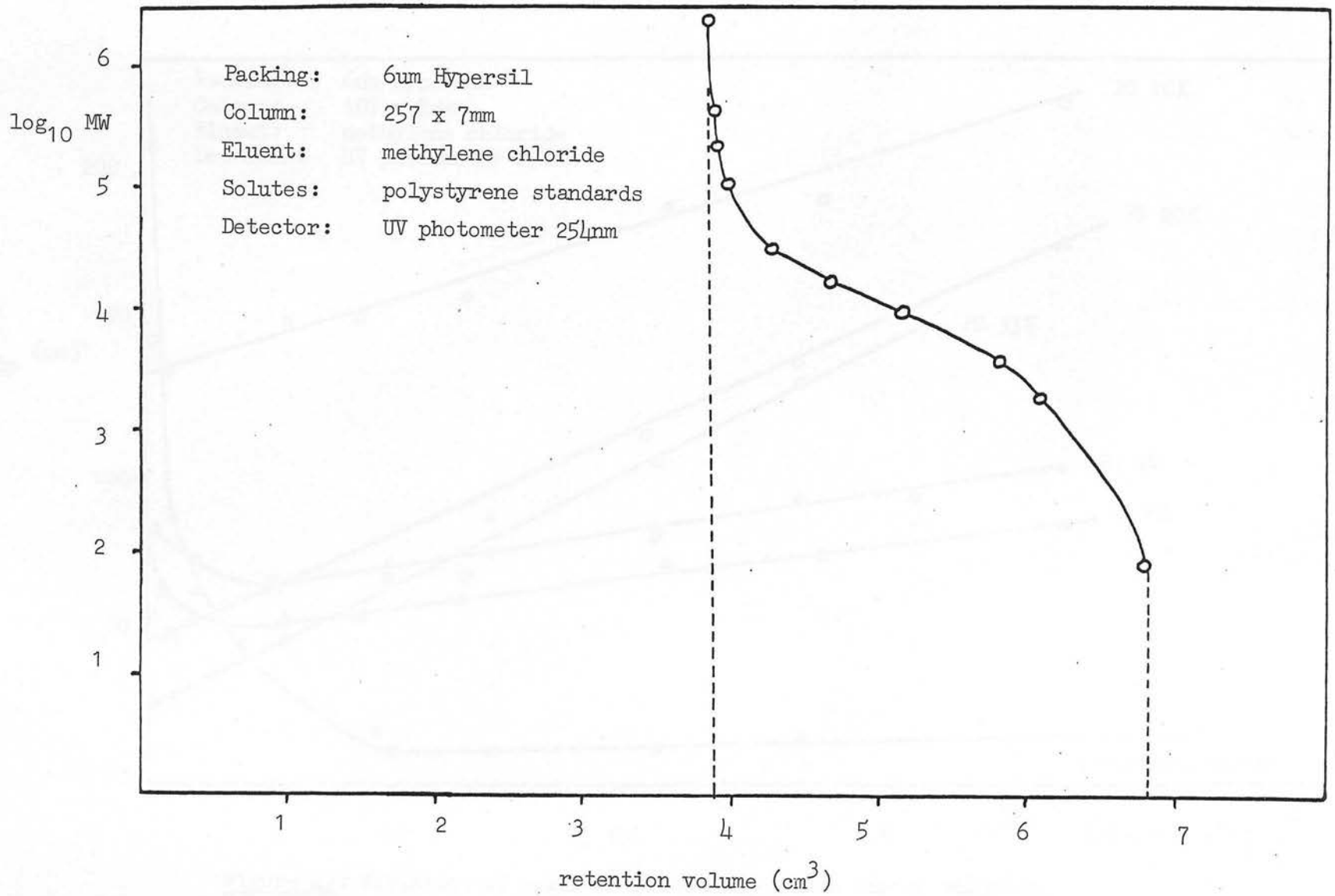

Figure 42: Calibration Curve for Hypersil

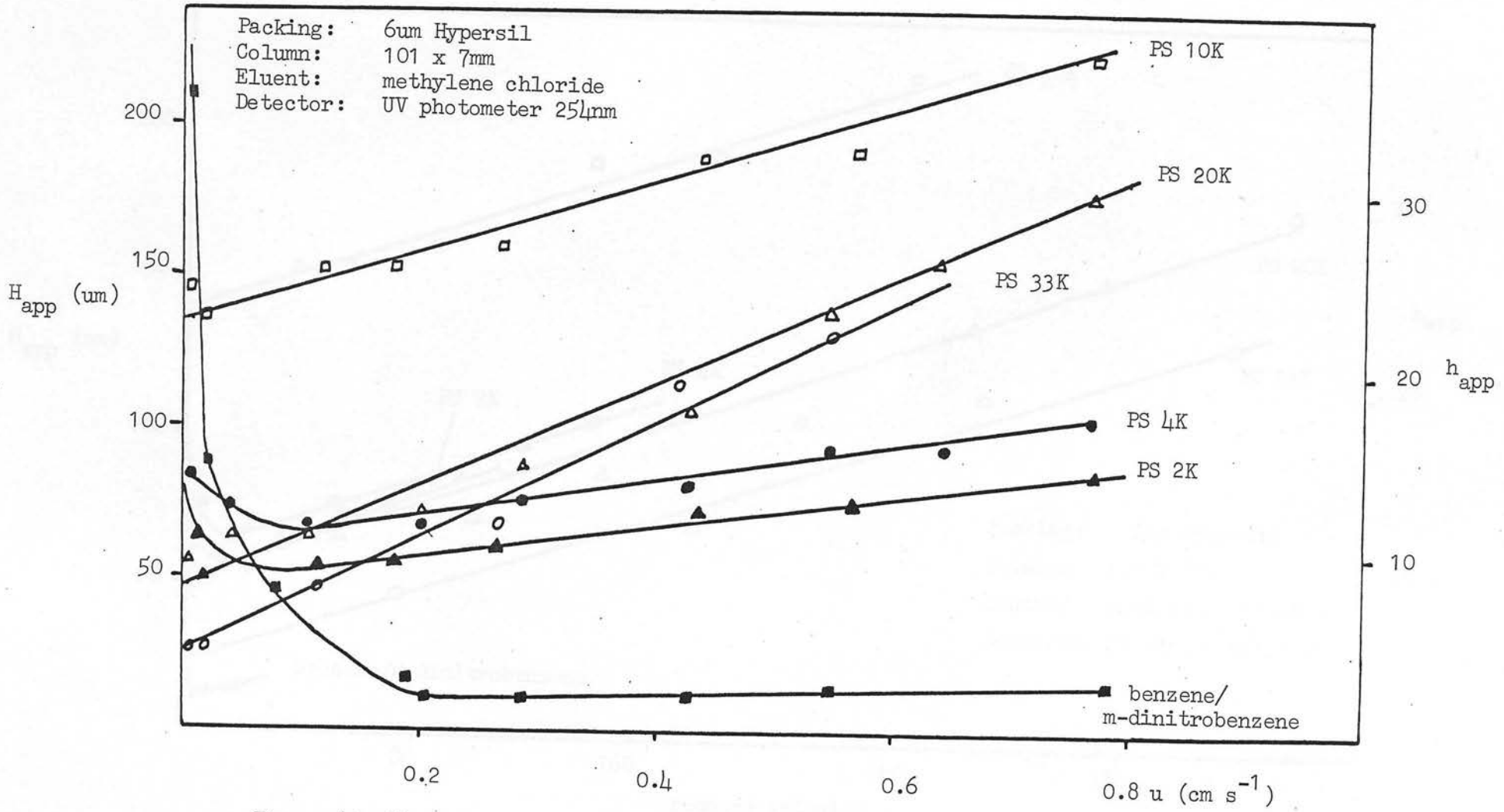

Figure 43: Variation of apparent plate height with linear velocity.

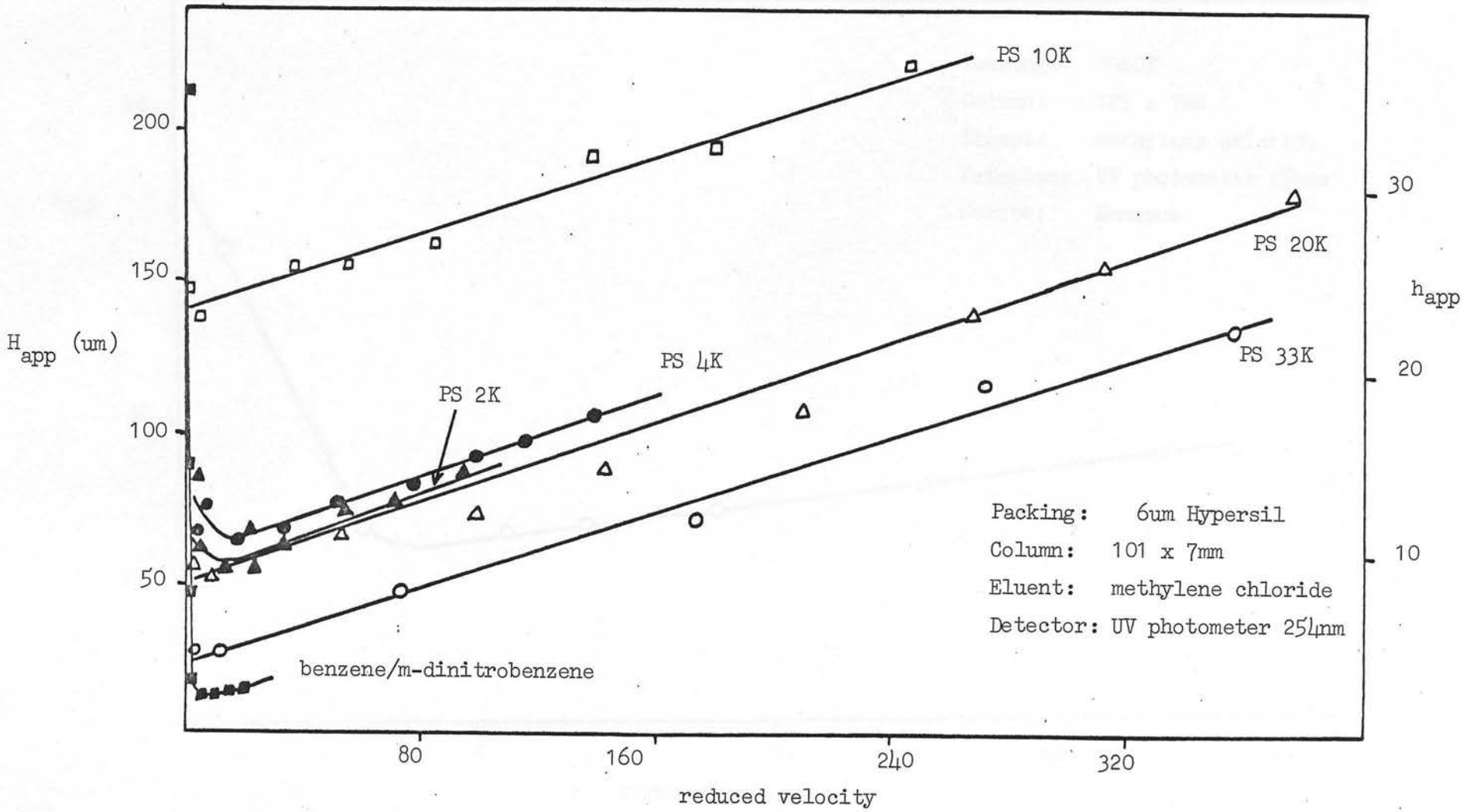

Figure 44: Variation of Apparent Plate Height with reduced velocity

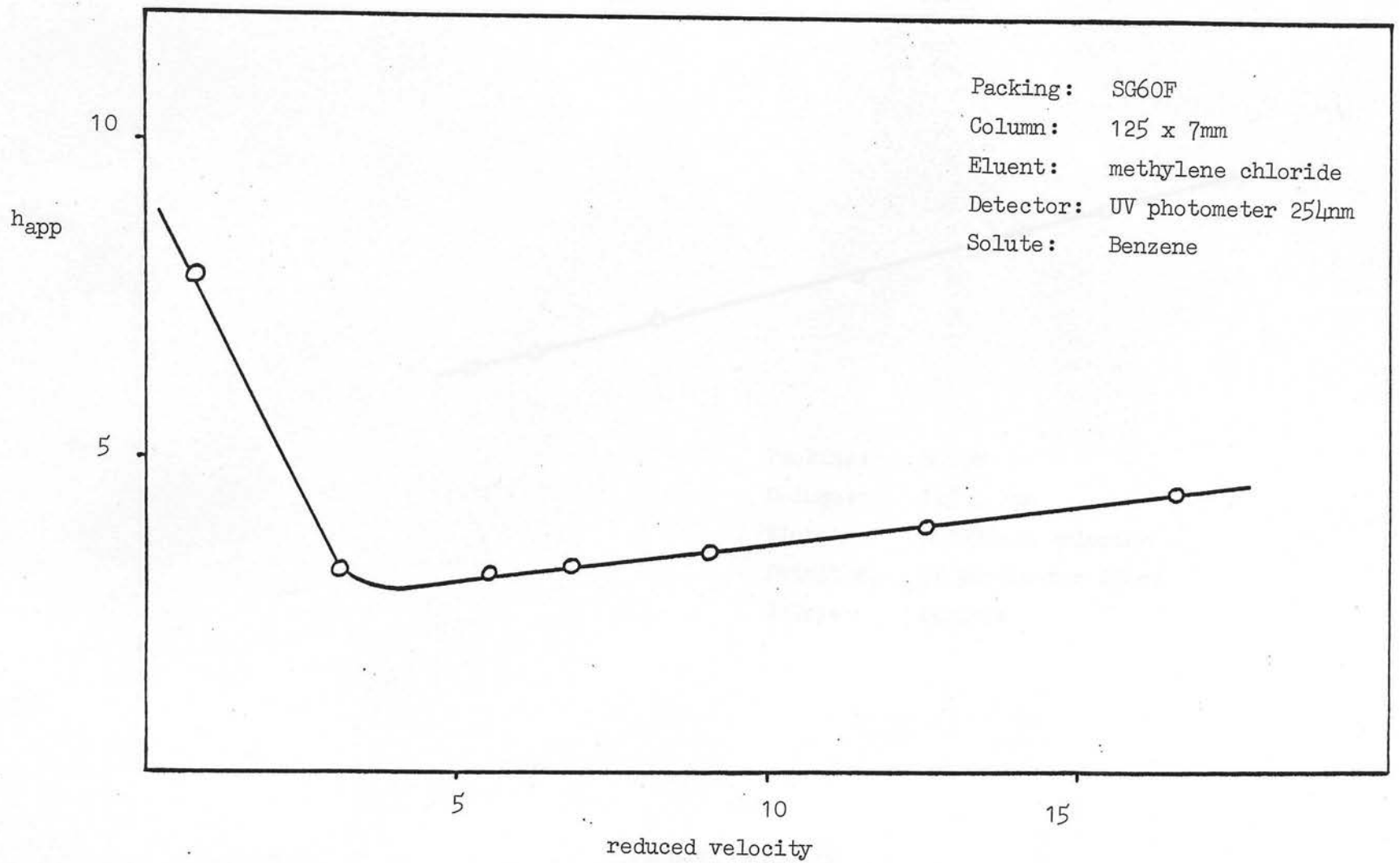

Figure 45: Reduced plate height versus reduced velocity curve for Benzene on SG60F

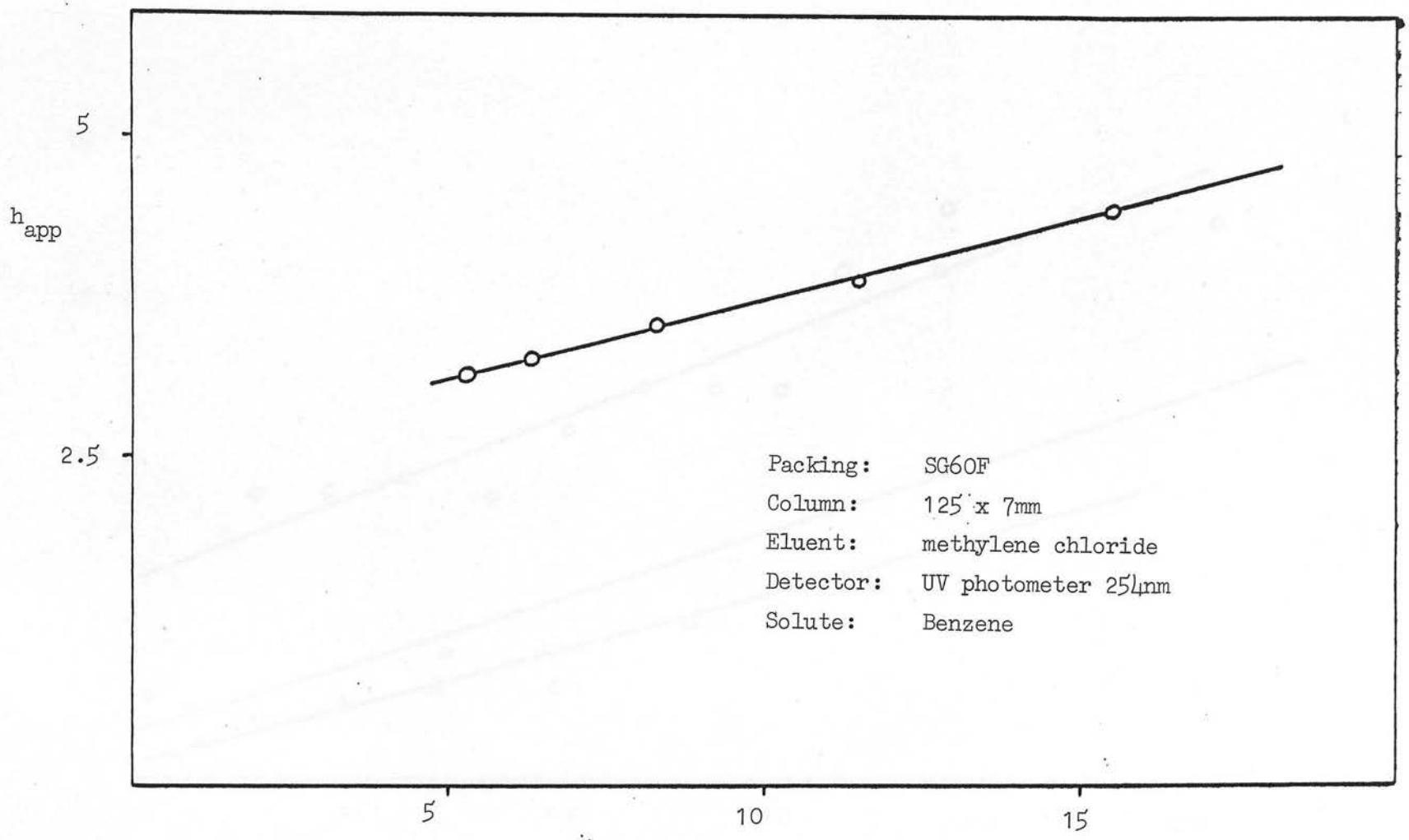

Figure 46: Reduced plate height versus reduced velocity curve for m-Dinitrobenzene on SG60F

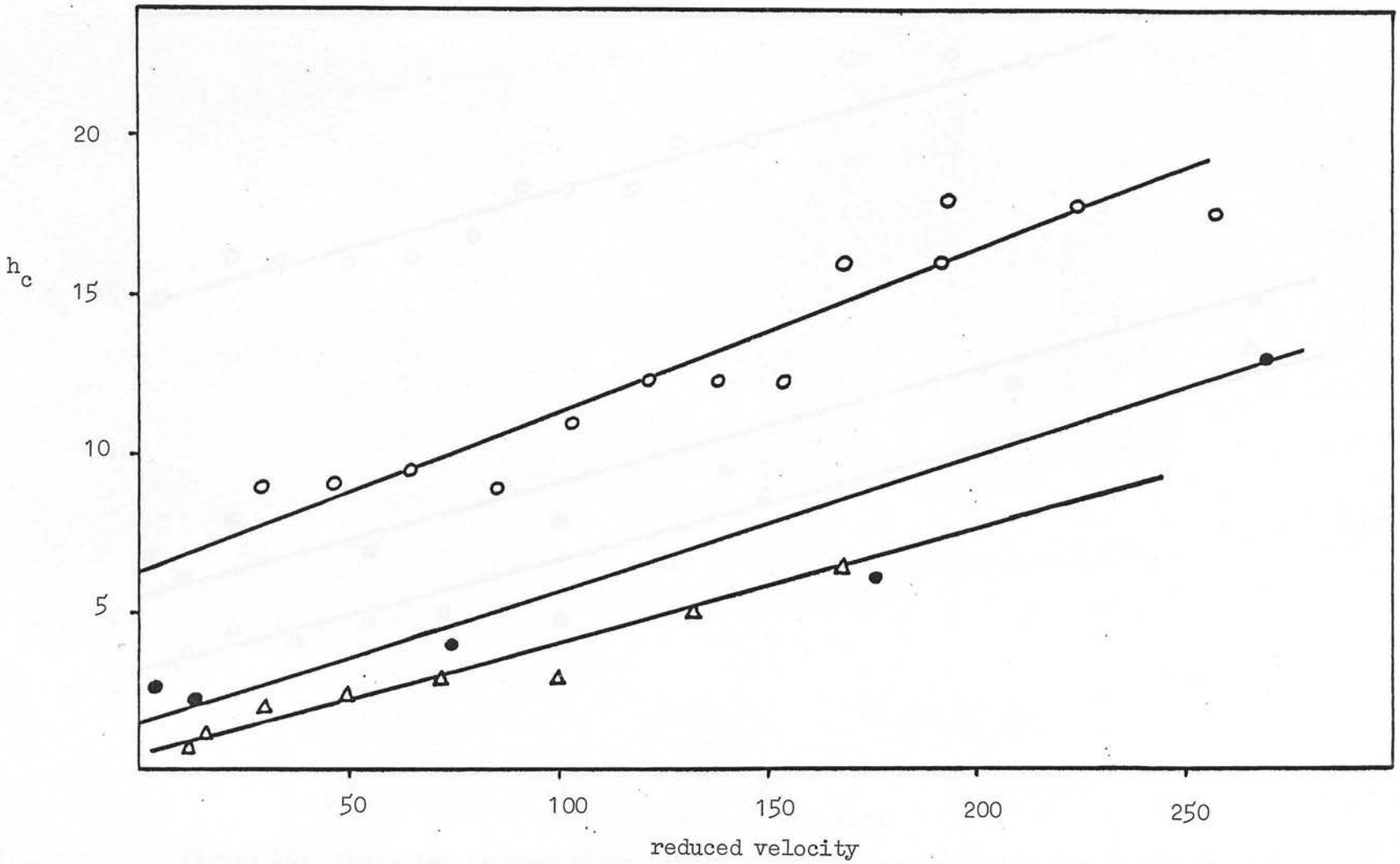

Figure 47: Corrected reduced plate height versus reduced velocity for PS 33K ($h_c = h_{app} - \frac{2}{\nu} - \nu^{0.33}$)

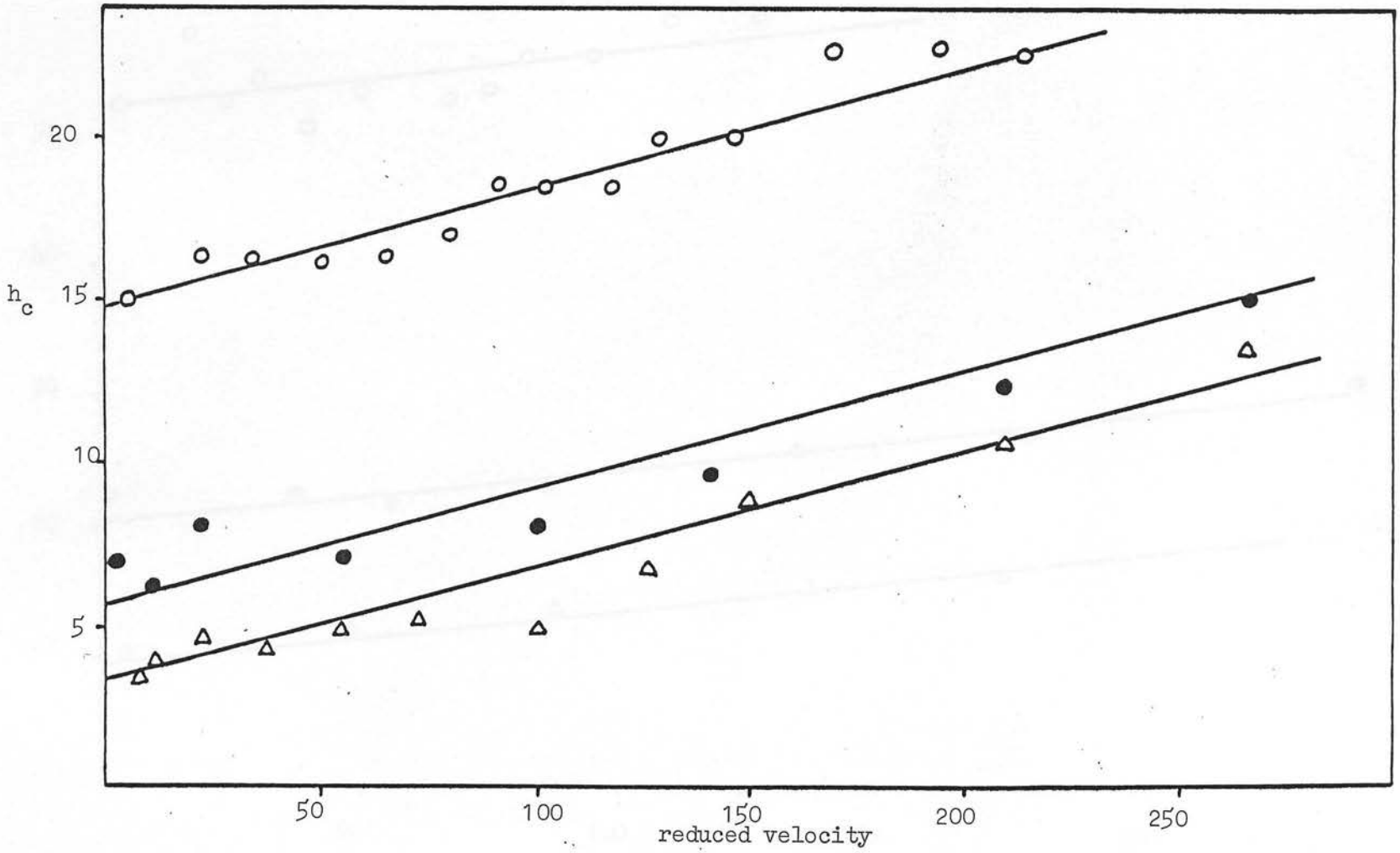

Figure 48: Corrected reduced plate height versus reduced velocity for PS 20K ($h_c = h_{app} - \frac{2}{\nu} - \nu^{0.33}$)

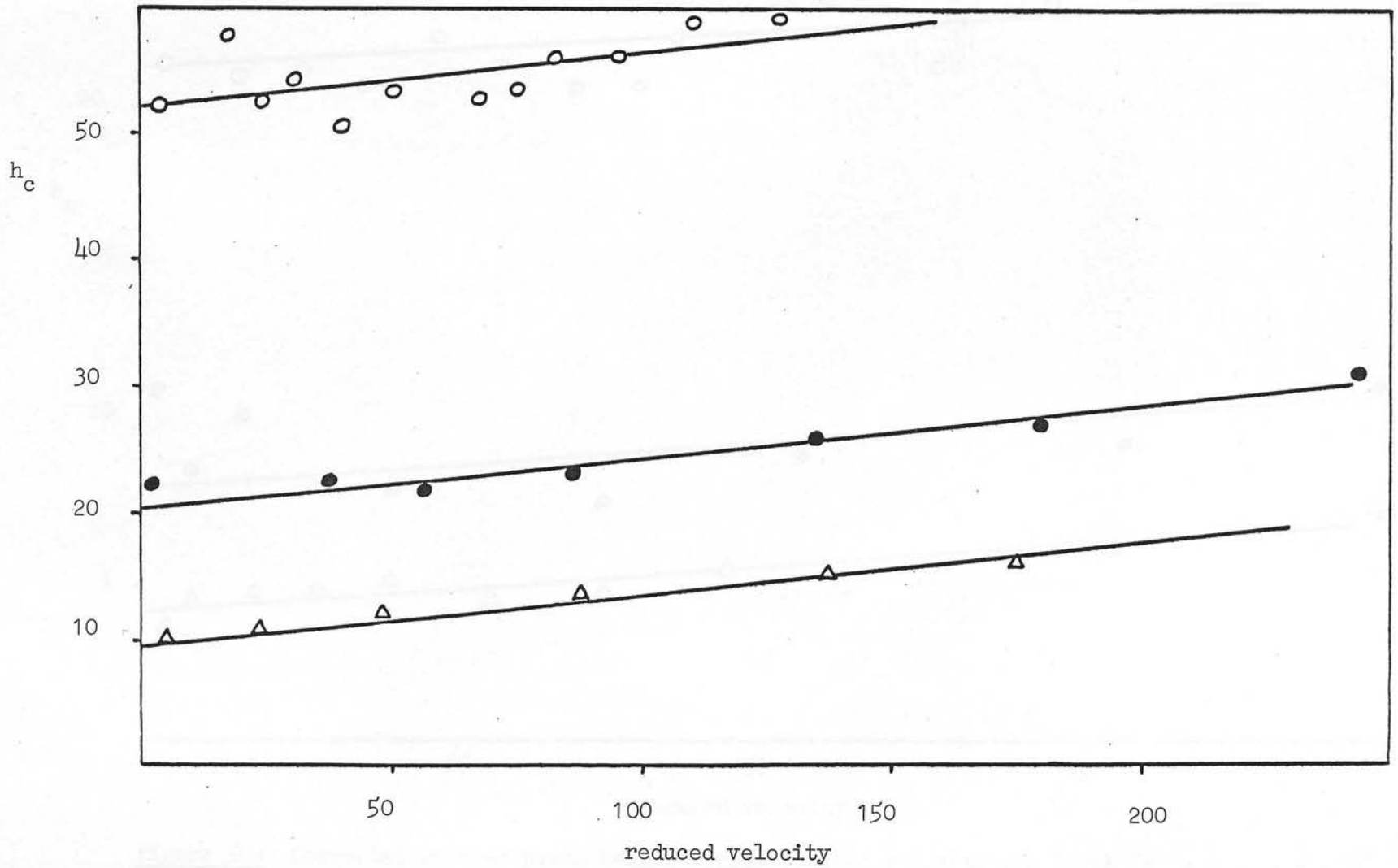

Figure 49: Corrected reduced plate height versus reduced velocity for PS 10K ($h_c = h_{app} - \frac{2}{\nu} - \nu^{0.33}$)

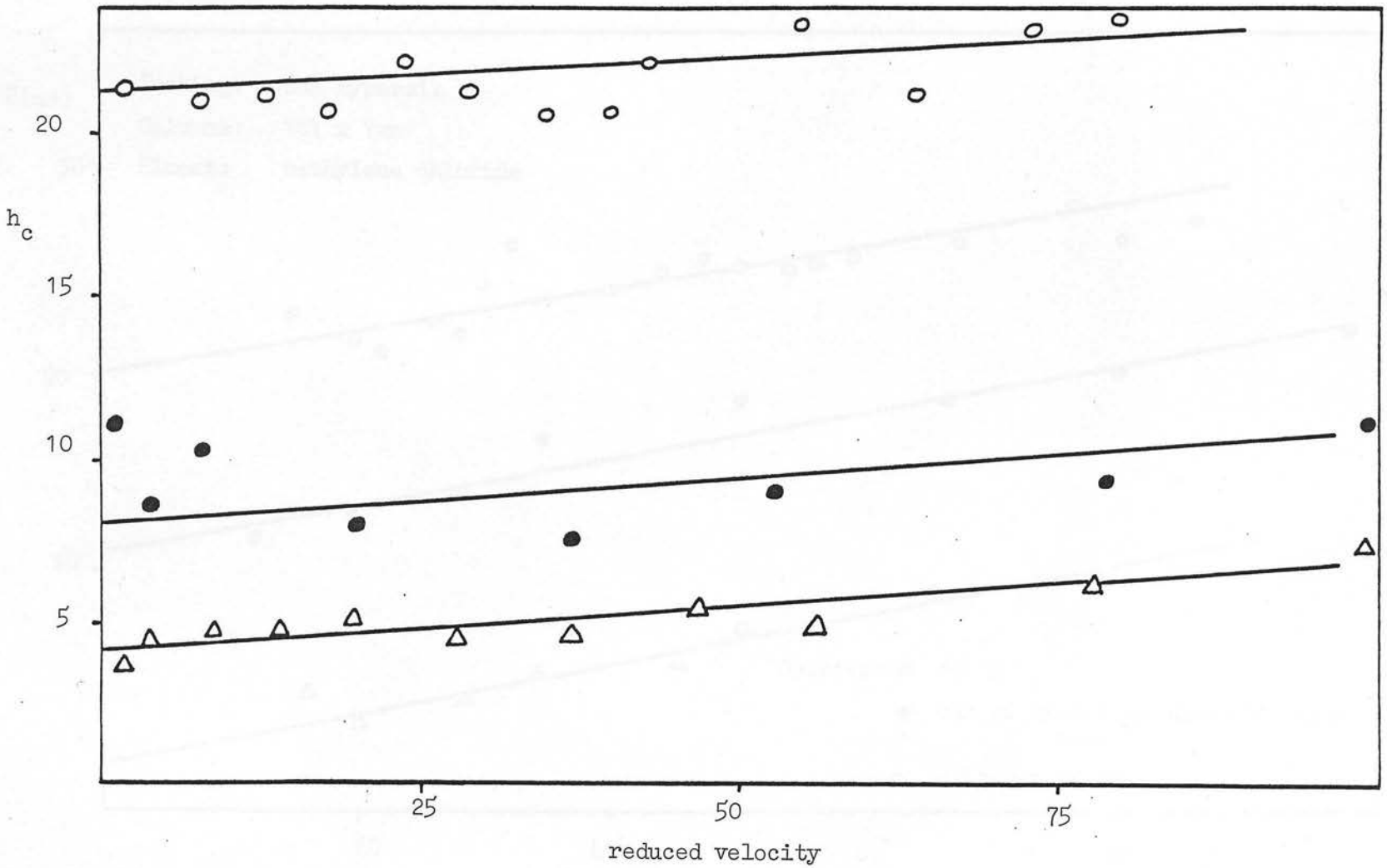

Figure 50: Corrected reduced plate height versus reduced velocity for PS 4K ($h_c = h_{app} - \frac{2}{\nu} - \nu^{0.33}$)

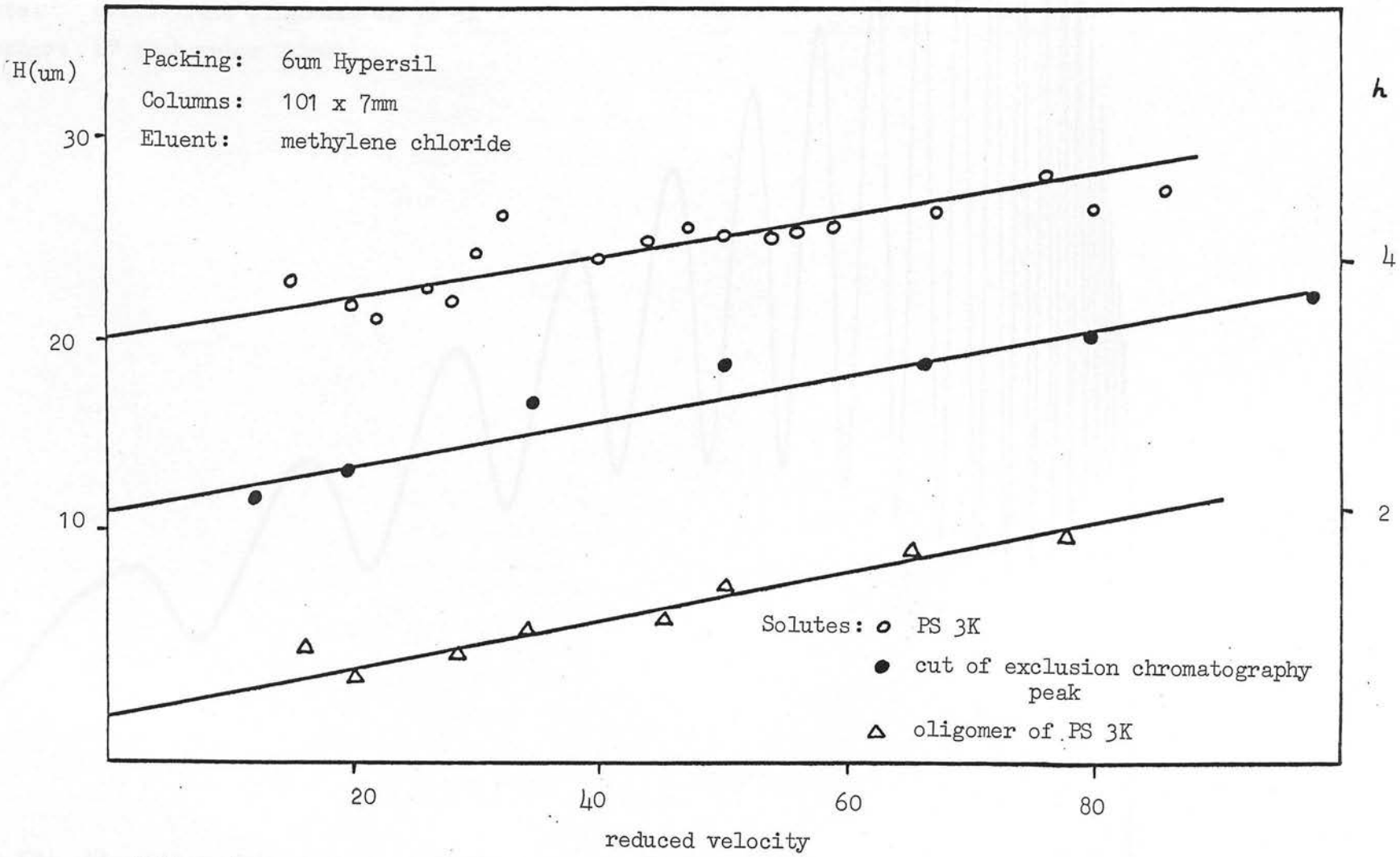

FIGURE 51: Plate height versus reduced velocity curves for PS 3K and PS 3K fractions

Packing: 6um Hypersil

Column: 101 x 7mm

Eluent: pentane/methylene chloride (80/20)

Solute: polystyrene oligomers in PS 3K

Detector: UV photometer 254nm

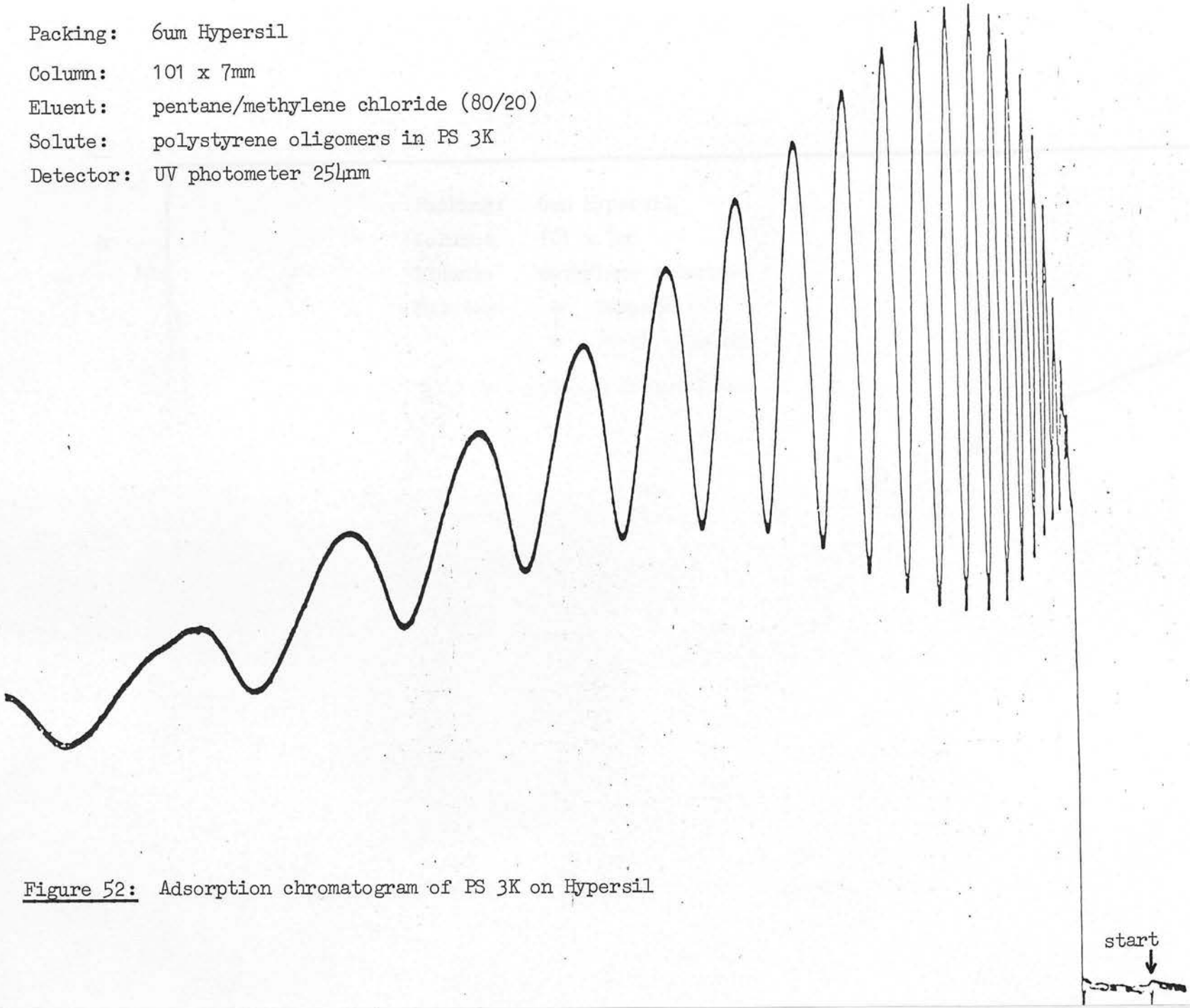

Figure 52: Adsorption chromatogram of PS 3K on Hypersil

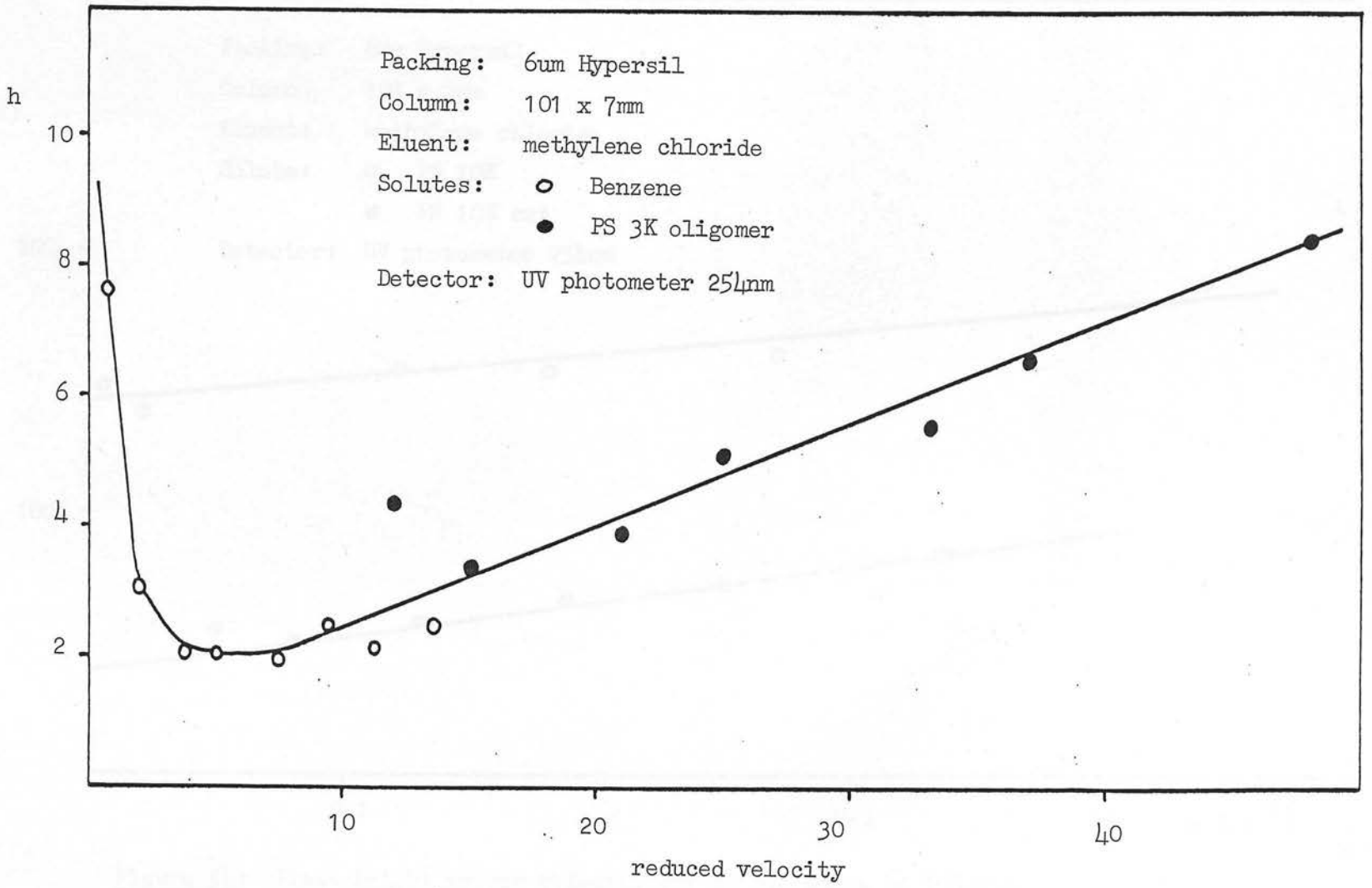

Figure 53: Reduced plate height versus reduced velocity for a PS 3K oligomer and Benzene

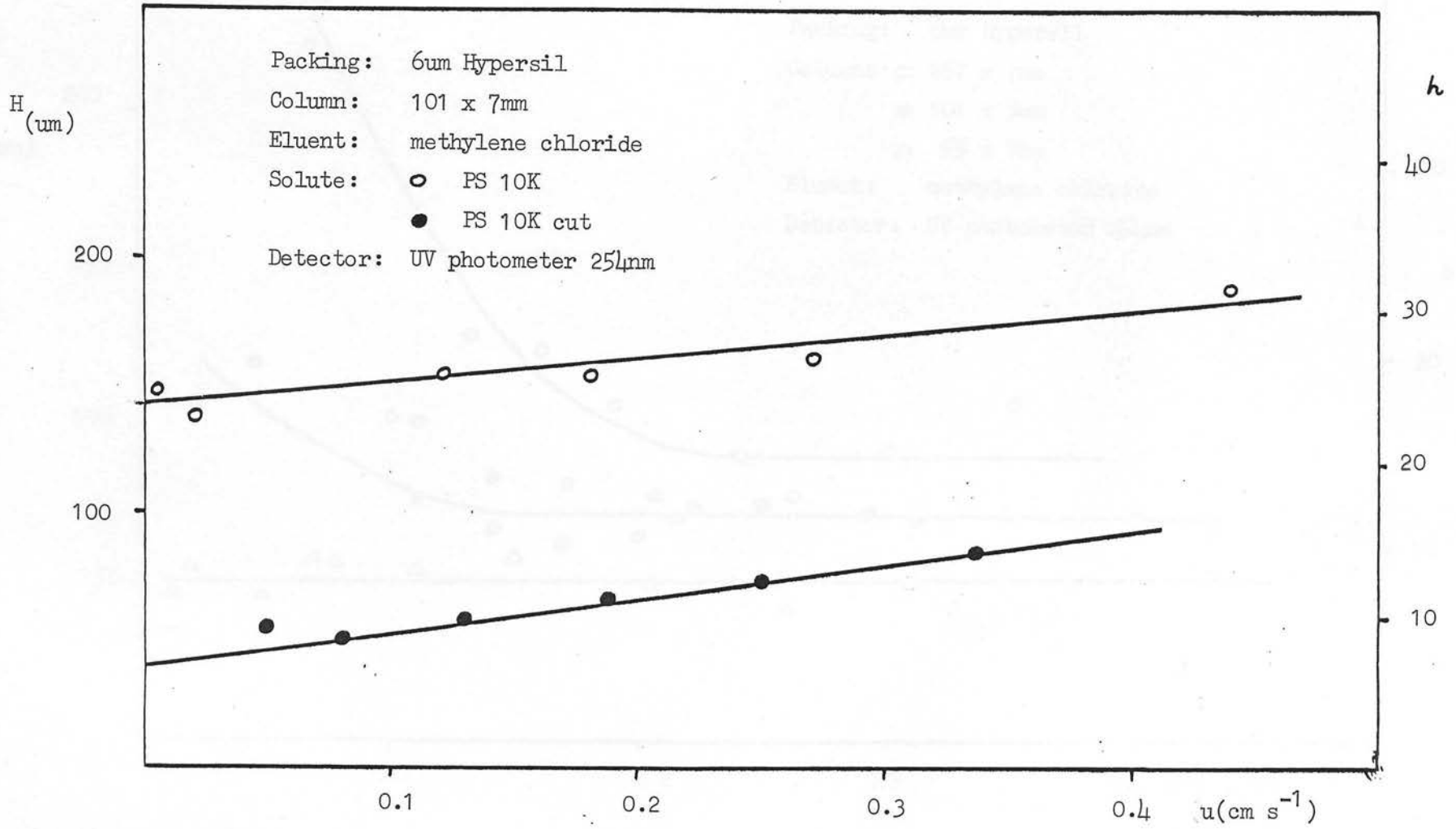

Figure 54: Plate height versus velocity for PS 10K and a PS 10K cut

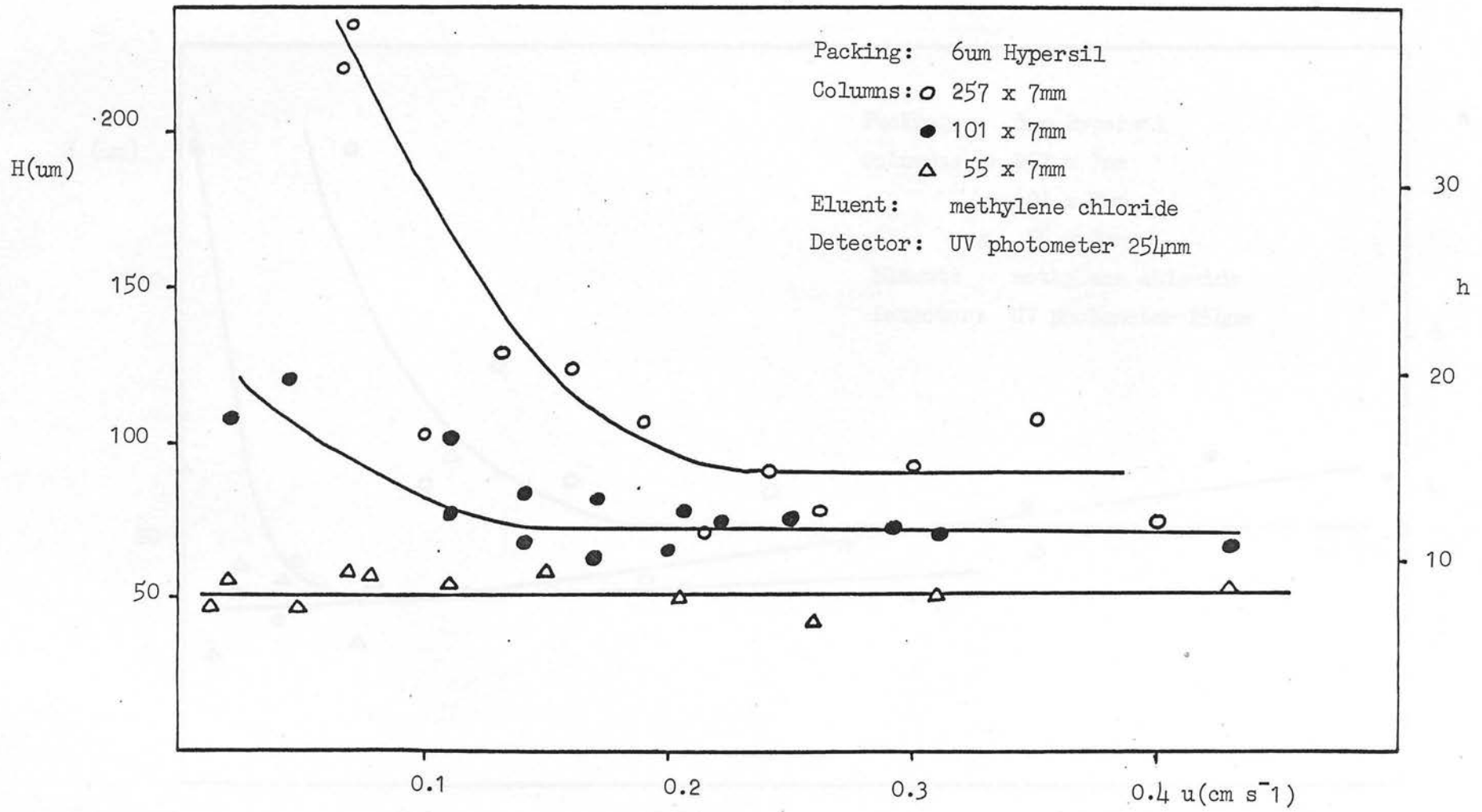

Figure 55: Variation of plate height with velocity for PS 2700K

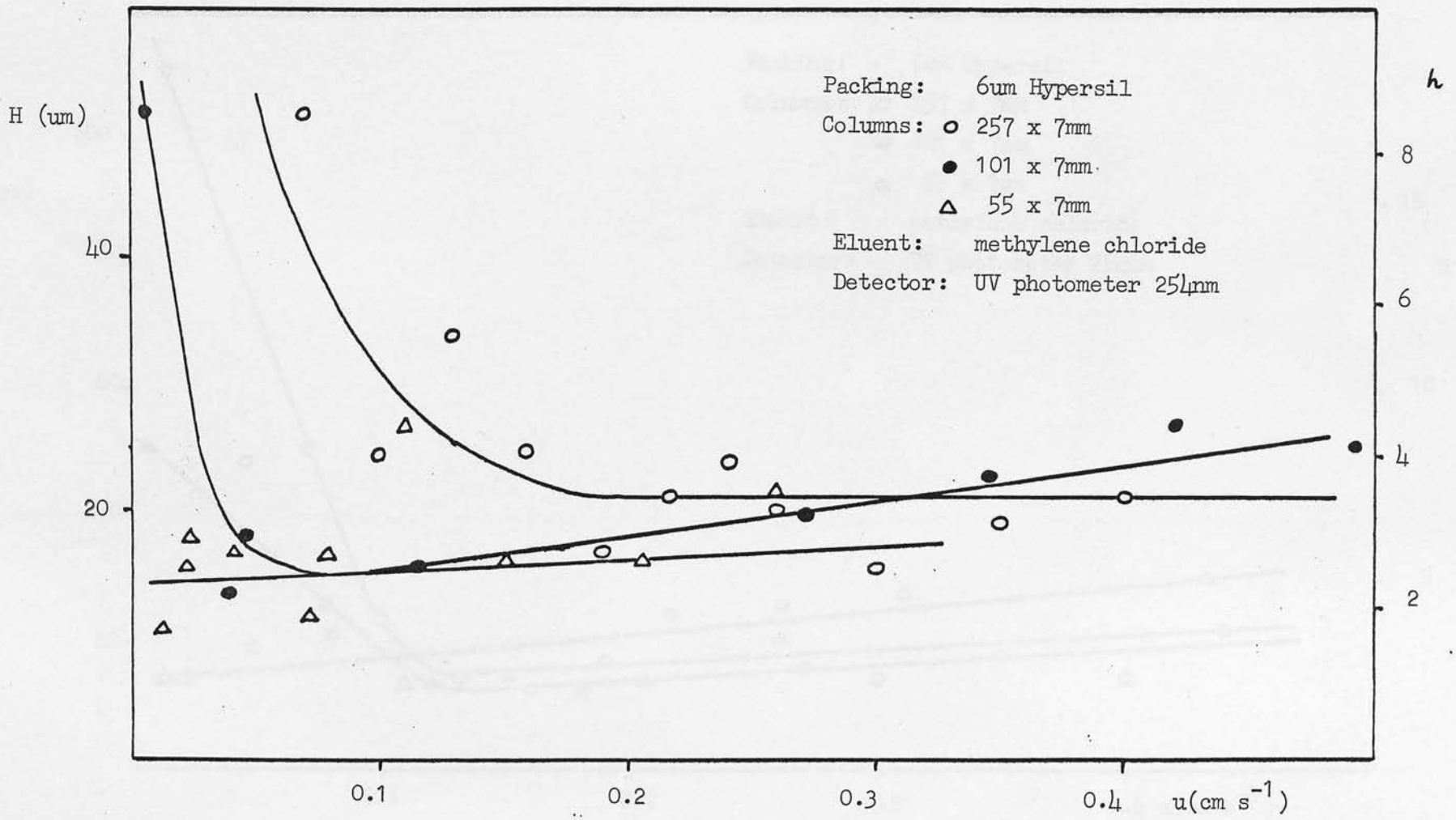

Figure 56: Variation of plate height with velocity for PS 470K

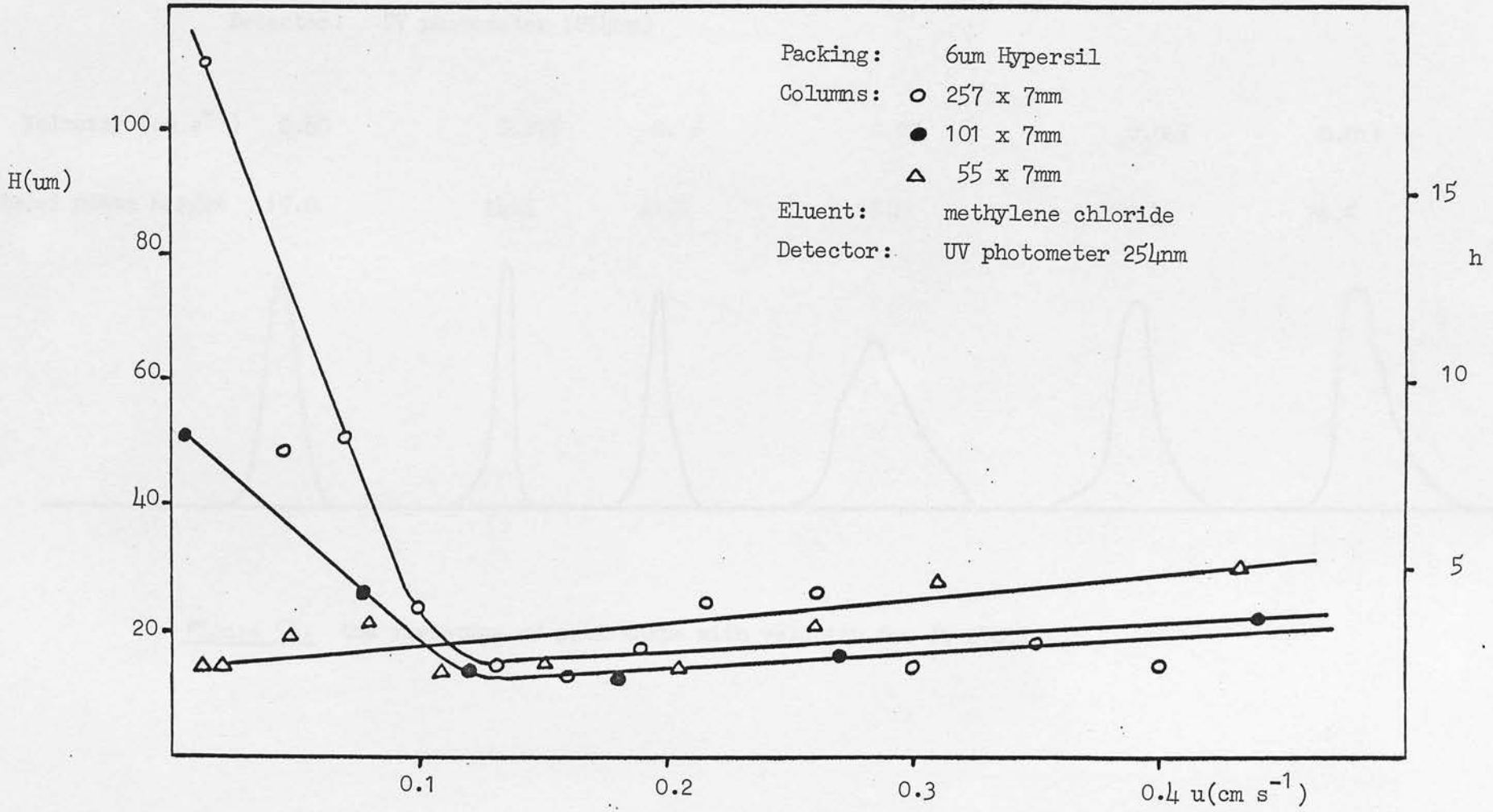

Figure 57: Variation of plate height with velocity for PS 200K

Packing: 6um Hypersil
Column: 257 x 7mm
Eluent: methylene chloride
Detector: UV photometer (254nm)

Velocity (cm s^{-1})	0.40	0.215	0.19	0.07	0.045	0.011
Reduced plate height	15.0	14.4	21.1	18.4	50.4	76.5

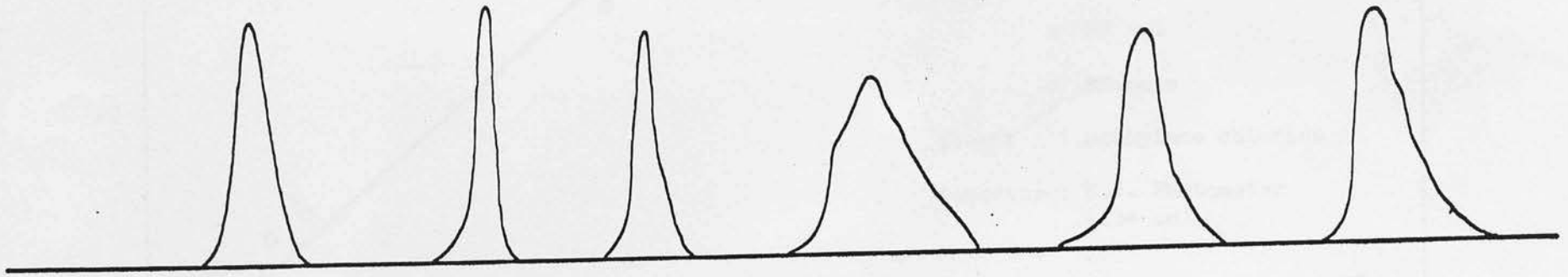

Figure 58: the variation of peak shape with velocity for PS 2700K

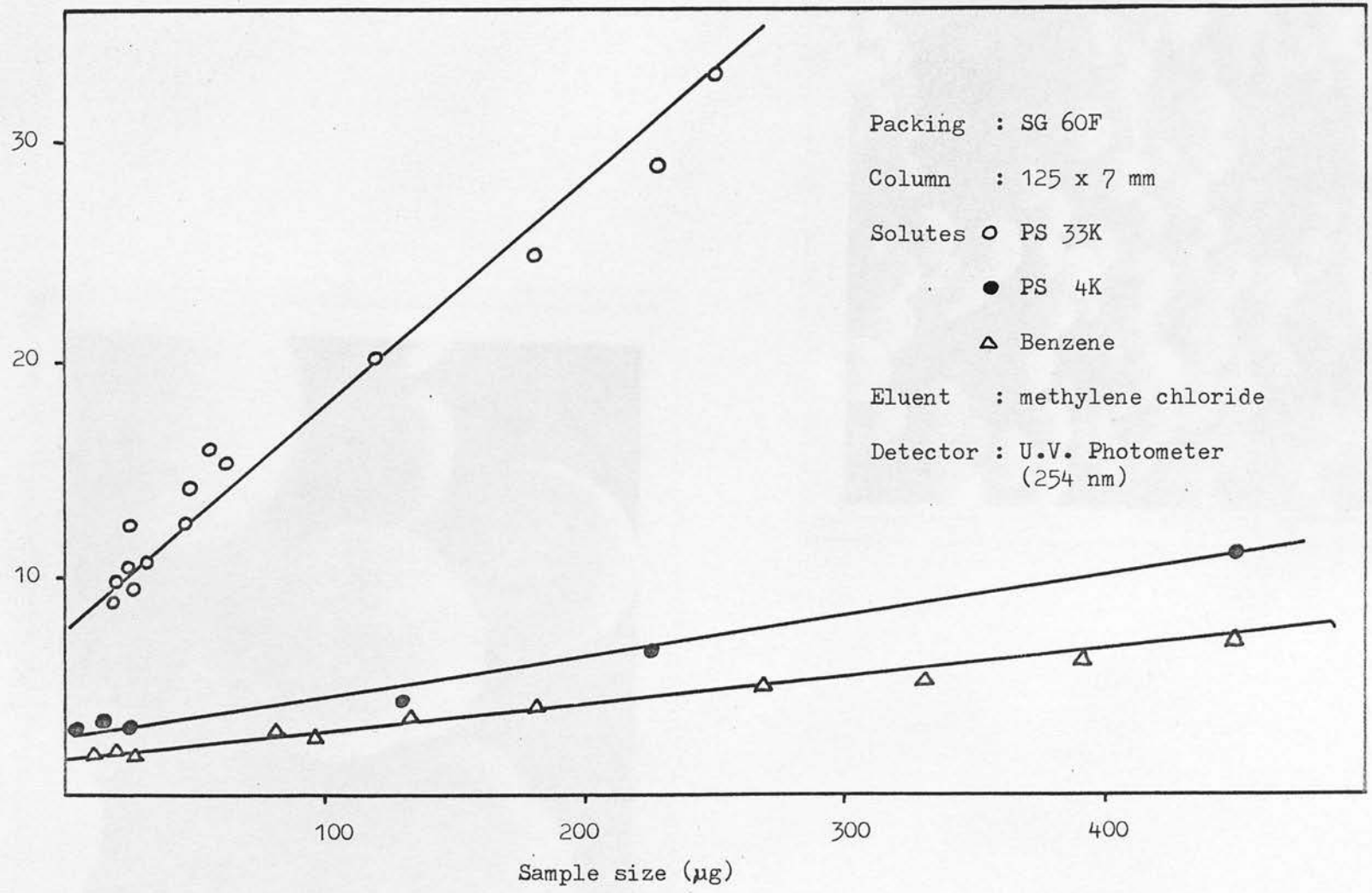

Figure 59 : Effect of sample size on column efficiency

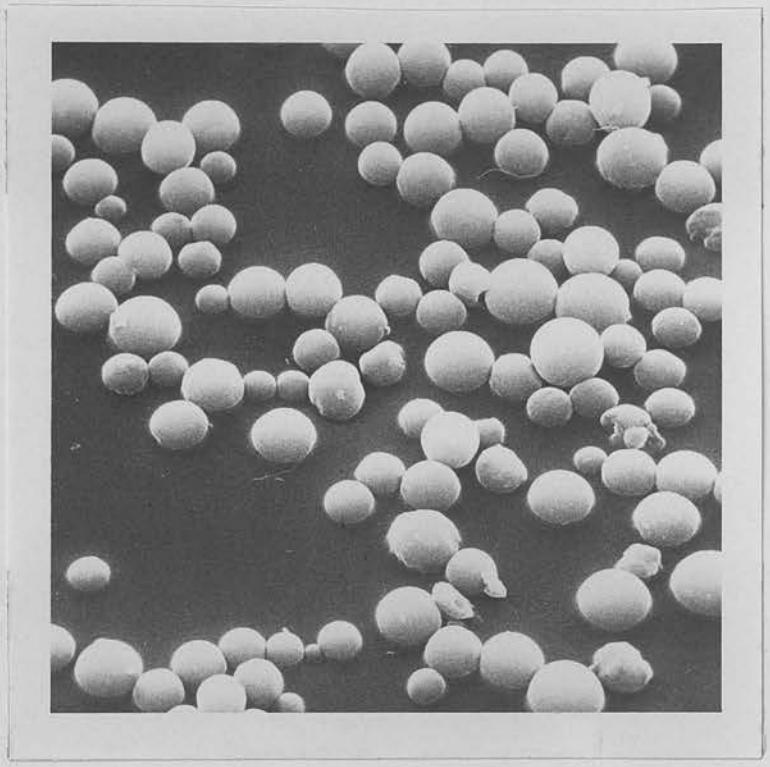

Electron Micrographs of Hypersil

Allowance for Polydispersity in the Determination of the True Plate Height in GPC

J. H. Knox / F. McLennan
Department of Chemistry, University of Edinburgh, Great Britain

Summary

In gel permeation chromatography (GPC), dispersion of a sharply injected sample arises both from the polydispersity, P, of the polmer sample and from the kinetic processes occurring within the column. The latter are described by the true plate height, H. It is shown that a current formula for deriving H from the observed band dispersion and the polydispersity is incorrect and that for samples with $P \leqslant 1.1$ *a good approximation is* $H = H_{app} - L(P-1)(1+\alpha)/x^2$ *where* H_{app} *is the apparent plate height calculated in the normal way from the experimental peak width and retention time or volume; L is the column length;* α *is a correction term whose value is 0.4 for* $P = 1.10$*; x is a measure of the relative molecular mass range covered by the packing material (x generally lies between 4 and 12 for GPC materials of narrow pore size distribution). It is concluded that the true plate height cannot generally be obtained from the elution peak of a polymer standard whose polydispersity is much larger than about 1.01.*

In gel permeation chromatography (GPC) dispersion of a sharply injected polymer sample arises both from the polydispersity, P, of the sample and from the kinetic processes occurring within the column. According to the theory of chromatography the kinetic dispersion of any sample of a pure compound (in the case of a polymer a monodisperse sample for which P = unity) eluted from a column of length, L, is related to the plate height, H, and the number of theoretical plates, N, by equations (1) and (2) respectively [1, 2].

$$H = L\left(\frac{\sigma_v}{V_R}\right)^2 \tag{1}$$

$$N = L/H = (V_R/\sigma_v)^2 \tag{2}$$

where σ_v is the standard deviation of the peak in volume units and V_R the elution volume. The effect of polydispersity will be to increase the peak width and so lead to an apparent increase in H and a decrease in N.

Bly has proposed the use of equations (3) or (4) to calculate the true values of H and N and correct for this effect of polydispersity [3, 4].

$$H = H_{app}/P^2 \tag{3}$$

$$\text{or } N = N_{app} \times P^2 \tag{4}$$

where H_{app} and N_{app} are calculated from the experimentally measured variance of the eluted peak. These equations have been used by subsequent workers [5, 6]. It is the purpose of this paper to show that equations (3) and (4) are incorrect and greatly underestimate the effects of polydispersity. The effect of polydispersity is in fact so large that even with P = 1.01 it is difficult to make accurate determinations of H and N.

The polydispersity, P, of a polymer sample is defined by equation (5) –

$$P = M_w/M_n \tag{5}$$

where M_w and M_n are the weight- and number-averaged relative molecular masses of the polymer sample. M_w and M_n are defined by equations (6) and (7) –

$$M_n = \int M\, f(M)\, dM \tag{6}$$

$$M_w = \frac{\int M^2 f(M)\, dM}{\int M f(M)\, dM} \tag{7}$$

where f(M) dM is the number fraction of polymer molecules having relative molecular masses in the range M to M + dM. A typical distribution showing M_n and M_w is given in Fig. 1. The polydispersity of this particular distribution is 1.09.

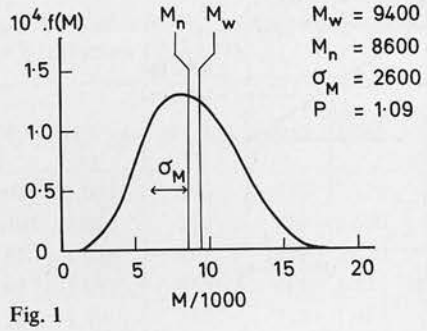

Fig. 1

● Number relative molecular mass distribution, f (M), as function of relative molecular mass M, for sample of moderate polydispersity, P = 1.09. Values of M are illustrative.

The second moment or variance of the distribution about the mean is given by equation (8) –

$$\sigma_M^2 = \int (M - M_n)^2 f(M)\, dM \qquad (8)$$

and it is readily shown (see Appendix 1) that whatever the form of f(M), σ_M^2 is related to M_n and M_w by equation (9) –

$$\left\{\frac{\sigma_M}{M_n}\right\}^2 = \left\{\frac{M_w}{M_n}\right\} - 1 = P - 1 \qquad (9)$$

This equation is quoted without proof by *Osterhoudt* and *Ray* [7]. Equation (6) and Fig. 1 show that σ_M is a substantial fraction of M_n even for a polymer sample with a polydispersity as low as 1.09. Fig. 2 shows a corresponding case where P = 1.01 and the distribution function is Gaussian. It is qualitatively clear that the polydispersity of even a relatively narrow polymer fraction will contribute substantially to the total width of the eluted peak in GPC. To obtain a quantitative measure it is necessary to consider the GPC calibration curve relating relative molecular mass to elution volume, an example of which is shown in Fig. 3. V_0 is the void volume of the packing (volume outside the particles); V_t is the void volume plus the volume of all pores accessible to a small molecule. M_u and M_l are the upper and lower relative molecular mass limits corresponding to the elution volumes V_0 and V_t respectively and obtained from the extrapolation of the linear portion of the calibration curve. M* is any intermediate relative molecular mass on the linear portion of the curve corresponding to an elution volume V*. The relative molecular mass selectivity of a GPC material is conveniently denoted by S, the reciprocal of the gradient of the linear portion of the calibration curve [3], that is –

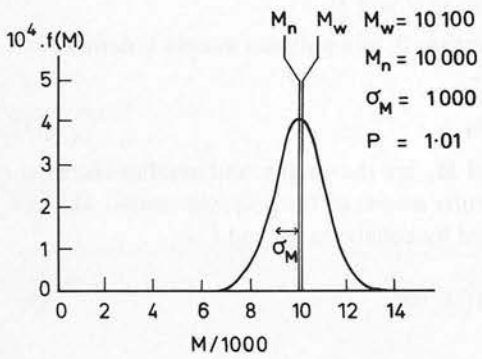

Fig. 2

- Gaussian relative molecular mass distribution function for high grade polymer standard P = 1.01. Values of M are illustrative.

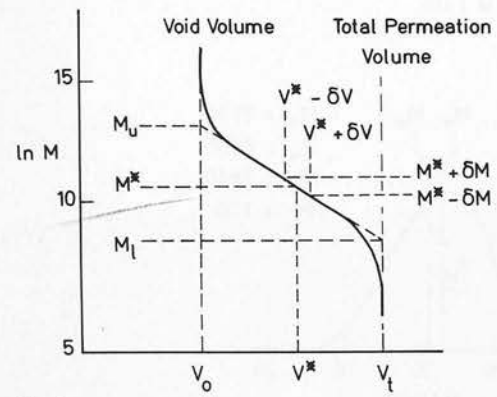

Fig. 3

- Illustrative calibration curve for gel permeation material showing dependence of elution volume, V, upon relative molecular mass M. Approximate molecular weight range resolvable 1000–25000.

$$1/S = -\, d\ln M/dV \qquad (10)$$

We thus have –

$$V_t = V_0 + S \ln (M_u/M_l) \qquad (11)$$

and for any intermediate relative molecular mass M close to M*

$$V_M = V^* + S \ln (M^*/M) \qquad (12)$$

Writing $M = M^* + \delta M$ then gives

$$\begin{aligned} V_M &= V^* + S \ln \frac{M^*}{M^* + \delta M} \\ &= V^* - S \ln \left(1 + \frac{\delta M}{M^*}\right) \\ &= V^* - \delta V \end{aligned} \qquad (13)$$

Equation (13) can be applied to a polymer sample where number average MW is $M_n = M^*$. The elution peak will then be centred on V* and the second moment of the peak on a volume basis will be –

$$\begin{aligned} \sigma^2_{V\ (\text{polydispersity})} &= \int_{-\infty}^{\infty} (\delta V)^2 f(M_n + \delta M)\, d(\delta M) \\ &= S^2 \int_{-\infty}^{\infty} \left[\ln\left(1 + \frac{\delta M}{M_n}\right)\right]^2 f(M_n + \delta M)\, d(\delta M) \end{aligned} \qquad (14)$$

For a polymer of narrow relative molecular mass range (i.e. low polydispersity) we may assume to a first approximation that f(M) is Gaussian, that is –

$$f(M) \equiv f(M_n + \delta M) = \frac{\exp\left[-\delta M^2/2\sigma_M^2\right]}{(2\pi\sigma_M^2)^{\frac{1}{2}}} \qquad (15)$$

σ_M being the standard deviation of the distribution. Figure 2 illustrates equation (15) where P = 1.01 and therefore $\sigma_M/M_n = 0.1$. The width of the distribution is again noticeable for this very low value of P. Insertion of f(M) from (15) into equation (14) followed by expansion of the logarithmic factor as a series and integration (see Appendix 2) lead to –

$$\sigma^2_{V\ (\text{dispersity})} = S^2\,(P - 1)\,(1 + \alpha) \qquad (16)$$

where α is a correction term given by –

$$\alpha = (11/4)\,(P - 1) + (137/12)\,(P - 1)^2 \qquad (17)$$

Values of α as a function of P are shown in Fig. 4.

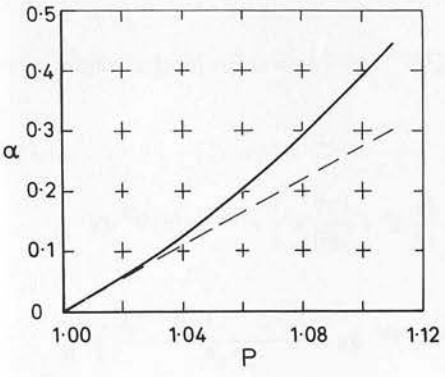

Fig. 4

Dependence of α (equation 17) on polydispersity P. Broken line gives asymptote for low α of (11/4) (P – 1).

Since variances from independent sources are additive we obtain for the total peak variance –

$$\sigma^2_{V\,(total)} = \sigma^2_{V\,(kinetic)} + \sigma^2_{V\,(polydispersity)} \qquad (18)$$

Using equation (1) for $\sigma^2_{V\,(kinetic)}$ and (16) gives –

$$\sigma^2_{V\,(total)} = \frac{H}{L} V_R^2 + S^2 (P-1)(1+\alpha) \qquad (19)$$

The apparent plate height and plate number are conveniently defined by analogy with equations (1) and (2) as

$$H_{app} = L\left\{\frac{\sigma_{V\,(total)}}{V_R}\right\}^2 \qquad (20)$$

$$N_{app} = \left\{\frac{V_R}{\sigma_{V\,(total)}}\right\}^2 \qquad (21)$$

We thus obtain

$$H_{app} = H + L(P-1)(1+\alpha)(S/V_R)^2 \qquad (22)$$

$$1/N_{app} = 1/N + (P-1)(1+\alpha)(S/V_R)^2 \qquad (23)$$

The ratio (V_R/S) is the hypothetical range of relative molecular mass measured in powers of e which would be eluted over a volume V_R. This ratio, denoted by x is generally with the range 4–12 for a GPC material of uniform pore size [2, 6, 8, 9] and is readily found from the calibration curve. Replacing (V_R/S) by x and rearranging gives finally –

$$H = H_{app} - L(P-1)(1+\alpha)/x^2 \qquad (24)$$

$$1/N = 1/N_{app} - (P-1)(1+\alpha)/x^2 \qquad (25)$$

Discussion

It is readily seen from equation (25) that for a monodisperse polymer (P = unity), $N = N_{app}$, while for a polydisperse polymer sample eluted from a column of infinite plate efficiency N_{app} has a maximum value given by –

$$N_{app(max)} = x^2/(P-1)(1+\alpha) \qquad (26)$$

Typical values of $N_{app(max)}$ are shown in Table I for different values of x and P. The contribution of polydispersity to peak dispersion in a moderately efficient column of $N \approx 1000$ will be relatively unimportant for entries above the stepped line but substantial for entries below the line.

Table I. Values of $N_{app(max)}$ for various values of P and x (equations 17 and 26)

P	(1 + α)	$N_{app\,(max)}$ x = 4	x = 8	x = 12
1.001	1.003	16 000	64 000	144 000
1.003	1.008	5 400	21 200	48 000
1.010	1.029	1 550	6 200	14 000
1.030	1.093	490	1 950	4 400
1.10	1.39	115	460	1 040

Table II shows the combined effects of polydispersity and kinetic dispersion on N_{app} for the case where x = 8. For entries above the stepped line the error in assuming $N = N_{app}$ is less than 15 %. It is seen that even for the least efficient column with N = 300 it is necessary to use a sample with a polydispersity of not more than 1.03 while if N = 1000 the polydispersity must be below 1.01. It becomes clear that the true plate number or plate height cannot generally be determined by elution of commercially available polymer standards whose polydispersities are rarely below 1.03 and in any case are not known with high enough precision to allow the precise calculation of the second terms in equations (22) to (25).

It is evident from the figures given in Table II that *Bly*'s formula will give values of N which are often far too low. This is emphasised by the comparison of the values of N calculated by formulae (4) and (25) shown in Table III. *Bly*'s formula gives acceptable accuracy only when N is close to N_{app}, in other words when the effects of polydispersity are negligible. Under all other conditions it gives results which are seriously in error. The figures in Table III again show that P must be below 1.03 for reliable values of N to be calculable. It is also necessary to know P rather accurately unless either N is very low, say below 300, or P is very low, say below 1.01.

Table II. Values for N_{app} for various values of P and N when x = 8 (equations 17 and 25)

P	(1 + α)	N_{app} N = 300	1 000	3 000	10 000	(1) ∞	of (2)
1.001	1.003	298	985	2 870	8 650	64 000	
1.003	1.008	296	955	2 630	6 800	21 200	
1.01	1.029	286	861	2 025	3 835	6 200	
1.03	1.093	260	661	1 225	1 635	1 950	
1.10	1.39	182	315	400	440	460	

(1) values in this column are $N_{app\,(max)}$ (see Table I)
(2) values in this row are true plate numbers N

Table III. Comparison of values of N calculated by Equations (4) and (25) for x = 8

	N_{app}	300	1 000	3 000
P	Eqn.			
1.01	25	315	1 190	5 800
	4	306	1 020	3 060
1.03	25	354	2 050	*
	4	318	1 060	3 180
1.10	25	860	*	*
	4	363	1 210	3 630

* For the given values of P and x the values of N cannot be attained owing to the dispersion due to the relative molecular mass range of the sample even with an infinitely efficient column.

Appendix 1

Relation of variance of relative molecular mass distribution to polydispersity (equations 8 and 9).

$$\sigma_M^2 = \int (M - M_n)^2 f(M)\, dM \qquad (8)$$

$$= \int M^2 f(M)\, dM - 2M_n M\, f(M)\, dM + M_n^2 f(M)\, dM$$

$$= \int M^2 f(M)\, dM - 2M_n^2 + M_n^2$$

$$= M_w M_n - M_n^2$$

$$\frac{\sigma_M^2}{M_n^2} = \frac{M_w}{M_n} - 1 = P - 1 \qquad (9)$$

Appendix 2

Evaluations of Integral of equation (14) using (15) for f(M).

$$I \equiv \frac{\sigma_{V\,(\text{polydispersity})}^2}{S^2} = \int_{-\infty}^{\infty} \left[\ln\left(1 + \frac{\delta M}{M_n}\right)\right]^2 \frac{\exp[-\delta M^2/2\sigma_M^2]}{(2\pi\sigma_M^2)^{\frac{1}{2}}}\, d(\delta M)$$

replacing $\delta M/M_n$ by x and $M_n^2/2\sigma_M^2$ by a gives

$$I = \int [\ln(1 + x)]^2\, e^{-ax^2}\, (a/\pi)^{\frac{1}{2}}\, dx$$

expanding the logarithm to several terms for $x < 1$ gives

$$\ln(1 + x) = x\{1 - (x/2) + (x^2/3) - (x^3/4) + \ldots\}$$

$$[\ln(1 + x)]^2 = x^2 \left\{1 - x + \frac{11}{12}x^2 - \frac{5}{6}x^3 + \frac{137}{180}x^4 - \right\}$$

Noting that $\int_{-\infty}^{\infty} x^{2n+1} e^{-ax^2} dx = 0$ for integral values of n we can write

$$I = \int_{-\infty}^{\infty} \left[x^2 + \frac{11}{12}x^4 + \frac{137}{180}x^6\right] e^{-ax^2} (a/\pi)^{1/2}\, dx$$

In general $\int_{-\infty}^{\infty} x^{2n} e^{-ax^2}\, dx = \frac{1.3.5 \ldots (2n-1)}{2^n a^n} \sqrt{\frac{\pi}{a}}$

Thus

$$I = \frac{1}{2a} + \frac{11}{4}\cdot\frac{1}{4a^2} + \frac{137}{12}\cdot\frac{1}{8a^3} + \ldots$$

$$= \left\{\frac{\sigma_M}{M_n}\right\}^2 + \frac{11}{4}\left\{\frac{\sigma_M}{M_n}\right\}^4 + \frac{137}{12}\left\{\frac{\sigma_M}{M_n}\right\}^6 + \ldots$$

Since $\left\{\frac{\sigma_M}{M_n}\right\}^2 = P - 1$ we obtain finally

$$I = (P-1)\left\{1 + \frac{11}{4}(P-1) + \frac{137}{12}(P-1)^2 + \ldots\right\} \qquad (16)$$

$$= (P-1)(1 + \alpha)$$

where

$$\alpha = (11/4)(P-1) + (137/12)(P-1)^2 \qquad (17)$$

References

[1] *J. C. Giddings*, "Dynamics of Chromatography Part 1", Marcel Dekker, New York, 1965.

[2] *L. R. Snyder* and *J. J. Kirkland*, "Introduction to Modern Liquid Chromatography", John Wiley, New York, 1974.

[3] *D. D. Bly*, J. Polym. Sci., A-1 **6**, 2085 (1968).

[4] *D. D. Bly*, Analyt. Chem. **41**, 477 (1969).

[5] *K. K. Unger*, *R. Kern*, *M. C. Ninou* and *K. F. Krebs*, J. Chromatog. **99**, 435 (1974).

[6] *K. K. Unger* and *R. Kern*, J. Chromatog. **122**, 345 (1976).

[7] *H. W. Osterhoudt* and *L. N. Ray*, J. Polym. Sci. C **21**, 5 (1968).

[8] *W. A. Dark* and *R. J. Limpert*, J. Chromatog. Sci. **11**, 114 (1973).

[9] *J. J. Kirkland*, J. Chromatog. Sci. **10**, 593 (1972).

Received: Sept. 23, 1976
Accepted: Oct. 11, 1976